UNIVERSIDADE FEDERAL DE MINAS GERAIS
PROGRAMA DE PÓS-GRADUAÇÃO EM SANEAMENTO, MEIO AMBIENTE E RECURSOS HÍDRICOS

Caique Prado Machado de Oliveira

PHOTOCATALYTIC RECYCLED MEMBRANES FROM TiO_2 AND GRAPHENE OXIDE (GO) AND THEIR APPLICATIONS IN THE TREATMENT OF WASTEWATER

Belo Horizonte
2022

Caique Prado Machado de Oliveira

PHOTOCATALYTIC RECYCLED MEMBRANES FROM TiO_2 AND GRAPHENE OXIDE (GO) AND THEIR APPLICATIONS IN THE TREATMENT OF WASTEWATER

Tese apresentada ao Programa de Pós-graduação em Saneamento, Meio Ambiente e Recursos Hídricos da Universidade Federal de Minas Gerais, como requisito parcial à obtenção do título de Doutor em Saneamento, Meio Ambiente e Recursos Hídricos.

Área de concentração: Meio Ambiente

Linha de pesquisa: Caracterização, prevenção e controle da poluição

Orientadora: Profª. Drª. Míriam Cristina Santos Amaral
Co-orientador: Prof. Dr. Marcelo Machado Viana
Prof. Dr. Jörg E. Drewes

Belo Horizonte
2022

Caique Prado Machado de Oliveira

PHOTOCATALYTIC RECYCLED MEMBRANES FROM TiO_2 AND GRAPHENE OXIDE (GO) AND THEIR APPLICATIONS IN THE TREATMENT OF WASTEWATER

Thesis presented to the Post-graduate Program in Sanitation, Environment and Water Resources of the Federal University of Minas Gerais, as a partial requirement to obtain the Doctorate's degree in Sanitation, Environment and Water Resources.

Focus area: Environment

Research line: Characterization, prevention and control of pollution

Advisor: Profª. Drª. Míriam Cristina Santos Amaral
Co-advisor: Prof. Dr. Marcelo Machado Viana
Prof. Dr. Jörg E. Drewes

Belo Horizonte
2022

Oliveira, Caique Prado Machado de.
O48p Photocatalytic recycled membranes from TiO_2 and graphene oxide (GO) and their applications in the treatment of wastewater [recurso eletrônico] / Caique Prado Machado de Oliveira .- 2022.
1 recurso online (xx, 187 f. : il., color.) : pdf.

Orientadora: Miriam Cristina Santos Amaral.
Coorientador: Marcelo Machado Viana.
Coorientador: Jörg E. Drewes.

Tese (doutorado) - Universidade Federal de Minas Gerais, Escola de Engenharia.

Apêndices: f. 179-187.

Bibliografia: f. 148-178.
Exigências do sistema: Adobe Acrobat Reader.

1. Engenharia sanitária - Teses. 2. Meio ambiente - Teses. 3. Água - Tratamento - Teses. 4. Grafeno - Teses. 5. Titânio - Teses. 6. Água - Poluição - Teses. 7. Sustentabilidade e meio ambiente - Teses. 8. Energia - Teses. 9. Água potável - Contaminação - Teses. 10. Reatores - Teses. 11. Membranas (Tecnologia) - Teses. 12. Poluição da água - Prevenção. 13. Fotocatálise - Teses. I. Amaral, Miriam Cristina Santos. II. Viana, Marcelo Machado. III. Drewes, Jörg E. IV. Universidade Federal de Minas Gerais. Escola de Engenharia. V. Título.

CDU: 628(043)

Ficha catalográfica elaborada pela bibliotecária Ângela Cristina Silva CRB/6 2361
Biblioteca Prof. Mário Werneck, Escola de Engenharia da UFMG

UNIVERSIDADE FEDERAL DE MINAS GERAIS
ESCOLA DE ENGENHARIA
CURSO DE PÓS-GRADUAÇÃO EM SANEAMENTO, MEIO AMBIENTE E RECURSOS HÍDRICOS

FOLHA DE APROVAÇÃO

Photocatalytic Recycled Membranes From TiO2 And Graphene Oxide (GO) And Their Applications In The Treatment Of Wastewater

CAIQUE PRADO MACHADO DE OLIVEIRA

Tese defendida e aprovada pela banca examinadora constituída pelos Senhores:

Prof. Miriam Cristina Santos Amaral

Prof. Marcelo Machado Viana (Coorientador)

Prof. Eduardo Henrique Martins Nunes

Profa. Regina de Fátima Peralta Muniz Moreira

Profa Fabiana Valéria da Fonseca

Profa Cintia Marangoni

Aprovada pelo Colegiado do PG SMARH

Versão Final aprovada por

Profa. Priscilla Macedo Moura

Coordenadora

Profª. Miriam Cristina Santos Amaral Moravia

Orientadora

Belo Horizonte, 12 de dezembro de 20

Documento assinado eletronicamente por **Cintia Marangoni, Usuário Externo**, em 19/12/2022, às 10:58, conforme horário oficial de Brasília, com fundamento no art. 5º do Decreto nº 10.543, de 13 de novembro de 2020.

Documento assinado eletronicamente por **Miriam Cristina Santos Amaral Moravia, Professora do Magistério Superior**, em 20/12/2022, às 14:27, conforme horário oficial de Brasília, com fundamento no art. 5º do Decreto nº 10.543, de 13 de novembro de 2020.

Documento assinado eletronicamente por **Eduardo Henrique Martins Nunes, Professor do Magistério Superior**, em 21/12/2022, às 12:15, conforme horário oficial de Brasília, com fundamento no art. 5º do Decreto nº 10.543, de 13 de novembro de 2020.

Documento assinado eletronicamente por **Regina de Fátima Peralta Muniz Moreira, Usuária Externa**, em 07/06/2023, às 09:02, conforme horário oficial de Brasília, com fundamento no art. 5º do Decreto nº 10.543, de 13 de novembro de 2020.

Documento assinado eletronicamente por **Fabiana Valéria da Fonseca, Usuária Externa**, em 07/06/2023, às 09:19, conforme horário oficial de Brasília, com fundamento no art. 5º do Decreto nº 10.543, de 13 de novembro de 2020.

Documento assinado eletronicamente por **Marcelo Machado Viana, Professor do Magistério Superior**, em 07/06/2023, às 11:11, conforme horário oficial de Brasília, com fundamento no art. 5º do Decreto nº 10.543, de 13 de novembro de 2020.

Documento assinado eletronicamente por **Priscilla Macedo Moura, Coordenador(a) de curso de pós-graduação**, em 12/06/2023, às 07:21, conforme horário oficial de Brasília, com fundamento no art. 5º do Decreto nº 10.543, de 13 de novembro de 2020.

A autenticidade deste documento pode ser conferida no site https://sei.ufmg.br/sei/controlador_externo.php?acao=documento_conferir&id_orgao_acesso_externo=0, informando o código verificador **1954907** e o código CRC **0F83D4BC**.

Referência: Processo nº 23072.272276/2022-63 **SEI nº 1954907**

AGRADECIMENTOS

A construção desse documento e a realização desse sonho envolve o suporte e carinho de muitas mãos... As primeiras a Quem quero agradecer e venerar são as de Deus que estiveram estendidas derramando suas bençãos, cumulando com seus dons e dando força e amparo em cada um dos dias dessa caminhada. A Ti, Senhor, toda minha gratidão!

Sei que Ele, de maneira gentil, também concederia Suas mãos de maneira física e elas puderam ser sentidas, dentre outras pessoas, pelas correções, direcionamentos, conselhos, conversas e apoio de meus orientadores: Professora Míriam, Professor Marcelo e Prof. Jörg. Professora Míriam é uma espécie de estilingue de sonhos. Propulsiona, incentiva, oportuniza e investe. Seu tempo, seu conhecimento, sua sabedoria. Sou muito grato por ter sido seu orientado no mestrado e doutorado, por ter aprendido tanto com a senhora e por cada oportunidade que me concedeu. Te admiro muito! Professor Marcelo é outra grata surpresa na minha vida, que me abriu a primeira porta da ciência, ainda na iniciação científica, e quem com toda sua motivação e paixão pela pesquisa me arrebatou também para área. Não foram raras as conversas recheadas de risadas e muito aprendizado ao longo desses anos de convívio. Obrigado por tudo que fez e ainda faz por mim. Minha estima sem tamanho! E no hall de orientadores, mais recentemente, tive o privilégio de conhecer Professor Jörg. Cada encontro com ele eram verdadeiras aulas. Sempre cirúrgico, preciso e com conhecimento que parece tender ao infinito. Embora não orientador formal, gostaria de ressaltar a presença do Konrad nessa trajetória acadêmica. Alemão dos mais abrasileirados que conheci. Coração bom sem tamanho. Obrigado por tudo! Refletindo acerca de tudo isso, não consigo pensar em mais nada a não ser me considerar um grande sortudo!

Para além das mãos acadêmicas, aquelas cheias do afago e de amor foram suporte em cada um dos dias. A dos meus pais, Fiora e Geraldo, certamente foram as mais afáveis e carregadas de muito suor e história. Sem dúvida alguma eu dedico esse título aos senhores! Devo tudo que a vida foi me propiciando à essas mãos aí que trabalharam incessantemente para me ensinar os valores do bem, da honestidade, da retidão e, sobretudo da importância do estudo. “Estudo em primeiro lugar”! Já ouvi reiteradas vezes que soa como mantra. E é nesse ínterim que hoje agradeço e celebro a vocês, meus doutores da vida.

Não posso deixar de mencionar meu irmão, Victor, sempre amigo e presente em todas as ocasiões, que vibra comigo como cada uma de suas conquistas e que no período recente foi me encontrar no sanduíche como incentivo em mais uma etapa desse período. Essa conquista é nossa!

Fui agraciado, também, pelas mãos de uma mulher incrível com quem tenho a honra de dividir a vida. Márcia é uma espécie de ponto de paz, fonte de alegria e calmaria nos meus dias mais difíceis e também nos mais felizes. Foi me encontrar duas vezes no período sanduíche e apesar do fuso não deixou de se fazer presente nem um segundo. Aguentou muitas noites e finais de semana que estive trabalhando, sempre me esperando com um sorriso largo e essas mãos cheias de amor. Muito obrigado! Devo muito disso aqui também a você!

Agradeço aos meus familiares, amigos, colegas, pares e todos aqueles que direta e indiretamente contribuíram para essa realização. Não irei citar nomes para não ser injusto de porventura deixar de mencionar um ou outro, mas cada um de vocês sabe a importância que têm para a consolidação desse momento.

Agradeço aos Professores que compõem a banca, pela gentileza de disponibilizar vossos tempos e conhecimento para o aprimoramento do presente trabalho! Obrigado de verdade.

Agradeço aos colegas de laboratório do Brasil e Alemanha. À Capes, DAAD, CNPq, Fapemig e todas as agências de fomento que propiciam nosso olhar para além fronteira e provisionaram os recursos financeiros para o desenvolvimento do presente trabalho.

Enfim, mãos que aqui muito ajudaram, deixo as minhas postas em sinal de muito obrigado!

“Se eu vi mais longe, foi por estar sobre ombros de gigantes.”

Isaac Newton

RESUMO

A poluição das águas, sua escassez e os desafios globais de energia têm levado a comunidade científica a desenvolver alternativas tecnológicas mais sustentáveis e eficientes de tratamento de águas residuárias. Especial atenção tem sido dada aos Contaminantes Emergentes (CEs) que já foram detectados em águas residuárias, superficiais, subterrâneas e até potável. Os efeitos destes CEs ainda não são totalmente esclarecidos, mas estudos apontam seus potenciais riscos toxicológicos. As ETAs e ETEs convencionais são ineficientes na remoção dos CEs, sendo requeridos tratamentos avançados para este propósito. Dentre os tratamentos avançados, as Membranas Fotocatalíticas são uma tecnologia em potencial, compostas pela união de catalisadores a membranas que geram mútuos benefícios. O catalisador mais utilizado nestes dispositivos é o dióxido de titânio (TiO_2) na forma de nanopartículas. No entanto, a dificuldade de sua recuperação em dimensões nanométricas e a necessidade de irradiação UV-C para sua ativação ainda limitam seu uso em larga escala. A imobilização do catalisador nas superfícies de membranas prefigura como alternativa promissora, portanto. A associação permite, também, a redução da incrustação nas membranas, por meio da degradação, por parte do catalisador, dos compostos causadores de incrustação. Dessa maneira, é mantido o fluxo de permeado e o consumo energético reduzido. Sendo assim, o objetivo deste projeto foi desenvolver e avaliar o desempenho de Membranas Fotocatalíticas compostas por membranas recicladas (membrana de osmose inversa pós vida útil convertida em membrana de ultrafiltração), nanopartículas de TiO_2 e óxido de grafeno (GO). Para isto, a metodologia foi alicerçada em cinco etapas. A primeira consistiu na síntese e caracterização da membrana fotocatalítica. A segunda em testes preliminares de remoção/degradação dos corantes negro de eriocromo T e azul de metileno, bem como monitoramento dos fluxos de permeado. A terceira no desenvolvimento do reator fotocatalítico de membrana seguida pela etapa de avaliação da capacidade da membrana na remoção de CEs de águas residuárias municipais pós tratamento secundário. Os parâmetros operacionais foram otimizados. Por fim, foi realizada análise econômica Capex e Opex do processo. O uso do GO, em função de suas excelentes propriedades de transferência eletrônica, teve por finalidade expandir a faixa de resposta à luz do TiO_2, e o emprego de membranas recicladas garantiu maior sustentabilidade e baixo custo ao processo, ampliando seu potencial de escalonamento. A utilização de membranas recicladas como suporte funcionou mais do que como uma estratégia de redução de custos, mas também como uma alternativa para redução de resíduos sólidos. Baixas adesões dos nanocompósitos TiO_2-GO às superfícies das membranas foram verificadas em modificações *self-assembly*, enquanto filtração e modificação com dopamina geraram membranas com camadas bem aderidas e homogêneas. Considerando a estabilidade, permeabilidade e eficiência de rejeição dos corantes, como substratos modelo, as membranas modificadas com o auxílio de dopamina-TiO_2-GO foram as mais promissoras (rejeições de aproximadamente 100%). Os nanomateriais aumentaram a hidrofilicidade da membrana e formaram uma camada hidratada que repele os contaminantes orgânicos e reduz a incrustação. Além da rejeição da membrana, adsorção (contribuição: ~10%) e fotocatálise (contribuição: ~20%) foram mecanismos adicionais para a remoção de poluentes. A membrana fotocatalítica modificada com dopamina-TiO_2-GO demonstrou ótima performance na remoção de seis diferentes compostos ativos farmacêuticos (PhACs), percebendo-se ganhos em termos

de eficiência de remoção (até 95,7%) e mitigação de incrustações para a membrana modificada em comparação com as membranas originais. A atividade fotocatalítica ainda contribuiu para uma degradação simultânea dos PhACs evitando a geração de uma corrente de concentrado com alta carga para posterior descarte. As membranas modificadas com dopamina, TiO_2 e GO, por apresentaram melhores desempenhos nos testes preliminares, foram selecionadas para uso em sistema de tratamento avançado de águas residuárias de Garching após tratamento na estação de tratamento. Mesmo após 10 meses de uso as membranas mantiveram estabilidade. Na operação do sistema com irradiação da membrana, foi avaliado o efeito da posição da lâmpada na fluência luminosa que atinge a membrana, sendo encontrados maiores valores no meio da membrana, fornecendo parâmetros para otimização do processo. A membrana foi avaliada nos seguintes sistemas: UV-C completo (irradiação e filtração), LED completo, filtragem, UV-C sozinho e o sistema LED sozinho. Em geral, os melhores resultados foram obtidos no sistema UV-C completo. Com reduções consideráveis de diclofenaco (92%) e antipirina (87%), as alterações no pH do efluente demonstraram uma tendência melhorada na atenuação da concentração de ECs em pHs mais altos. Para análise de viabilidade técnica do uso da membrana fotocatalítica, foi considerada a implementação de um sistema de tratamento terciário de águas residuais de uma população de aproximadamente 31.000 pessoas. O CapEX calculado foi de US$ 1,23 por metro cúbico e o Opex foi de US$ 3,75 por metro cúbico. Tais valores são superiores aos custos dos processos convencionais e até mesmo de alguns processos avançados, sendo que a maioria dos custos Opex foram associados ao consumo de eletricidade. Se o sistema fosse simplificado usando irradiação natural, como a luz solar, e removendo o sistema de aeração, o novo Opex seria de US$ 0,23 por metro cúbico, comparável a outras técnicas avançadas, como o carvão ativado granular. Vale ressaltar que as membranas fotocatalíticas têm a vantagem de não produzirem lodo e gerar concentrado com menor carga, com consequente menor custo de tratamento de concentrado, além de não gerar um passivo ambiental. Como resultado, todas essas variáveis devem ser consideradas e a tecnologia se mostra promissora para escalabilidade futura.

Palavras-chave: Reatores Fotocatalíticos de Membranas; Membranas Recicladas; Contaminantes Emergentes; tratamentos avançados.

ABSTRACT

Water pollution, scarcity, and global energy challenges have prompted the scientific community to develop more sustainable and efficient wastewater treatment technologies. Emerging Contaminants (ECs) that have already been detected in wastewater, surface water, groundwater, and even drinking water have received special attention. Although the effects of these ECs are not fully understood, studies indicate that they may pose toxicological risks. Conventional WTPs and WWTPs are ineffective at removing ECs, necessitating advanced treatments. Among the advanced treatments, Photocatalytic Membranes are a promising technology that combines catalysts and membranes to generate mutual benefits. Titanium dioxide (TiO_2) nanoparticles are the most commonly used catalyst in these devices. However, the difficulty of recovering it in nanometric dimensions and the requirement for UV-C irradiation for its activation continue to limit its widespread use. As a result, immobilization of the catalyst on membrane surfaces prefigures as a promising alternative. The association also cooperates for the reduction of incrustation on membranes through the degradation of the compounds that cause fouling by the catalyst. Permeate flow is maintained while energy consumption is reduced. Therefore, the objective of this project was to develop and evaluate the performance of Photocatalytic Membranes composed of recycled membranes (post-life reverse osmosis membrane converted into ultrafiltration membrane), TiO_2 nanoparticles and graphene oxide (GO). For this, the methodology was based on five stages. The first consisted in the synthesis and characterization of the photocatalytic membrane. The second in preliminary tests of removal/degradation of eriochrome black T and methylene blue dyes, as well as monitoring of permeate fluxes. The third in the development of the photocatalytic membrane reactor followed by the evaluation of the membrane's ability to remove ECs from municipal wastewater after secondary treatment. Operating parameters have been optimized. Finally, an economic CapEX and OpEX analysis of the process was carried out. The use of GO, due to its excellent electronic transfer properties, was intended to expand the light response range of TiO_2, and the use of recycled membranes ensured greater sustainability and low cost to the process, expanding its potential for scale-up. The use of recycled membranes as a support worked more than a cost reduction strategy, but also as an alternative to reduce solid waste. Low adhesions of TiO_2-GO nanocomposites to membrane surfaces were verified in self-assembly modifications, while filtration and dopamine modification generated membranes with well-adhered and homogeneous layers. Considering the stability, permeability and the rejection efficiency of the dyes, as model substrates, the membranes modified with the aid of dopamine-TiO_2-GO were the most promising (approximately 100% rejections). The nanomaterials increased the hydrophilicity of the membrane and formed a hydrated layer that repels organic contaminants and reduces fouling. In addition to membrane rejection, adsorption (contribution: ~10%) and photocatalysis (contribution: ~20%) were additional mechanisms for pollutant removal. The photocatalytic membrane modified with dopamine-TiO_2-GO demonstrated excellent performance in the removal of six different active pharmaceutical compounds (PhACs), achieving gains in terms of removal efficiency (up to 95.7%) and fouling mitigation for the modified membrane compared to the original membranes. The photocatalytic activity also contributed to a simultaneous degradation of the PhACs, avoiding the generation of a concentrated stream with

a high charge for later disposal. Membranes modified with dopamine, TiO_2 and GO, in reason of their better performances in preliminary tests, were selected for use in an advanced wastewater treatment system in Garching after treatment at the treatment station. Even after 10 months of use, the membranes maintained stability. In the operation of the system with irradiation on the membrane, the effect of the position of the lamp on the luminous fluency that reaches the membrane was evaluated, with higher values being found in the middle of the membrane, providing parameters for optimization of the process. The membrane was evaluated in the following systems: complete UV-C (irradiation and filtration), complete LED, filtration, UV-C alone and the LED system alone. In general, the best results were obtained on the complete UV-C system. With considerable reductions of diclofenac (92%) and antipyrine (87%), changes in effluent pH demonstrated an improved trend in attenuating the concentration of ECs at higher pHs. For the technical feasibility analysis of the use of the photocatalytic membrane, the implementation of a tertiary wastewater treatment system for a population of approximately 31,000 people was considered. The calculated CapEX was US$1.23 per cubic meter and the Opex was US$3.75 per cubic meter. Such values are higher than the costs of conventional processes and even some advanced processes, and most Opex costs were associated with electricity consumption. If the system were simplified using natural irradiation such as sunlight and removing the aeration system, the new Opex would be $0.23 per cubic meter, comparable to other advanced techniques such as granular activated carbon. It is noteworthy that photocatalytic membranes have the advantage of not producing sludge and generating concentrate with a lower load, with consequent lower cost of concentrate treatment, in addition to not generating an environmental liability. As a result, all these variables must be considered and the technology shows promise for future scalability.

Keywords: Photocatalytic Membrane Reactors; Recycled Membranes; Emerging Contaminants; advanced treatments.

LIST OF FIGURES

Figure 1 - Possible routes of Emerging Contaminants in the environment. 28
Figure 2 - PMRs configurations: a) suspended catalyst and membrane inside the reactor; b) suspended catalyst and membrane outside the reactor; c) immobilized catalyst/membrane with support function d) immobilized catalyst/membrane with support and filtration function. 31
Figure 3 - Fouling types. 45
Figure 4 - Possible photocatalytic mechanism in a TiO_2-GO membrane. 47
Figure 5 - Surface coating nanocomposite membrane fabrication (a) self-assembly (b) cross-linker aid. 57
Figure 6 - a) Scheme of the self-assembly mechanism of TiO_2-GO nanocomposites on the surface of polysulfone membranes; adapted from Gao; Hu; Mi, (2014b) with copyright permission. b) Scheme of the layer-by-layer mechanism. 58
Figure 7 - Interactions between the membrane surface and TiO_2-GO nanocomposites. 60
Figure 8 - Benefits and drawbacks of each nanocomposite membrane fabrication technique. 61
Figure 9 - Surface hydrophilicity of the membranes modified with TiO_2-GO. 69
Figure 10 - Schematic design of the experimental apparatus. 87
Figure 11 - Samples of membranes modified with TiO_2-GO. a) self-assembly modification; b) washing after self-assembly modification; c) filtration modification of the suspension, and d) modification using dopamine. 88
Figure 12 - Schematic representation of the RO membranes characteristics before and after recycling process. 88
Figure 13 - SEM micrographs of the recycled membrane (a) and cross-sectional image of the recycled membrane (b) and micrograph of new RO membrane (c). 89
Figure 14 - SEM micrographs of the membrane modified by filtration (a), membrane modified by Dop+TiO_2+GO (b), membrane modified by Dop+TiO_2 (c). Red dots indicate the presence of the element titanium. 91
Figure 15 - Schematic representation of the adhesion mechanisms in the filtration, dop+TiO_2 and dop+TiO_2+GO modification routes. 92
Figure 16 - Fourier infrared spectroscopy of the recycled membrane and recycled modified membrane with dopamine, TiO_2 and GO. 94
Figure 17 - (a) Water flux under different pressures and (b) hydraulic permeability of the obtained membranes. 95

Figure 18 - (a) Rejection efficiency of the eriochrome black dye by the modified membranes, and (b) hydraulic permeability during removal of the eriochrome black T dye. 98
Figure 19 - Methylene blue removal by the Dop+TiO_2+GO membrane under UV irradiation (254 nm) and in the combination of both. 100
F**igure 20** - Concentration of PhACs on the permeate without irradiation, permeate with irradiation, rejection efficiency of the Dop+TiO_2+GO photocatalytic membrane without, and with irradiation at 254 nm. 101
Figure 21 - Schematic representation of the experimental apparatus. 109
Figure 22 - Geometrical calculation strategy for the light fluence. 113
Figure 23 - Zeta potential versus pH for the recycled and modified membrane. 115
Figure 24 - Thermogravimetric analysis of the recycled and modified membranes. 116
Figure 25 - AFM micrographs of the (a) RO membrane after cleaning process, (b) recycled membrane, (c) Modified membrane with TiO_2-GO, (d) modified membrane after use. 118
Figure 26 - (a) SEM micrograph of the modified membrane after use and (b) SEM micrograph with elemental map indicating the presence of titanium element. 119
Figure 27 - Light fluence as a function of the position on the membrane surface. 120
Figure 28 - Parameters removals by different treatment techniques. 122
Figure 29 - TOrCs removals by different treatment techniques. 124
Figure 30 - Principal components analysis of the different techniques and evaluated parameters. 127
Figure 31 - TOrCs removals in different pHs. 128
Figure 32 - Schematic representation of the treatment system. 132
Figure 33 - Costs comparison between photocatalytic membranes obtained by commercial and recycled UF 135
Figure 34 - Percentage impact of each equipment on Capex. 137
Figure 35 – Comparison between the operational costs obtained for photocatalytic membranes and the costs reported by Foureaux et al. (2020) for conventional membrane separation processes. 141

LIST OF TABLES

Table 1 - Photocatalytic membranes reactors with photocatalytic membranes based on TiO_2-GO. 33

Table 2 - Membranes modified with TiO_2-GO nanocomposites and the main methods of preparing these nanomaterials. 50

Table 3 - Usual characterization techniques for modified membranes with TiO_2-GO nanocomposites. 64

Table 4 - Summarization of TiO_2-GO nanocomposite membranes applications. 71

Table 5 - Specifications of the different modification routes. 84

Table 6 - Roughness parameters of the different membranes. 118

Table 7 - TOrCs main characteristics. 122

Table 8 - Summary of cost variables considered for estimation of photocatalytic membrane production. 133

Table 9 – Summary of cost variables considered for estimation of capital expenses (Capex) of the tertiary treatment unit. 136

Table 10. Operational costs for the tertiary treatment of secondary wastewater by photocatalytic membranes. 140

LIST OF ACRONYMS

ABS 254 - Absorbance at 254 nm

AFM – Atomic force microscopy

Al_2O_3 – Aluminum Oxide

ALRS - Adsorption layer reactor synthesis

AO7 - Acid Orange 7

ATR-FTIR - Attenuated total reflectance – Fourier transform infrared spectroscopy

BSA – Bovine serum albumin

CA – Cellulose acetate

CB – Conduction band

CNT – Carbon nanotubes

COD – Chemical Oxygen Demand

CuO – Copper oxide

DI – Distillated

DP – Diphenhydramine

EC50 - Effect concentration

ECs – Emerging contaminants

EDX – Energy Dispersive X-Ray Analysis

EPS - extracellular polymeric substances

EtOH – Ethanol

Fe_3O_4 – Ferric oxide

GO – Graphene oxide

HA – Humic acid

LED - Light-emitting diode

MB – Methylene blue

MC – Methylene chloride

MF - Microfiltration

$MgSO_4$ – Magnesium sulfate

MO – Methyl orange

MWCO - Molecular weight cut-off

Na_2SO_4 – Sodium sulfate

NaCl – Sodium chloride

NaOCl – Sodium hypochlorite

NF – Nanofiltration

PA – Polyamide

PAN – Polyacrylonitrile

PDMS – Polydimethylsiloxane

PEG - Polyethylene glycol

PES - Polyethersulfone

PI – Polyimide

PMRs - Photocatalytic Membrane Reactors

PSF - Polysulfone

PSSA – poly (4-styrenesulfonic acid)

PU - Polyurethane

PVA – polyvinyl alcohol (PVA)

PVC - Polyvinylchloride

PVDF – Polyvinylidene fluoride

RhB – rhodamine B

RO – reverse osmosis

SDS – sodium dodecyl sulfate

SEM – Scanning electron microscopy

SiO_2 – Silicon oxide

SDS - Dodecyl sulfate

SUS – Sistema Único de Saúde - Health Unic System

TAC - Cellulose triacetate

TEM - Transmission electron microscopy

TFC – Thin film composite

TGA - Thermogravimetric analysis

TiO_2 – Titanium dioxide

TN – Total nitrogen

TNS – TiO_2 nanosheets

TOC - Total organic carbon

TUM - Technical University of Munich

UF – Ultrafiltration

UV – Ultraviolet

VB – Valence band

WHO – World health organization

WTP - Water treatment plant

WWTP – Wastewater treatment plant/process

XPS – X-ray photoelectron spectroscopy

XRD - X-ray diffraction

ZnO – Zinc oxide

LIST OF PUBLICATIONS AND CONGRESSES

- OLIVEIRA, C. P. M.; FERNANDES, I. F.; KOCH, K.; DREWES, J. E.; VIANA, M. M.; AMARAL, M. C. S. TiO_2-Graphene oxide nanocomposite membranes: A review. Separation and Purification Technology, v. 280, p. 119836, 2022.

- OLIVEIRA, C. P. M.; MOREIRA, V. R.; LEBRON, Y. A. R.; VASCONCELOS, C. K. B.; KOCH K.; VIANA, M. M.; DREWES, J. E.; AMARAL, M. C. S. Converting recycled membranes into photocatalytic membranes using greener TiO_2-graphene oxide nanomaterials. Chemosphere, v. 306, p. 135591, 2022.

- OLIVEIRA, C. P. M.; SANTOS, C. V.; DE PAULA, E. C.; VIANA, M. M.; AMARAL, M. C. S. Patent filing application: Notificação de invenção NI 16/2022 - Membranas recicladas fotocatalíticas a partir de TiO_2 e Óxido de Grafeno (GO). March, 14th, 2022.

- OLIVEIRA, C. P. M; VIANA, M. M.; AMARAL, M. C. S. Euromembrane. Greener Photocatalytic Membrane Reactor for Refinery Wastewater Polishing. 2021. (Congress).

- OLIVEIRA, C. P. M.; KOCH, K. DREWES, J. E.; VIANA, M. M.; AMARAL, M. C.S. Silubesa 2022. Membranas recicladas fotocatalíticas a partir de TiO_2 e Óxido de Grafeno (GO) para remoção de fármacos. June 29 to July 01, 2022 (Congress).

- OLIVEIRA, C. P. M.; SPERLE, P.; DREWES, J. E. VIANA, M. M.; AMARAL, M. C. S. V Workshop de Tecnologias Limpas e III Jornada de Tecnologias Limpas. Layout otimizado de um reator fotocatalítico de membrana para tratamento de águas residuárias. 28th to 30th September 2022.

Other works

- Awarded business idea in the "E-Hackathon en Agua, Saneamiento e Higiene en Asentamientos Informales de América Latina y el Caribe (2020)", Banco Interamericano de Development and BID Lab, CEWAS and Young Water Solutions. Subject: Recycled membranes for gray water treatment.

- DAAD fellowship (2021/2022) at the Technical University of Munich (Germany) in the Chair of Urban Water Systems Engineering under the supervision of Prof. Dr. Jörg Drewes and Dr. Konrad Koch (sandwich PhD).

SUMÁRIO

CHAPTER 1 - INTRODUCTION 25

1.1 BACKGROUND 26

1.1.1 EMERGING CONTAMINANTS 26
1.1.2 PHOTOCATALYTIC MEMBRANE REACTORS (PMRS): PHOTOCATALYTIC MEMBRANES 30
1.1.3 USE OF GRAPHENE OXIDE AS AN ADDITIVE TO IMPROVE THE CHARACTERISTICS OF PHOTOCATALYTIC MEMBRANES 34
1.1.4 RECYCLED REVERSE OSMOSIS (RO) MEMBRANES 37

1.2 JUSTIFICATION 38

1.3 HYPOTHESES 40

1.4 OBJECTIVES 40

1.4.1 GENERAL OBJECTIVE 40
1.4.2 SPECIFIC OBJECTIVES 40

1.5 DOCUMENT STRUCTURE 41

CHAPTER 2 - TIO_2-GRAPHENE OXIDE NANOCOMPOSITE MEMBRANES: A REVIEW 42

2.1 - INTRODUCTION 43

2.2 - TIO_2-GO NANOCOMPOSITES INCORPORATION IN POLYMERIC MEMBRANES 47

2.3 - GO BENEFITS TO THE TIO_2-GO NANOCOMPOSITES AND THEIR IMPACTS ON MEMBRANE PERFORMANCE 53

2.4 – MAIN POLYMERIC MATERIALS FOR TIO_2-GO NANOCOMPOSITE MEMBRANES 54

2.5 – DESIGN AND FABRICATION OF TIO_2-GO NANOCOMPOSITE MEMBRANES 56

2.5.1 BLENDING 56
2.5.2 SURFACE COATING 56
2.5.3 FILTRATION 59

2.6 - TIO_2-GO MEMBRANES CHARACTERIZATION TECHNIQUES 62

2.7 – IMPACTS OF THE TIO_2-GO LOADING IN THE MEMBRANE PERFORMANCE 65

2.8 – FOULING CONTROL IN TIO_2-GO NANOCOMPOSITE MEMBRANES 67

2.8.1 DEGRADATION OF FOULING COMPOUNDS BY PHOTOCATALYSIS 67
2.8.2 ANTIBACTERIAL PROPERTIES 68
2.8.3 INCREASED HYDROPHILICITY OF MEMBRANES 69

2.9 – TIO_2-GO NANOCOMPOSITE MEMBRANES APPLICATIONS 70

2.10 - CONCLUSIONS AND PERSPECTIVES 77

CHAPTER 3 - CONVERTING RECYCLED MEMBRANES INTO PHOTOCATALYTIC MEMBRANES USING GREENER TIO_2-GRAPHENE OXIDE NANOMATERIALS 79

3.1 INTRODUCTION 80

3.2 MATERIALS AND METHODS 82

3.2.1 REAGENTS 82
3.2.2 FABRICATION OF THE PHOTOCATALYTIC MEMBRANES 83
3.2.3 PHOTOCATALYTIC MEMBRANES CHARACTERIZATIONS 85
3.2.4 IMPACT OF THE MODIFICATIONS IN THE MEMBRANE PERFORMANCES 85

3.2.5 PHARMACEUTICAL ACTIVE COMPOUNDS REMOVAL 86
3.3 RESULTS AND DISCUSSION 87
3.3.1 CHARACTERIZATION OF THE PHOTOCATALYTIC MEMBRANES 87
3.3.2 REJECTION OF PHACS 101
3.4 CONCLUSIONS 103
CHAPTER 4 - USE OF PHOTOCATALYTIC RECYCLED TIO_2-GO MEMBRANES FOR THE REMOVAL OF TORCS FROM WASTEWATERS 104
4.1 INTRODUCTION 105
4.2 MATERIALS AND METHODS 108
4.2.1 MATERIALS 108
4.2.2 MODIFIED MEMBRANE PREPARATION 108
4.2.3 PHOTOCATALYTIC REACTOR DESIGN 109
4.2.4 PHOTOCATALYTIC AND FILTRATION TESTS 110
4.2.5 ANALYTICAL METHODS 111
4.2.6 CALCULATION 111
4.3 RESULTS AND DISCUSSION 113
4.3.1 MEMBRANE CHARACTERIZATION 113
4.3.2 THE IMPACT OF LIGHT POSITION ON THE FLUENCE RADIATION INCIDENT ON MEMBRANE SURFACE 119
4.3.3 MEMBRANE PERFORMANCE ON THE WASTEWATER TREATMENT 121
4.3.4 REMOVAL OF EMERGING CONTAMINANTS 122
4.5 CONCLUSIONS 128
CHAPTER 5 - PHOTOCATALYTIC RECYCLED MEMBRANES FOR MUNICIPAL WASTEWATER TREATMENT: ECONOMICAL EVALUATION 129
5.1 INTRODUCTION 130
5.2 MATERIAL AND METHODS 131
5.2.1 PHOTOCATALYTIC MEMBRANE PREPARATION 131
5.2.2 WASTEWATER TREATMENT PLANT 131
5.2.3 DATA COLLECTION, CAPEX AND OPEX CALCULATION 132
5.3 RESULTS AND DISCUSSION 133
5.3.1 PHOTOCATALYTIC MEMBRANE FABRICATION COSTS 133
5.3.2 CAPEX 136
5.3.3 OPEX 138
5.4 CONCLUSIONS 142
CHAPTER 6 - FINAL CONSIDERATIONS AND SUGGESTIONS FOR FUTURE WORKS 143
REFERENCES 147
APPENDIX 178

CHAPTER 1

Introduction

1.1 BACKGROUND

1.1.1 Emerging contaminants

The World Health Organization (WHO) estimates that more than a billion people do not have access to clean water. More than 4,000 children die every day due to water pollution worldwide (DHARUPANEEDI *et al.*, 2019). According to a United Nations report, a quarter of the world's population will suffer from poor water conditions by the middle of this century (WANG *et al.*, 2017). There is still a growing demand for water resources due to the increase in population and high consumption in the industrial and agricultural sectors. Furthermore, of all the water available globally, only 3% is fresh, and a good portion of this percentage has been polluted due to human activities (MURGOLO *et al.*, 2019).

In recent years, among the sources of water pollution, special attention has been given to Emerging Contaminants (ECs) such as drugs, hormones, personal hygiene products, fertilizers, heavy metals, microplastics, among others (ENICK; MOORE, 2007; KLAVARIOTI; MANTZAVINOS; KASSINOS, 2009). The ECs can be released into the environment through feces, urine, agricultural runoff, industrial and domestic effluent discharges and are persistent in the conventional wastewater treatment processes (WWTP), which can contaminate drinking water supply sources (VERGILI, 2013). Studies have already detected ECs in raw water at concentrations of ng L^{-1} to μg L^{-1}, which were present even after the drinking water treatment process (WANG *et al.*, 2019; ZHANG *et al.*, 2019).

Among the different definitions given to Emerging Contaminants, a very comprehensive one is suggested by the United States Geological Survey Institute (2017) as being:

> Any chemical of synthetic or natural origin or any microorganism that is not commonly monitored in the environment but has the potential to cause adverse ecological and human health effects.

Thus, in general, they usually have the characteristics of being anthropogenic chemical products, predominantly unregulated, persistent in the environment, present in trace concentrations, and capable of altering the physiology of target receptors (BHANDARI *et al.*, 2009).

The adverse effects of ECs and their by-products on the aquatic environment are not yet fully understood (STADLMAIR *et al.*, 2018). However, it has been reported that after long periods

of exposure to these, humans, animals, and plants may show abnormal chronic physiological changes, such as infertility and cancer (LIN, 2017).

A class of emerging contaminants, in particular, that of endocrine disruptors, composed of polychlorinated biphenyls, phthalates, bisphenol A, polybrominated diphenyl ethers, Ethinyl estradiol, among others, affect the physiological hormonal system of animals and humans (DE OLIVEIRA *et al.*, 2020b; FRYE *et al.*, 2012). Studies have detected sexual disorders such as polycystic ovaries, reduced male fertility, and cancers of the prostate, testis, and breasts, depending on the exposure dose and period of contact with such compounds (DE OLIVEIRA *et al.*, 2020b). The feminization of male fish has also been detected when these animals have been exposed to estrogen for a prolonged period, even in low concentrations (JUKOSKY; WATZIN; LEITER, 2008).

It is also pointed out the relationship of some ECs with the development of antibiotic-resistant strains and bacterial genes (ORVOS *et al.*, 2002). Especially in the context of biological treatments, common to municipal WWTP, there may be the formation of resistant species that can pose risks to human health and cause changes in aquatic systems. For this reason, due to the eco-toxic potential, there is a great demand for efficient, low-cost, and environmentally friendly strategies for removing these contaminants.

ECs enter ecosystems through different sources divided into five broad categories: domestic wastewater, industrial effluents, hospital effluents, agricultural activities, and livestock activities (Fig. 1) (ROUT *et al.*, 2021). Among the ECs, drugs are mainly inserted into the environment through human and animal excreta. These compounds, after being consumed, are partially metabolized and eliminated by feces and urine reaching wastewater treatment plants. A similar route occurs with personal hygiene products, such as shampoos, sunscreens, toothpaste, among others, discharged at treatment stations through washing activities. Effluents from industries producing various chemical products contribute to the presence of a wide range of ECs in the environment, as well as hospital effluents that are composed of a conjugate of drugs. The effluents from agriculture and livestock are usually found in the form of pesticides and hormones, respectively, used to increase productivity (SANTOS *et al.*, 2020).

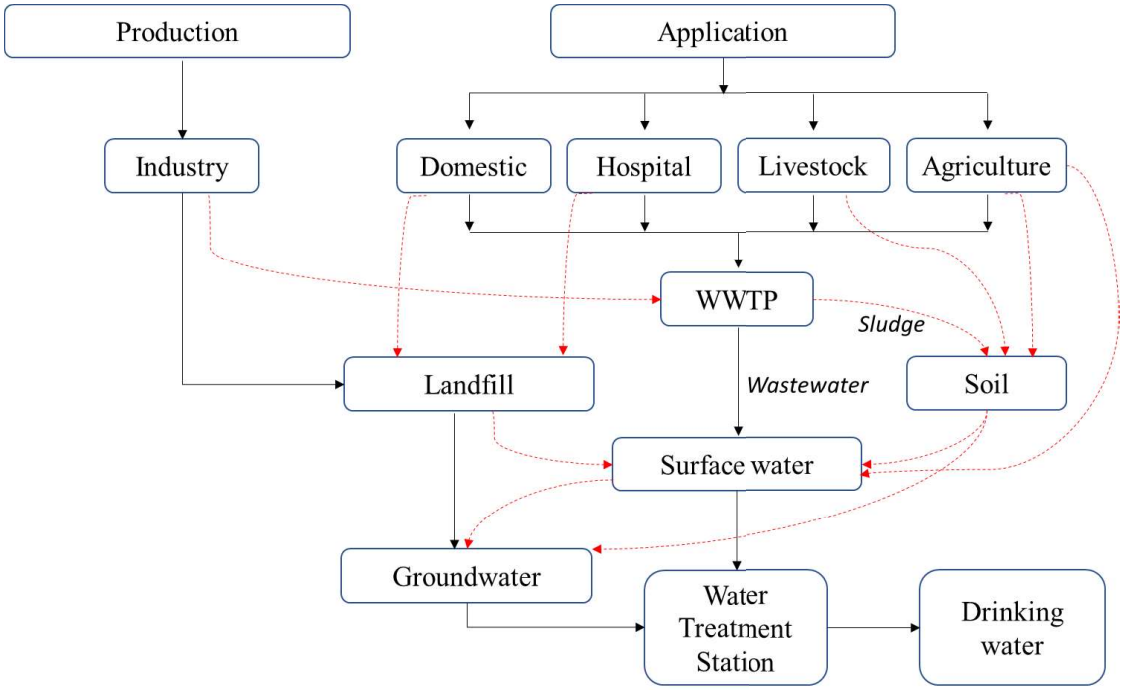

Figure 1 - Possible routes of Emerging Contaminants in the environment.

Source: adapted from ROUT *et al.* (2021).

The contamination of water bodies by ECs is associated with the inefficiency of removing these components by conventional methods of treatment and leaks in the wastewater collection networks (SANTOS, 2014). Moreover, in Brazil, as in other developing countries, there is still the discharge of untreated sewage in the water bodies. Brazil's Ministry of Regional Development Data show that only 49.1% of the generated sewage in the country is treated (BRASIL, 2019).

According to Kasprzyk-Hordern *et al.* (2009), the discharge of effluents from wastewater treatment plants is considered the primary cause of the occurrence of ECs in surface waters. In the case of drinking water, the occurrence of ECs is dependent on the quality of the sources of supply, seasonality, and socioeconomic aspects of the collection region. Although studies indicate safe levels, the concern regarding the products of transformation of these components and its long-term effects arouse the scientific community's apprehension (LUO *et al.*, 2014).

Recent work conducted by Santos and collaborators (2020) confirmed concentrations that confer high toxicity, at least to one trophic level, of 60% of 28 drugs evaluated in surface and treated waters in Brazil, and attested the inefficient removal of them by drinking water treatment

stations. The study also detected doses of atorvastatin in the treated water that pose potential risks to public health.

As mentioned, most conventional drinking water treatment plants and wastewater treatment plants were not designed to remove the ECs, proving to be inefficient in this regard. It occurs because ECs have stable structures, low volatility, besides being small, polar, highly soluble in water, and highly mobile, which hinder their removal (VERGILI, 2013). Their persistence and resistance to degradation characterize them, therefore, as recalcitrant pollutants.

Wastewater treatment plants typically employ primary, secondary, and, eventually, tertiary treatment. Tiwari and collaborators (2017) observed different ECs removal percentages at each treatment stage, and for the primary, removal efficiency varies from 20-50%. In comparison, rates of 30-70% are achieved by the secondary. In addition, more than 90% is reached by the tertiary. In contrast, cases of negative removal of ECs are reported in wastewater treatment plants, in which the concentrations of specific contaminants after treatment are higher than before. This fact can be explained by enzymatic biological treatment mechanisms capable of reversing smaller and conjugated molecules to their parent compounds (RHOUT *et al.*, 2021).

This whole context of inefficiency in removing ECs by conventional treatments is also justified by the recent development of sensitive analytical techniques for detecting low concentrations (ng L^{-1} or μ L^{-1}) of these compounds in environmental samples. Therefore, investigations into the occurrence and detection of these contaminants in the environment have been taking place, more precisely, ostensibly in the last two decades (BAILLY *et al.*, 2013).

The severity of contamination of water bodies by ECs can be even more severe in developing countries, such as Brazil, where less than half of the generated wastewater is treated (BRASIL, 2019), and the use of drugs without a medical prescription is a frequent practice, owing to insufficient health services. Thus, more advanced treatment techniques are required, such as adsorption with activated carbon, ozonation, advanced oxidative processes, and membrane separation processes, to remove these ECs. In this field, a potential technology is the Photocatalytic Membrane Reactors (PMRs).

1.1.2 Photocatalytic Membrane Reactors (PMRs): Photocatalytic Membranes

PMRs are devices that combine the separation properties of membranes with the power of chemical transformations of catalysts, consisting of a green technology that increases the potential of each one of the techniques, generating a synergistic effect that reduces environmental and economic impacts (MOLINARI; LAVORATO; ARGURIO, 2017). The membranes allow continuous operations to recover the catalyst in systems where the reaction and separation of the products occur simultaneously, favoring the displacement of the chemical balance towards the products (degraded pollutants). On the other hand, catalysts degrading the compounds in the feed allow the mitigation of fouling and maintenance of the flux in the membranes, reducing energy costs and, consequently, operating expenses (LEONG *et al.*, 2014; MOZIA, 2010).

PMRs can be built in two different configurations. One is with the catalyst as a suspended powder in the reaction mixture followed by a membrane unit (DE OLIVEIRA *et al.*, 2020a). The other concerns the catalyst immobilized on the membrane surface (DAROWNA *et al.*, 2017). The configuration with the suspended catalyst has the main advantage of obtaining large yields of pollutants degradation due to the high specific surface area of the particles. The catalyst load can also be adjusted in this configuration. However, it presents some drawbacks, such as the difficulty in separating and recovering the catalyst, particle agglomeration with a consequent reduction in reaction yield, and membrane fouling due to the deposition of the catalyst.

On the other hand, in the immobilized configuration, these problems are avoided. The membrane acts as a selective barrier to contaminants, keeping them in the reaction medium and supporting the catalyst. The last configuration is in accordance with the principles of process intensification, as a new catalyst recovery step is not necessary. However, the light irradiation above the membrane can damage its structure and reduce its useful life (ROMAY *et al.*, 2020).

Variations of the above mentioned PMR configurations are reported in the literature, as shown in Figure 2. Regarding the suspended configuration, the membrane can be submerged in the reactor (Fig. 2-a) or disposed of outside (Fig. 2-b). The membrane is subject to more significant pressure drops when located outside the reactor, and oscillations in the concentration of the

catalyst in the reaction medium may occur. In the immobilized configuration, the membrane can act only as a catalyst support (Fig. 2-c) or have a separation function (Fig. 2-d).

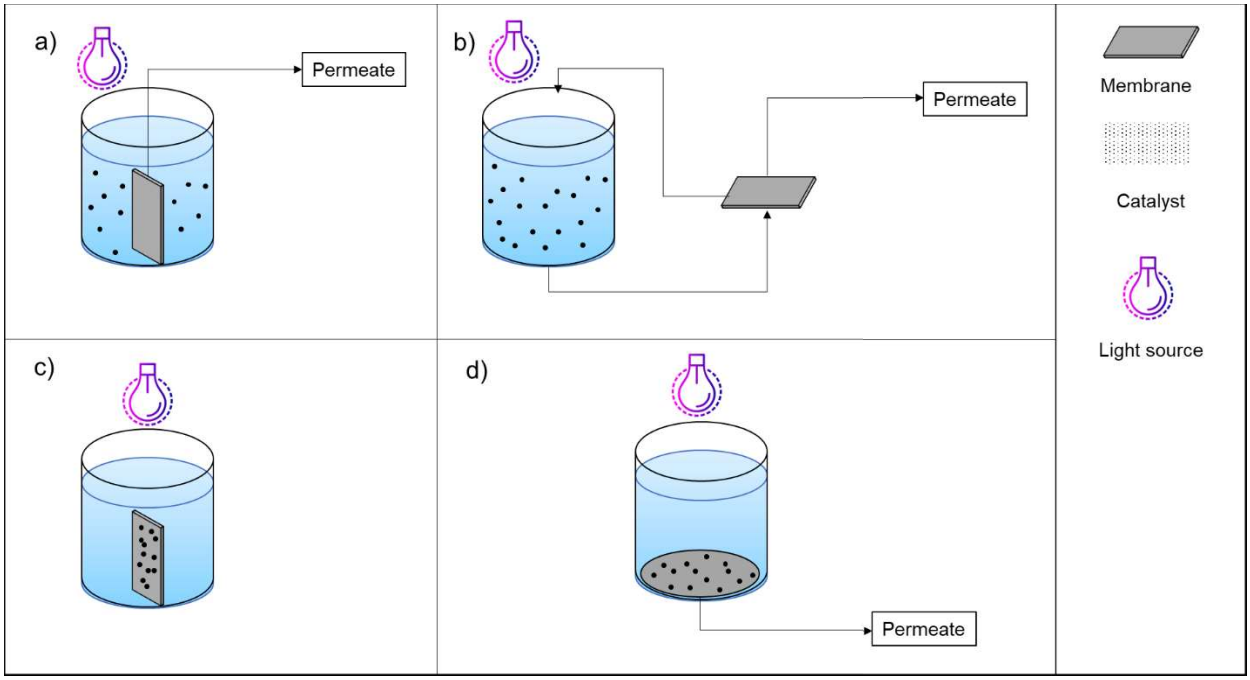

Figure 2 - PMRs configurations: a) suspended catalyst and membrane inside the reactor; b) suspended catalyst and membrane outside the reactor; c) immobilized catalyst/membrane with support function d) immobilized catalyst/membrane with support and filtration function.

Source: Adapted from Romay *et al.* (2020)

The most widely used catalyst in PMRs studies is titanium dioxide (TiO_2) in nanoparticulate form due to its high specific surface area. However, in these dimensions and being free, its recovery is complex, and the expansion of its use on a large scale is limited, thus its immobilization on the membrane surface is a promising alternative (FARALDOS and BAHAMONDE, 2017). The catalyst action mechanism occurs mainly through the formation of highly oxidizing hydroxyl radicals. When irradiated by radiation with a wavelength below 387 nm, the oxide has its electrons migrated from the valence band (VB) to the conduction band (CB), leaving positive vacancies in the valence band. Electrons in CB and positive gaps in VB can react with oxygen and water adsorbed on the catalyst surface, respectively, giving rise to radicals that trigger a series of oxide-reduction reactions that can promote the mineralization of pollutants in the environment (NGOs; MOHAMMAD; NG, 2019).

Many studies focus on the development of PMRs for degradation of synthetic matrices and focus mainly on the efficiency of the degradation/removal process (ATHANESEKOU *et al.*

2015; FISCHER *et al.*, 2015; RAMASUNDARAM *et al.*, 2013). Nevertheless, there is a great need for the use of such devices in complex, real matrices that consider, in addition to the intervening operational factors, the economic, environmental, and technical factors of a possible scaling and implementation of the process on a large scale (CAI *et al.*, 2018). Assessments of the stability of the developed systems are also scarce. The use of such technology for the treatment of wastewater after a secondary process is a promising alternative for removing ECs, thus reducing the impacts on water bodies caused by the discharge of effluents.

The removal of ECs using PMRs in the treatment of water and wastewater, in addition to mitigating the impact on water bodies, will provide quality water in the supply sources, guaranteeing safe water for the population. The technology can also be used to municipal wastewater reclamation. The reuse alternative has been recognized as a mean of maximizing water sources and reducing the freshwater consumption, consisting of a solution to the scarcity problem (XU; BELLONA; DREWES, 2010).

Even with the described advantages, one of the limitations in using TiO_2 is related to the need for ultraviolet radiation for its activation. Expanding this range of activation for sunlight is a highly explored study area, whether through doping with metals, semiconductors, or sensitizers. An exponent material for expanding the range of response to light by TiO_2 is graphene oxide (GO) due to its excellent electron transfer properties (MIN *et al.*, 2012; NAIR and JAGADEESHBABU, 2017).

In addition to having a high capacity for electronic transfer, GO also has a high surface area and high adsorption capacity, making it an important candidate for hybrid use in TiO_2-GO nanocomposites in PMRs. The association can provide the catalyst activation under solar irradiation and greater contact with contaminants, increasing the pollutants residence time and the percentage of degradation (DADVAR *et al.*, 2017; YOO *et al.*, 2011; ZHAO *et al.*, 2012).

Table 1 shows a compilation of studies that developed photocatalytic reactors using TiO_2-GO as membranes modifying materials in the configuration of catalyst fixed to the membrane by different techniques.

Table 1 - Photocatalytic membranes reactors with photocatalytic membranes based on TiO_2-GO.

Membrane Material	Modification Material	Modification Method	Main results	References
Polyvinylidene fluoride (PVDF)	TiO_2-GO	Phase inversion	-Photodegradation of 50-70% bovine serum albumin (BSA) -Water flow twice as large as the pristine membrane -Self-cleaning property under UV irradiation	XU *et al.* (2016a)
Aromatic polyamide (PA)	TiO_2-GO	Interfacial polymerization	- 98.8% Na_2SO_4 rejection -Water flow twice as large as the pristine membrane	WANG *et al.* (2017a)
Polyvinylidene fluoride (PVDF)	TiO_2-GO	Phase inversion precipitation	-Modified membrane flow four times greater than pristine	WU *et al.* (2019)
Polysulfone (PSF)	TiO_2-GO	Layer by layer	-Increased kinetics of methylene blue degradation (60-80% faster) compared to the pristine membrane under UV irradiation and 3-4 times faster under solar irradiation	GAO; HU; MI (2014a)
Cellulose	TiO_2-GO	Vacuum filtration	-92% degradation of methylene blue after 110 minutes of UV irradiation -Recovery of 96% initial flow after 100 minutes of UV irradiation	ZHU *et al.* (2017)
Polyacrylonitrile (PAN)	TiO_2-GO	Layer by layer	-58.8% removal of methylene blue after 250 minutes of UV irradiation -Membrane irradiation 40 minutes before filtration increased the water flow from 1.67 to 1.87 L m^{-2} h^{-1}	YAN *et al.*, (2019)
Aromatic polyamide (PA)	TiO_2-GO	Layer by layer	-Resistance to chlorine through adsorption in GO -Increased membrane hydrophilicity	SHAO *et al.*, (2017a)

Although the theme has already been explored by several studies, as shown in table 1, there is still information lack about the functioning of PMRs based on TiO_2-GO under prolonged

periods of operation. Analysis of the stability of the generated membranes and more adequate cleaning protocols also constitute knowledge gaps in the area. Evaluating these devices in the treatment of complex matrices, such as sewage, in removing emerging contaminants also needs further consideration.

1.1.3 Use of graphene oxide as an additive to improve the characteristics of photocatalytic membranes

Graphene is a hydrophobic sheet with a single atomic layer of graphite discovered by Novoselov and Geim (NOVOSELOV *et al.*, 2004). Graphene oxide (GO) is a carbon nanomaterial of a hydrophilic nature obtained by the oxidation of graphene. In the oxidation process, epoxide and phenol hydroxyl groups are generated in the basal plane and carboxylic at the edges of the material (GAO *et al.*, 2012; LIU *et al.*, 2010), giving it important characteristics (GAO *et al.*, 2013b). In recent years, GO has attracted significant attention from the scientific community for the preparation of nanocomposite membranes for the treatment of water and wastewater, including desalination, removal of toxic ions and emerging pollutants (URSINO *et al.*, 2018), because this nanomaterial can improve the mechanical and thermal properties of polymeric membranes.

A large portion of the polymeric membranes is hydrophobic. This characteristic is one of the main reasons for its propensity to fouling since organic incrustations are attracted to surfaces and pores of these membranes. Deposition prevention and treatment methods, such as cleaning and backwashing, only remove reversible fouling, but irreversible leads to a permanent decline in flux. Therefore, modifications in membranes preparation techniques are required to improve their performance (JHAVERI; MURTHY, 2016). Among the forms of fouling, the biological is one of the most complexes. It is a consequence of the irreversible adhesion of bacterial cells to the membrane surface and, once it is formed, its removal is challenging. Graphene oxide is as an alternative to the solution of such problems, as it has the potential to promote the lysis of bacterial cells and offer anti-adhesive properties, reducing the incrustation deposition, especially the biological one (SALEEM; ZAIDI, 2020). The antibacterial activity of the oxide is due to the sharp edges of its sheets that can promote the rupture of the membrane bacterial cells and the leakage of their genetic material (AKHAVAN; GHADERI, 2010; LIU *et al.*, 2011).

Several authors have studied the association of GO with TiO_2 for modifying the membrane surface (as reported in Table 1). The association is justified by the limitations of TiO_2 alone in the total photodegradation of pollutants due to its fast rate of electron-hole pair recombination (CHEN; MAO, 2007) and the need for UV irradiation for its activation. Weak interactions are also reported between the catalyst and the polymeric membranes, generating unstable membranes (GAO *et al.*, 2013b). GO can act as a cross-linker between TiO_2 particles and between them and the membrane (ZHU *et al.*, 2011). The strong contact between GO sheets and TiO_2 can increase charge transfer and increase photocatalytic activity. Gao and collaborators (2013) proposed that the electrons in the TiO_2 conduction band are transferred to the GO, decreasing the recombination rate, increasing the photocatalytic activity. The same authors pointed out the band-gap reduction of the materials through their integration, providing activation by sunlight.

When using nanoparticles to modify membranes, there is a great tendency for their agglomeration due to the high surface/volume ratio they have in these dimensions. Agglomeration is harmful because it reduces the efficiency and performance of the membrane through the blocking of pores, resulting in a drop in flux, even under high pressures (URSINO *et al.*, 2018). The use of GO associated with TiO_2 reduces the aggregation of nanoparticles and promotes a more uniform dispersion. TiO_2, because it is a rigid structure between the GO sheets, can also prevent the compaction of the latter, increasing the percolation of the fluid (XU *et al.*, 2013a).

In addition to the reported advantages of mitigating fouling in membranes and improving the photocatalytic activity of TiO_2 by association with graphene oxide, there is also an increase in the permeability of membranes by adding graphene oxide in its composition to specific concentrations (SALEEM; ZAIDI, 2020). With the proviso that high concentrations of GO decrease the permeability but increase the resistance to fouling. These phenomena occur because water can flow through the oxide nanochannels, and their hydrophilic functional groups, such as hydroxyl and carboxyl, facilitate the adsorption of water molecules. According to Wenzel's model theory (ZHAO *et al.*, 2019; ZHAO; GAO; VAN DER BRUGGEN, 2019), for membranes covered with hydrophilic materials, the hydrophilicity of the membrane surface will increase with the increase of the membrane surface roughness (ZHU *et al.*, 2020). In such a way, membranes with high permeate flux and operational stability can be obtained.

Gao and collaborators (2014) studied the effects of modifying polysulfone membranes with TiO_2-GO. Removal of 70% of the methylene blue dye was observed by photodegradation under solar irradiation after 5 hours of the experiment. The removal percentage was practically the same obtained at a similar time under UV irradiation. In addition, the authors verified the stability of the water flux, in a steady-state, around twice higher for the modified membrane when irradiated by sunlight compared with the unmodified one also irradiated, and attributed the result to the increased hydrophilicity of the membrane promoted by the modification.

Gao and collaborators (2013b) studied commercial cellulose acetate membranes modified with TiO_2-GO and obtained total degradations of rhodamine B and acid orange 7 (AO7) after 20 and 30 minutes, respectively, under UV irradiation, endorsing the relevance of the association of the materials in the degradation of foulants, thus ensuring the maintenance of the flux for more extended periods of operation compared to membranes without modification. The permeate flux in the removal/degradation of humic acid molecules was also evaluated. The flux in the steady state with the modified membranes was around nine times greater than the membranes without modification. The authors attributed this better performance to the degradation of humic acid by TiO_2-GO. A dense layer of humic acid was formed on the membrane surface without UV irradiation, whereas almost no deposition of this same compound was identified under irradiation.

Dadvar et al. (2017) compared the nanofiltration membranes without modification and hybrids with TiO_2-GO and found pollutants (methyl orange) removal five times faster by the hybrid membranes than those without modification. In addition, the energy consumption of hybrids was half that of pristine.

Safarpour; Vatanpour and Khataee, (2016) point out that high rejection of dyes by membranes with TiO_2 and GO may be associated with the repulsive effect of the dye molecules and the charged surface of the membranes. Other authors attribute high removals of the eryochrome black dye by GO-modified membranes due to the adsorption of the dye by π-π bonds with the membrane (CAO et al., 2020).

The search for membranes modifications to improve their performances is a reality. However, the studies carried out in the literature occurs by synthesizing new membranes or modifying the surface of new commercials. When thinking about the sustainability of processes, there is still a gap in investigating changes in membranes at the end of their lifespan.

1.1.4 Recycled reverse osmosis (RO) membranes

Reverse Osmosis technology is used to remove contaminants from water at the ionic level. It is a semipermeable membrane, a selective barrier, where under the application of an external force, the passage of water is allowed, and the ions are rejected (SEMIAT, 2015). Most of the used RO membranes are made of thin-film composite (TFC) in polyamide, which have three layers, the first being a thin and dense layer of aromatic polyamide that is the selective part, another a microporous support of polysulfone, and, finally, a thicker polyester base (ANTONY *et al.*, 2016).

In 2016, the number of reverse osmosis (RO) desalination facilities in the world were over 13,000 units (PAULA, 2017), and this is the most widely used desalination technology due to its lower energy costs when compared to evaporation/distillation using thermal processes (SHENVI, ISLOOR, ISMAIL, 2015). Large desalination units employ tens of thousands of membrane modules. In general, the RO units' lifespan is 5 to 7 years (PAULA, 2017), a factor that highlights the large number of modules that are periodically replaced and discarded. Estimates are that more than 14,000 tons of RO residues are generated per year (DE PAULA; AMARAL, 2018). The residues from the membrane modules are considered inert solid waste and, in most cases, disposed of in landfills.

Given this problem, alternatives for reusing or recycling the used modules are prefigured as of great importance. Possible direct use in systems that require lower yields, or oxidative conversion via chemical attack with the removal of the dense aromatic polyamide layer for the production of porous membranes for application in less demanding processes, such as microfiltration (MF) and ultrafiltration (UF), are reported. For conversion, several oxidizing agents can be used: potassium permanganate, sodium hypochlorite, sodium hydroxide, among others. (ANTONY *et al.*, 2016).

The use of recycled RO membranes as a substitute for UF or MF, at low cost, represents an excellent benefit for wastewater treatment operations, whether industrial or domestic, as well as is a possibility to humanitarian water treatment projects or even can be used in the pre-treatment of desalination processes (GARCÍA-PACHECO *et al.*, 2015; LAWLER, 2013). A study conducted by De Paula and Amaral (2018) found that recycled UF membranes have a cost of 1% compared to acquiring new ones.

Paula (2017), studying the use of recycled RO membranes for the treatment of surface water from three rivers in Minas Gerais (Brazil), obtained excellent results in terms of permeate flux, which remained with all monitored parameters (pH, electrical conductivity, apparent color, and turbidity) practically constant over 8 hours of permeation and low tendency to membrane fouling. It also found that 100% of the *Escherichia coli* bacteria present in surface water samples were removed after treatment with recycled membranes, indicating a potential method for producing drinking water. The membranes were also used in wastewater treatment after the secondary process achieving 92% organic matter removal, 99% turbidity removal, and 98% color removal, thus presenting the potential to generate reuse water for fewer noble purposes.

The membrane market has shown high growth, whether for industrial use or in water and wastewater treatments. The trend should continue since the global water demand is growing and environmental regulations increasingly demanding (SUBRAMANI and JACANGELO, 2015). In this sense, modifications in membranes are extensively studied, especially those that use nanoparticles (NASROLLAHI *et al.*, 2021). However, new membranes are used for this purpose. Recycled membranes are therefore a promising alternative to support photocatalytic membranes, as they reduce pollution through reverse logistics, replacing new materials by recycled materials (HENRIQUES and CATARINO, 2015; KURDVE *et al.*, 2015).

1.2 JUSTIFICATION

Given the panorama exposed in the introduction, the present work aims to contribute to the advancement of scientific knowledge regarding advanced domestic wastewater treatment processes. Based on the expected results, it aims to propose a technological alternative that adds economic and environmental benefits associated with reduced operation times, robust maintenance and high process efficiency. The technology consists of developing photocatalytic membranes inserted in the class of photocatalytic membrane reactors, which can remove Emerging Contaminants (ECs). Such compounds are pollutants of aquatic environments that attract special attention due to their potential toxic effects on humans, animals, and plants.

The motivation found is based on the ever-increasing water demand associated with the decrease in water supply, and the fact that ECs are complex and challenging to treat structures, in which conventional water and wastewater treatment processes are ineffective in their removal. Therefore, to study and develop advanced technologies for their treatment is

necessary. In this regard, photocatalytic membrane reactors are a promising alternative that adds mutually beneficial effects to membranes and catalysts. Thus, they can solve the problems resulting from fouling and flux reduction in the membranes. In addition to the separation of contaminants, they promote their degradation in a single operational step through photocatalysis promoted by the catalyst. On the other hand, the membrane allows the confinement and retention of catalysts in nanometric dimensions and controls the residence time of the compounds in the photodegradation. In this way, the technology is in line with the principles of process intensification.

Most of the studies reported in the literature use PMRs in the form of suspended catalysts. This has an operational problem: the tendency to scale on the membrane surface due to the catalyst's deposition. Moreover, the vast majority of them use UV radiation to activate the catalyst, which represents a considerable energy expenditure in the treatment and hinders its expansion. Another point of attention is that a large part of the works uses commercial catalysts. One of the novelties of the present study is that TiO_2 synthesized by a greener route by our research group will be used, providing greater sustainability to the process.

The combination of GO and TiO_2 proposed in the present work is a promising alternative that can allow the use of the system under solar irradiation, reduce costs, and facilitate the expansion of implementation. In addition, studies that include real effluents in their evaluations are pretty rare, being synthetic effluents or isolated molecules generally used for degradation. Moreover, are also rare studies that evaluate the stability of membranes in PMRs over the operation time, and those that do report loss of membrane integrity after a certain period. To overcome these problems and fill these gaps, the present study will test the surface modifying technique with dopamine aid in order to guarantee greater stability and strong fixation of the materials on the membrane surface. Furthermore, the matrix to be treated will be domestic wastewater after secondary treatment.

Using recycled membranes in the technology (reverse osmosis membranes (RO) post-lifespan converted into ultrafiltration (UF) membranes) also increases the sustainability of the process and reduces the costs for its development and implementation, facilitating the expansion of scale. More than that, it reduces the amount of inert solid waste discarded annually from these materials. When treating secondary effluent, the technology can generate water with quality of reuse for less noble purposes in countries where the practice is allowed, increasing the water

availability of the regions. The fact that a low-cost reactor can be generated makes it possible to use it in decentralized treatment in informal communities or with limited purchasing power for safe water, especially in regions of socioeconomic vulnerability in Brazil. The use of such membranes in PMRs is unprecedented and is in line with the circular economy.

1.3 HYPOTHESES

Based on the premise that it is possible to synthesize photocatalytic membranes from TiO_2, GO, and recycled ultrafiltration membranes, the following hypotheses were formulated for the present study:

H1 – Given the strong enough interactions between the materials involved in obtaining the photocatalytic membrane (TiO_2, GO, and polysulfone/polyamide), a stable membrane that remains intact to the studied operating conditions can be produced.

H2 - The photocatalytic membrane can remove Emerging Contaminants from wastewater after secondary treatment.

H3 - Fouling is mitigated in the photocatalytic membrane compared to the pristine specimen.

1.4 OBJECTIVES

1.4.1 General Objective

The objective of the present study is to develop an integrated system of membranes with catalysts called Photocatalytic Membrane Reactor (PMR), obtained by a photocatalytic membrane based on titanium dioxide, graphene oxide, and recycled membrane, and evaluate the PMR performance in the advanced treatment of wastewater, to remove emerging contaminants (ECs).

1.4.2 Specific Objectives

- Obtain a photocatalytic membrane from titanium dioxide, graphene oxide, and recycled membrane (reverse osmosis membrane (RO) post-lifespan converted into ultrafiltration (UF) membrane).

- Evaluate the effectiveness of the modified photocatalytic membrane from titanium dioxide and graphene oxide concerning its potential for the degradation of model organic molecules (simulating pollutants).
- Evaluate the effectiveness of the synthesized photocatalytic membrane in wastewater treatment after the secondary treatment to remove ECs.
- Determine the best-operating conditions for the PMR regarding the removal of ECs.
- Evaluate the membrane stability over an extended operation time (months).
- Carry out an economic evaluation (CAPEX and OPEX) of the studied process.

1.5 DOCUMENT STRUCTURE

The document is structured in six chapters. The first one is the introduction about the project topic, the justification, hypothesis, and objectives. The second chapter concerns a review article about membranes modified with TiO_2-GO nanocomposites and can be read independently. The third chapter is another paper regarding the obtained photocatalytic membranes, their characterization and preliminary applications, the fourth presents another paper of the use of the membranes for the removals of trace organic chemicals of domestic wastewater. The fifth presents an economical evaluation of the photocatalytic membrane treatment system. Finally, the last chapter depicts the considerations obtained by the achieved results and the suggestions for future works. Each chapter can be read independently.

CHAPTER 2

TiO_2-Graphene Oxide nanocomposite membranes: a review

2.1 - INTRODUCTION

The ever-increasing demand for water and the scarcity of water sources are driving the development of robust water and wastewater treatment technologies (DHARUPANEEDI *et al.*, 2019). Membrane separation processes are among the key technologies because of their advantages: high efficiency, modularity, no need for phase changes, mild temperatures operation, and high selectivity (BET-MOUSHOUL *et al.*, 2016; NASROLLAHI *et al.*, 2021). Membranes can be manufactured using different materials, whether organic (polymers) (ABADIKHAH *et al.*, 2019a; ZHANG *et al.*, 2016) or inorganic (ceramic) (MARZOUK *et al.*, 2021; SCHNITTGER *et al.*, 2021), and most of those studied and commercially used are polymeric due to their chemical stability, flexibility, lower cost and mechanical resistance (JHAVERI; MURTHY, 2016b).

Although membrane separation processes are an efficient treatment technology that produces high-quality water, they consist of only a separation process where two streams are generated. To produce high-quality water, one stream with a high concentration of contaminants called concentrate is produced, which needs further consideration (JOO; TANSEL, 2015; YANG *et al.*, 2018). Moreover, an inherent drawback of the process is the fouling, which causes a loss of performance, reduced permeate flux, and limited selectivity, in addition to increased operating costs (LEVITSKY; TAVOR; GITIS, 2021; MOSER *et al.*, 2018). The inadequate separation of low molecular weight substances, e.g., emerging contaminants, such as antibiotics, endocrine disruptors, and hormones, is another potential limitation of the process. These emerging contaminants are persistent in aquatic environments and can lead to the development of resistant bacterial genes, mutagenic effects, and impairment of the reproductive system of animals and humans (DE OLIVEIRA *et al.*, 2020b; SANTOS *et al.*, 2020a). With the aim of solving these drawbacks of the membrane separation processes, several nanomaterials are reported in the literature for membrane modifications, including TiO_2 (TEOW *et al.*, 2015), ZnO (BAI; LIU; SUN, 2012), Fe_3O_4 (HUANG *et al.*, 2012), CuO (CHOUDHURY *et al.*, 2018), Al_2O_3 (AMANIPOUR *et al.*, 2012), graphene oxide (GO) (MENG *et al.*, 2018), carbon nanotube (CNT) (BAEK *et al.*, 2014), SiO_2 (JIN *et al.*, 2012), etc. Due to their high surface-to-volume ratio, these nanomaterials have outstanding characteristics such as photocatalytic potential, adsorptive capacity, antibacterial property, and high hydrophilicity, among others. Therefore, the use of nanocomposites associated with membranes can reduce the fouling vulnerability and the load of the concentrate streams besides removing the low-weight molecular substances by

photocatalysis. Thus, the combination of membrane separation processes with nanomaterial is considered a promising alternative to overcome existing bottlenecks.

Membranes modified with nanocomposites are advanced membranes to improve water and wastewater treatment by taking advantage of the properties of nanomaterials. These nanomaterials can be introduced into the polymeric matrix of the membranes (AKBARI *et al.*, 2018; SAFARPOUR; VATANPOUR; KHATAEE, 2016; XU *et al.*, 2016b) or deposited as a coating on their surfaces (GAO; HU; MI, 2014b; TRAN *et al.*, 2020a, 2020b). Usually, the addition of nanomaterials alters the properties of the membranes, with the improvement of their separation performance, increased permeability, flux stabilization, and impression of an anti-fouling behavior (WU *et al.*, 2018; YOUNAS *et al.*, 2017).

The integration of membrane separation processes with nanocomposites expands the possibilities of treatment by the technology, besides improving the characteristics of polymeric membranes. Removal of emerging pollutants can be achieved by integrated membrane separation and photocatalytic oxidation processes (CAI *et al.*, 2018; ROUT *et al.*, 2021; SZYMAŃSKI; MORAWSKI; MOZIA, 2018). Retention of toxic ions, like arsenic, is also achieved by adsorption and oxidation (CHI-JUNG *et al.*, 2020; ZHANG *et al.*, 2018). The association allows the treatment of industrial and domestic wastewater effluents to generate high-quality water with the potential to be reused (REZAKAZEMI *et al.*, 2018), reducing the problem of water scarcity.

Among the nanocomposites used in the membrane modifications, photocatalysts, as titanium dioxide (TiO_2), are highly explored. Advanced oxidative processes with heterogeneous catalysis produce active species capable of degrading and mineralizing organic pollutants or reducing the valence of inorganic substances to decrease its toxicity (XU *et al.*, 2018a; ZAKERITABAR *et al.*, 2020). The association of membranes with catalytic nanomaterials reduces the number of steps in the treatment processes, consequently diminishing operating costs, since the membranes act as both a structure for immobilizing materials and as a selective barrier in only one unit (IGLESIAS *et al.*, 2016). Nanomaterials can then be used in several cycles.

Polymeric membranes are mostly hydrophobic and, therefore, prone to the deposition of organic compounds on their surfaces. Moreover, the treated matrices are often characterized by

complex compositions with many pollutants (REN *et al.*, 2021). The deposition of pollutants onto the membrane pores or on the membrane surface during permeation enhances fouling, which is one of the key operational challenges of the technology. It leads to a flux decline, selectivity loss, membrane lifespan reduction, and increases energy consumption and operating costs due to the increase in transmembrane pressure. Fouling can occur due to the deposition or adsorption of colloids (IGBINIGUN *et al.*, 2016), macromolecules, particles, salts (DUONG *et al.*, 2016), extracellular polymeric substances (EPS), or microbial cells (YANG *et al.*, 2021), on the surface or pores of membranes (GUO; NGO; LI, 2012; LI *et al.*, 2020a). The different fouling types are illustrated in Figure 3 depending on their foulants.

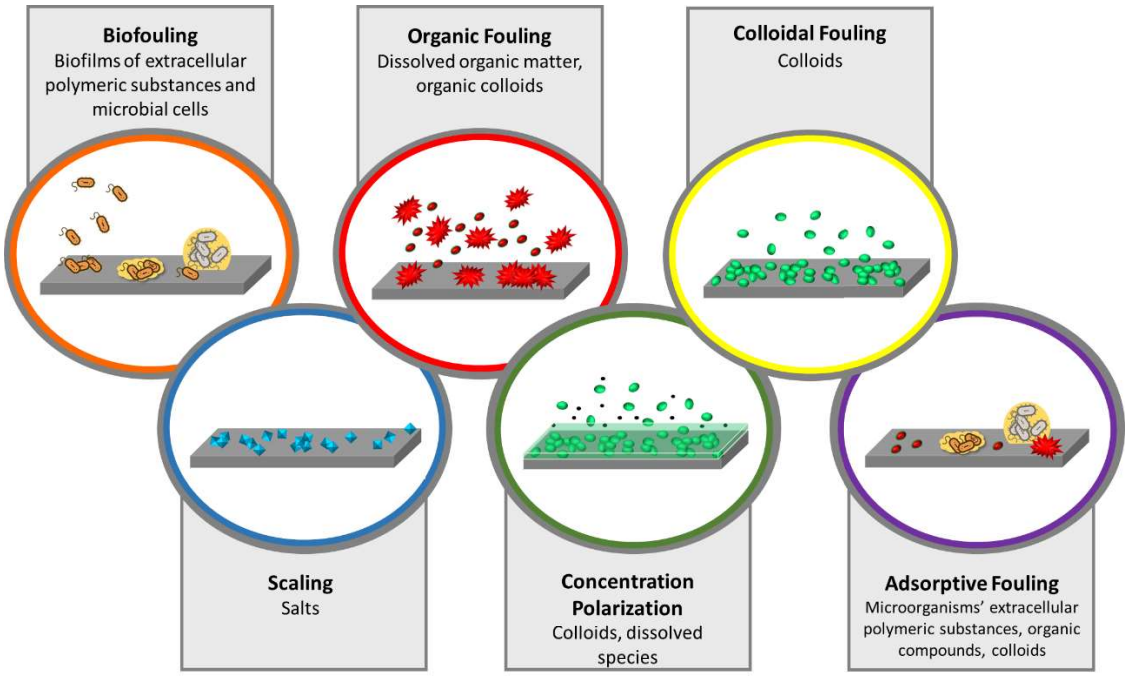

Figure 3 - Fouling types.

Fouling, that is poorly adhered to the membranes, can be removed by backwashing or physical and chemical cleaning, respectively. However, some fouling is irreversible due to chemosorption to the membrane (JHAVERI; MURTHY, 2016b). Thus, the development of fouling-resistant membranes capable of degrading foulants is a valuable research area that has received significant attention in recent years.

As previously stated, the combination of membrane separation processes with nanomaterials with catalytic properties is a promising alternative to fouling mitigation. Membrane fouling is reduced with the degradation of the compounds in the feed (ZHU *et al.*, 2018). Especially in

the context of wastewater treatment by biological systems associated with membranes, such as membrane bioreactors (MBR), biofouling can be mitigated with the application of nanocomposites membranes by enhancing microbial lysis and the promotion of fewer adherent surfaces (MANOHARAN; YOUNG-HO, 2020).

In addition to acting to reduce fouling through photocatalysis, the modifications of membranes with nanocomposites aim to overcome the permeability/selectivity trade-off. In operational terms, membranes are desirable that generate the highest possible permeate flux and the highest selectivity (MA; PING; DONG, 2017). However, these characteristics are often antagonistic. The use of TiO_2-GO nanocomposites with membranes is a promising alternative to achieve this goal, owing to their photocatalytic property and, also, due to the ability to increase the hydrophilicity of the membranes by the presence of oxygenated groups of the nanocomposites. Moreover, fast flow channels are formed by the almost frictionless tunnels between the GO nanosheets (YIN; DENG, 2015). The combination of TiO_2 with GO enhances the performance of each material compared to their individual applications. GO can reduce the band-gap of TiO_2-GO nanocomposites and enables its activation by visible light, widening the possibilities of applications. The conjugation also avoids the agglomeration of the nanoparticles, increasing the specific surface area available for photocatalysis. On the other hand, the rigid TiO_2 structure prevents the collapse of the lamellar sheets of the GO in the membrane modifications.

In reason of the promising properties of membranes modified with nanocomposites, several studies have focused on their development (ALMEIDA *et al.*, 2016; BAO *et al.*, 2020; LI *et al.*, 2019b; ONG; MOHAMMAD; NG, 2019). Some reviews have also been published in recent years on the subject (LI *et al.*, 2021; NASROLLAHI *et al.*, 2021; QING *et al.*, 2020; REN *et al.*, 2021). However, no review so far focused on polymeric membranes modified with TiO_2-GO composites to the best of our knowledge. We believe that the TiO_2-GO nanocomposite membranes literature has reached a level where a review of the achieved advances in the area is necessary. Therefore, this review aims to describe the main membranes materials used in obtaining TiO_2-GO nanocomposites membranes, the processes of obtaining the nanocomposites (TiO_2-GO), the benefits achieved with the modifications of the membranes, the design of obtaining the membranes, the nanocomposite fillers loading, and applications of these novel modified membranes.

2.2 - TiO_2-GO NANOCOMPOSITES INCORPORATION IN POLYMERIC MEMBRANES

Among the studied nanomaterials associated to membranes, nanoparticulate TiO_2 is the most extensively used due to its low cost compared to other nanomaterials, low toxicity to humans, and its chemical and thermal stabilities (JHAVERI; MURTHY, 2016b). TiO_2 also remains unchanged after photocatalytic degradation of organic compounds and acts as a disinfectant. Upon being irradiated by UV light, the oxide electrons are excited from their valence band to their conduction band, leaving positive gaps in the valence band. This electron-hole pair has a strong reducing and oxidizing activity, respectively, capable of reacting with water and oxygen from the medium, generating oxygenated radicals, such as hydroxyl ($OH^{\cdot}$) and superoxide anion ($O_2^{\cdot}$). The generated radicals can react with organic molecules and microorganisms contributing to their degradation or inactivation (HORIKOSHI; SERPONE, 2020; MARINHO; DACHAMIR, 2021) (Fig. 4). After a cycle of photodegradation, the catalyst returns to its initial condition and is available in new cycles (DE OLIVEIRA *et al.*, 2020a).

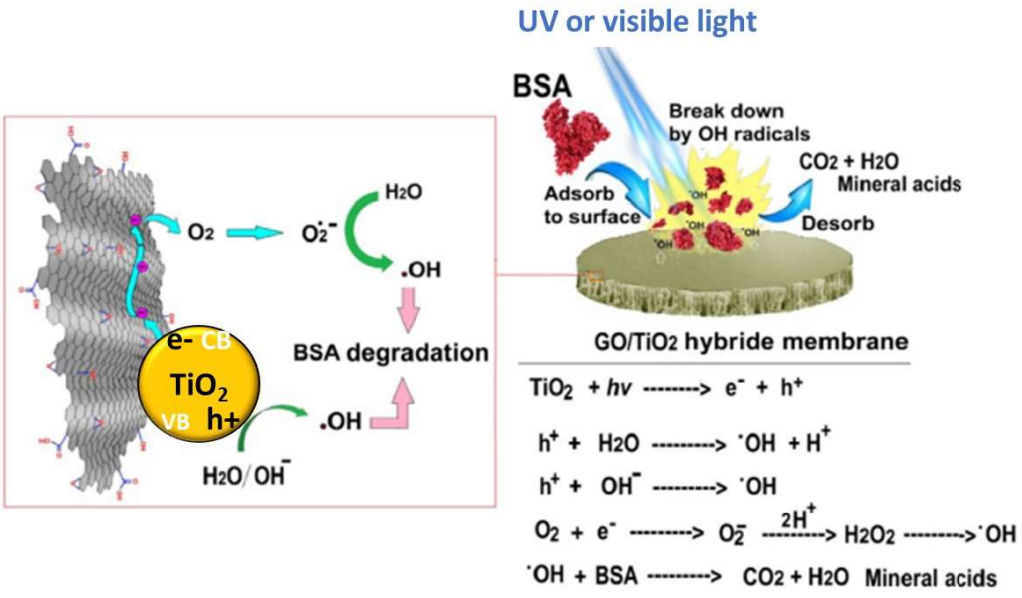

Figure 4 - Possible photocatalytic mechanism in a TiO_2-GO membrane.Adapted from Nasrollahi *et al.* (NASROLLAHI *et al.*, 2021) with copyright permission.

The photocatalytic activity of the TiO_2 promotes the oxidation of pollutants, contributing to the removal efficiency of the process with the generation of a lower load concentrate. The photocatalysis also decreases membrane fouling by promoting the degradation of feed compounds, thus generating self-cleaning surfaces, keeping the permeation stable

(MOLINARI; LAVORATO; ARGURIO, 2017). The lysis of bacteria cells mitigates the biofouling. The photo-induced hydrophilicity by the oxide due to its oxygenated functional groups (PEDERSEN *et al.*, 2018) also reduces the deposition of organic substances and increases the permeate flux. This is because the permeability of the modified membranes is influenced by their hydrophilicity, roughness, and porosity.

However, despite the described advantages, TiO_2 is only activated at sufficiently energetic wavelengths. Among the different crystallographic phases of the semiconductor, anatase is the most commonly used, and its band-gap is 3.2 eV, which means that the catalyst is activated by irradiations in the UV region of the electromagnetic spectrum (<387 nm) (CHEN; CHEN; CHEN, 2017). Thus, its large-scale use is limited by the energy expenditure due to non-solar activation. Also, the high surface energy of the oxide increases the possibility of aggregation of the nanoparticles, which reduces photocatalytic activity and can promote the blocking of membrane pores (MOZIA *et al.*, 2015). Some alternatives such as conjugation with other semiconductors, doping with metals, non-metals, and coupling with carbonic materials have been successfully addressed to solve these problems (REN *et al.*, 2021).

The use of GO associated with TiO_2 has been extensively studied, due to important characteristics of this carbonic material, such as high surface area, presence of a large amount of oxygenated functional groups, and excellent electron transfer properties (SALEEM; ZAIDI, 2020; URSINO *et al.*, 2018a). The high surface area associated with a large number of functional groups in GO promotes intimate contact with TiO_2 and the components of the medium to be degraded. In this way, TiO_2 aggregation is avoided and the photodegradation is increased. The electronic transfer properties of GO decrease the electron-hole recombination rate in the TiO_2, as well as reduce the nanocomposite band-gap. Therefore, the association of the nanomaterials enhances photocatalysis and enables visible light activation (GAO *et al.*, 2013; GAO; HU; MI, 2014b).

GO is a carbon nanomaterial obtained by oxidizing graphene, which can be massively produced by exfoliating graphite (CHEN *et al.*, 2018). It has a hydrophilic nature due to a large number of functional groups (-OH, -COOH, -C-O-C, -C=O) in its two-dimensional structure. This material improves the thermal and mechanical properties of polymeric membranes. Its sharp edges also confer antibacterial properties by disrupting the cellular structure of microorganisms (SONG *et al.*, 2018). The non-oxidized regions of the GO form tortuous, almost frictionless

nano-channels that act as high-speed permeation routes for water molecules (JIA; SHI, 2016). However, such channels are not stable and can collapse, limiting the applications of GO alone associated with membranes. Unattached GO sheets on membrane surfaces can also be easily removed by rinsing with water (MENG *et al.*, 2018). Besides, the interaction between the oxide sheets causes narrow channels that can reduce the permeate flux (LIU; WANG; ZHANG, 2015; WEI *et al.*, 2016). The association of rigid materials, such as TiO_2 with GO, prevents the collapse of the lamellar structure and improves the permeation performance (WANG *et al.*, 2017b). In such a way, associating TiO_2 to the GO improves the performance of both materials in the modifications of membranes.

Although some studies use anatase and rutile phases, in general, commercial TiO_2 catalysts in the anatase crystallographic phase are used in the membrane modifications. Hummer's method is the most used for GO synthesis due to its effectiveness consolidated by the scientific community.

Table 2 presents a compilation of studies using TiO_2-GO nanocomposites for modifying membranes, the ways of obtaining the nanomaterials, and the main characteristics of the modified membranes.

Table 2 - Membranes modified with TiO_2-GO nanocomposites and the main methods of preparing these nanomaterials.

Membrane	TiO_2 nanoparticles	GO	TiO_2:GO mass ratio	Modifying method	Main characteristics of nanocomposite membranes	Reference
Polyamide nanofiltration	Commercial (10-25 nm)	Graphite exfoliation using the Hummer's method	1:2	Electrospinning/ Electrospraying	The obtained membranes had a hydrophilic character with a contact angle varying between 46.5-50 °. Membranes modified only with GO showed a permeability of 7.62 L m^{-2} h^{-1} bar^{-1}, whereas for those with TiO_2 the permeability increased to 13.77 L m^{-2} h^{-1} bar^{-1}. This improvement was explained by the increase in the interlayer space of the GO sheets by the addition of TiO_2. The membranes were able to remove 92.05% and 99.36% of the methylene blue and methyl orange dyes (10 mg L^{-1}), respectively. The rejection mechanisms were screened by physical size and electrostatic repulsion. For this reason, a higher removal of methyl orange was achieved due to its negative charge similar to GO.	(CHEN *et al.*, 2018)
Polyethersulfone	Hydrolysis of $Ti(SO_4)_2$	Graphite exfoliation using the Hummer's method	1:3	Blending (Interfacial polymerization)	The roughness of membranes modified with nanocomposites was reduced compared to that without modification up to specific concentrations of the nanomaterial. Above 0.3% wt TiO_2-GO the roughness increased. The authors argue that the roughness affects the adsorption and desorption of foulants on the membrane surface. Smoother surfaces of hydrophilic membranes reduce fouling.	(WANG *et al.*, 2017b)

Membrane	TiO_2 nanoparticles	GO	TiO_2:GO mass ratio	Modifying method	Main characteristics of nanocomposite membranes	Reference
Polyamide nanofiltration	Hydrothermal synthesis from orthotitanate	Graphite exfoliation using the Hummer's method	1:9	Blending (Interfacial polymerization)	The surfaces of the membranes modified with the nanocomposites were smoother compared to the membrane without modification. The authors attributed the reduction of roughness to the hydrogen bonds between the functional groups of the composites and the polyamide layer. The contact angle reduced from 67° (pristine) to 47.2°, in the case of the membrane modified with TiO_2-rGO (0.02% wt).	(SAFARPOUR *et al.*, 2015)
Polysulfone	Commercial TiO_2 nanoparticles (322 nm diameter, 80% anatase, and 20% rutile)	Graphite exfoliation using the Hummer's method	1.5:1	Blending	The modified membrane showed a more porous surface compared to that without modification. The contact angle of the modified membrane decreased from 73.75° (pristine) to 65.25°, due to the affinity of the water molecules with Ti-O. A greater hydrophilicity prevents the deposition of organic matter on the membrane surface. The modified membranes also showed greater tensile strength.	(KUSWORO *et al.*, 2021)
Poly(vinylidene difluoride-co-trifluoroethylene)	Commercial TiO_2 (10-40 nm)	Graphite exfoliation using the Hummer's method	100:1	Electrospinning	The authors measured the band-gap of TiO_2 (3.01 eV) and of TiO_2-GO nanocomposite (2.21 eV). The reduction in the value was due to the GO's ability to absorb in the visible region. Degradation tests of methylene blue dye (10^{-5} mol L^{-1}) under visible light irradiation, with the nanocomposite modified membrane (8% wt), revealed 99% degradation after 90 minutes. Membranes modified with only TiO_2 (20% wt) were tested for comparison and showed	(ALMEIDA *et al.*, 2016)

Membrane	TiO_2 nanoparticles	GO	TiO_2:GO mass ratio	Modifying method	Main characteristics of nanocomposite membranes	Reference
Unsupported membrane	Synthesis from Tetrabutyl titanate ($Ti(OC_4H_9)_4$)	GO dispersions (17.3 mg mL^{-1})	10:1	Sol-gel	degradation of 63% only. The increase in efficiency was attributed to the decrease in the band-gap value. Membranes with 2.73 eV band-gap energy were obtained. The GO addition reduced the membrane pore size. The membrane molecular weight cut-off was 1224 Da.	(XIA *et al.*, 2018)

2.3 - GO BENEFITS TO THE TIO_2-GO NANOCOMPOSITES AND THEIR IMPACTS ON MEMBRANE PERFORMANCE

As previously described, the use of GO associated with TiO_2 improves the performance of the semiconductor, and both increase the performance of the modified membranes. One of the first study that described the association of these nanomaterials was that of Williams *et al.* (WILLIAMS; SEGER; KAMT, 2008). The authors proposed a mechanism that proved to be valid in other studies, in which the electrons generated by the UV irradiation of TiO_2 can interact with the GO sheets, reducing some groups of its surface, and the remaining electrons are relocated along the basal planes. Such electrons can react with adsorbed O_2 to form $O_2^{\cdot -}$ radicals that can oxidize pollutant molecules in the medium. This effective charge transfer between TiO_2 and GO reduces the electron-hole recombination rate of the semiconductor and increases the photocatalytic activity of TiO_2 in the TiO_2-GO composite. Another function of the GO in the nanocomposite is to act as a sensitizer since the charge transfer from the GO to TiO_2, forming a p/n junction between the materials, and leaving a doped hole in the GO, has already been confirmed (MORALES-TORRES *et al.*, 2012). In such a way, the photocatalytic activity can be amplified to visible light through the direct excitation of electrons from the GO to the TiO_2 conduction band. The GO band-gap depends on functional groups present in its structure and the oxygen:carbon ratio (HASAN *et al.*, 2017). Values that are close to 2.1-2.2 eV are reported in the literature, which corresponds to an activation at wavelengths around 550 to 560 nm, that is, in the visible light region of the electromagnetic spectrum (VELASCO-SOTO *et al.*, 2015). In the following paragraphs, studies describing membranes modified with TiO_2-GO in the treatment of pollutants are reported, emphasizing the gains in selectivity and photocatalytic performance due to the presence of GO in the nanocomposite.

Zhang *et al.*, (2021d) tested the efficiency of Polyacrylonitrile (PAN)/β-cyclodextrin (β-CD) nanofiber membranes modified with TiO_2-GO nanocomposites in removing methylene blue (MB) and methyl orange (MO) dyes (10 mg L^{-1}). The modified membrane with the TiO_2:GO mass ratio 8:2 removed 93.52 ± 1.83% and 90.92 ± 1.52% of MB and MO, respectively, under irradiation of natural light (noon on a sunny day) for 5 hours. MB removals of approximately 32%, 82%, 65%, and MO removals of approximately 30%, 75%, and 60% were achieved for the membrane without modification, modified only with TiO_2, and modified only with GO, respectively. The authors observed that GO increased the photocatalytic activity of the

nanocomposite; however, excessive doses reduced the absorption of light by TiO_2. The removal by the membrane modified only with GO was attributed to its excellent ability to adsorb organic components through electrostatic π-π interaction and hydrogen bonds.

Xu *et al.*, (2016a) tested the photocatalytic properties of ultrafiltration PVDF membranes modified with TiO_2-GO nanocomposites to remove bovine serum albumin (BSA) (1 g L^{-1}). After 120 minutes of UV irradiation, removals of 8%, 46%, 53%, and 80% were achieved for the membrane without modification, modified only with GO, modified only with TiO_2, and modified with TiO_2-GO, respectively. The superior photocatalytic performance was attributed to the integration of nanomaterials. In addition, the authors observed that the photodegradation kinetics of the membrane modified with TiO_2-GO was 108% faster than that modified only with TiO_2 and 153% faster than that modified only with GO. Still, in this study, it was verified that the flux (operating pressure: 1 bar) of pure water (487.8 L m^{-2} h^{-1}) remarkable increased by the addition of the nanocomposite in comparison to the membrane without modification (157.1 L m^{-2} h^{-1}), modified with TiO_2 (302.4 L m^{-2} h^{-1}) and GO (398.7 L m^{-2} h^{-1}).

(SURIANI et al., 2019) observed an increase in the performance of nanofiltration PVDF membranes modified with TiO_2-GO in the filtration of methylene blue dye (10 ppm) without irradiation. Both the unmodified membrane and those modified only with GO and with the TiO_2-GO composite showed very similar rejection rates, equal to 92.79%, 92.81%, and 92.79%, respectively. However, the permeate flux (operating pressure: 2 bar) of the membrane increased from 1,146 L m^{-2} h^{-1}, in the case of the unmodified membrane to 4,476 L m^{-2} h^{-1} in the case of the modified one only with GO, and 7,770 L m^{-2} h^{-1} for the one modified with TiO_2-GO. In such a way, the permeability-selectivity trade-off is resolved.

2.4 – MAIN POLYMERIC MATERIALS FOR TIO_2-GO NANOCOMPOSITE MEMBRANES

Different polymeric materials have been used in the preparation of membranes modified with TiO_2-GO nanocomposites, as well as different routes of modification. Polymers such as polyamide, PVDF, PSF, PES, nylon, poly (4-styrenesulfonic acid) (PSSA), polyvinyl alcohol (PVA), PVC, CA, Nafion, polyetherimide, TAC are reported in the literature. Table A.1 (Appendix) shows some studies of different polymeric materials used in membranes modified with TiO_2-GO nanocomposites.

As shown in Table A.1, most of the membranes modified with TiO_2-GO nanocomposites are flat sheets used in plate and frame configuration. Further studies of modifications should be carried out also in spiral and hollow fiber configurations since these configurations present a greater packaging factor than flat (BAKER, 2004), and from an economic point of view, they are more attractive to the treatment processes.

Most studies report the modification of polysulfone membranes because they are widely used in water and wastewater treatment due to their high thermal stability and good mechanical resistance. However, this material is prone to fouling and has a low permeate flux, as it is nonpolar (NGUYEN *et al.*, 2019). Therefore, modifications with TiO_2-GO aim to increase the permeability with the maintenance of high rejection of contaminants. Some studies report membranes with photocatalytic capacity (GAO *et al.*, 2013; SUNDARAN *et al.*, 2020; TAGHIZADEH; KEBRIA; QADERI, 2019), and others aim to increase hydrophilicity by incorporating nanocomposites regarding this polymer (HOSSEINI *et al.*, 2017; SIRINUPONG *et al.*, 2018). Some studies promote the modification by physically contacting with the membrane surface (DIOGO JANUÁRIO *et al.*, 2020; SEHATI *et al.*, 2015) and others by blending the polymeric solutions (BAIG *et al.*, 2019; CORREA *et al.*, 2017).

Another polymer widely used in the modified membranes is polyamide, owing to its wide usage in RO and NF membranes. Usually, these membranes are composed of a thin film, and the selective layer has high salt rejection; however, the permeate flux is low, requiring the use of higher pressures to promote permeation. The addition of nanocomposites to these membranes has the main purpose of increasing the hydrophilicity of the material and, consequently, the permeate flux. Another aim is to increase the resistance to chlorine, and to reduce bio-fouling through the biocidal potential of TiO_2-GO. For these membranes, most of the studies describes the interfacial polymerization as the most common obtaining method, in which the nanocomposites are mixed with the casting solutions [69].

Abadikhah *et al.*, (2019b) modified TFC polyamide membranes with amino-functionalized TiO_2-GO using interfacial polymerization. Functionalization was performed to increase the compatibility of the composite with the polyamide. The authors point out that high doses of nanocomposites in this modification can negatively affect the movement of monomers through interfacial polymerization and limit successful polymer formation. Therefore, although higher

doses of nanocomposites increase hydrophilicity and flux, attention must be paid to the membrane's rejection capacity.

2.5 – Design and fabrication of TiO_2-GO nanocomposite membranes

The usual methods for nanocomposite membranes fabrication are blending, surface coating, and filtration.

2.5.1 Blending

The technique for preparing nanocomposite membranes using blending consists of mixing the TiO_2-GO nanocomposites to a polymeric matrix in an organic solvent. The solution is solidified by phase separation which can occur by diffusion induced, temperature induced or solvent evaporation (SALEH; GUPTA, 2016). The main advantage of the blending of TiO_2-GO in the polymeric matrix of the membrane is the reduction in leaching of the catalyst (MÉRICQ *et al.*, 2015). Besides, a more uniform dispersion of particles along the transverse and vertical directions of the membrane is reported. In this way, the obtained membrane efficiency increases by intensifying the contact of the materials with the feed water. Greater adherence of materials to the polymer matrix is compared to other preparation techniques also reported. Additionally, it is possible to increase permeability up to certain concentrations by the formation of pores close to the nanocomposites. However, under high concentrations, the probability of formation of agglomerates increases, which will generate a larger number of larger pores, reducing the membrane rejection efficiency. Wang *et al.*, (2017b) obtained nanofiltration membranes modified with TiO_2-GO through blending. The modified membranes showed a doubled permeate flux compared to the pristine membrane in using a 0.2% of TiO_2-GO. When using the 0.3% ratio, the permeability was reduced compared to the pristine specimen, showing increased resistance to transport due to high doses. It is noteworthy to mention that blending with TiO_2-GO differs from blending with only GO. With only GO, the material sheets can compact themselves in a lamellar manner to cause pore blockage leading to an overall reduced permeability.

2.5.2 Surface coating

In the preparation of nanocomposite membranes using surface coating, nanomaterials are deposited on the surface of a synthesized membrane. The process can take place through simple contact of the materials with the membrane surface, called self-assembly (Fig. 5-a), or through

the use of adhesion agents called cross-linkers (Fig. 5-b). In the case of self-assembly, there must be interactions between the functional groups of the membranes and the nanomaterials. When using cross-linkers, they act as “glue” between the structures. Usually, the materials are placed in contact with the membrane surface for a while and, afterward, the non-adherent residue is removed. This technique faces the problem of loss of active material, especially for cases of cross-flow filtration, because the adhesion process can be weak. However, the operational simplicity for preparing the modified membranes is an important advantage.

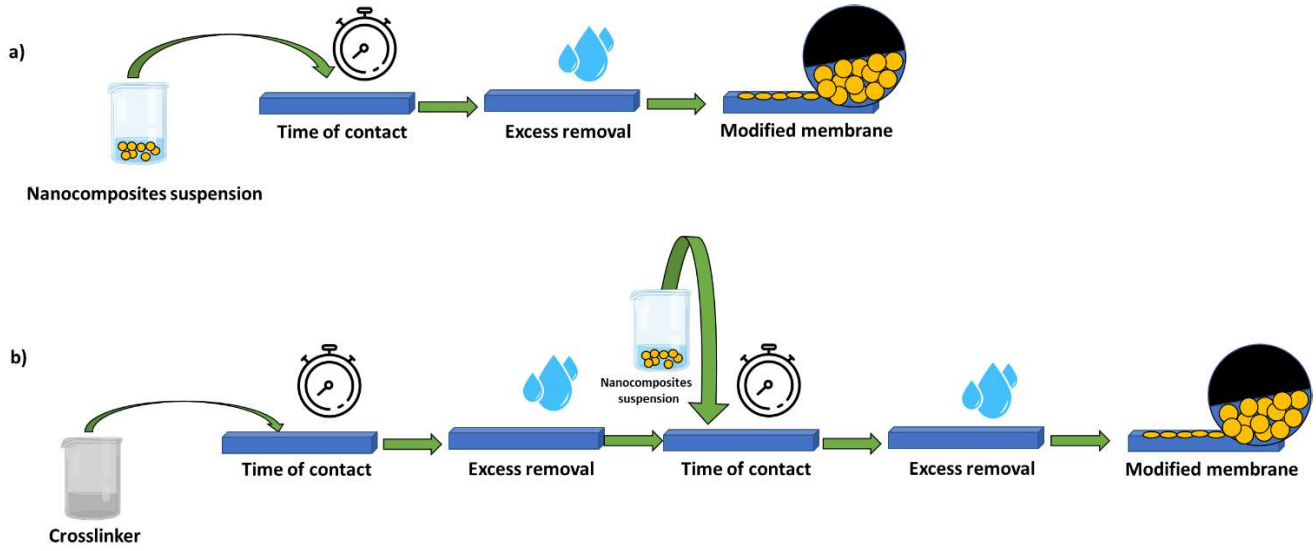

Figure 5 - Surface coating nanocomposite membrane fabrication (a) self-assembly (b) cross-linker aid.

Gao *et al.* (GAO; HU; MI, 2014b) promoted the modification of commercial polysulfone UF membranes with TiO_2-GO through a variation of the self-assembly method called layer-by-layer. A TiO_2 suspension was placed in contact with the membrane and stirred on its surface for 3 hours. Subsequently, GO solution was poured onto the membrane surface and it was soaked with 95% ethanol and irradiated by UV light to form strong bonds between TiO_2 and GO. The authors attributed the adhesion of TiO_2 to the membrane surface to the Ti-O bond formed between the Ti^{+4} and hydroxyl of the oxide and the sulfonic groups of the membrane, and between TiO_2 and GO through hydrogen bonding between Ti^{+4} and carboxylic groups in GO. The modified membrane was able to degrade approximately 70% of the methylene blue dye (50 mg L^{-1}) after 5 hours of solar irradiation. The authors attributed the performance to the association of materials that reduces the band-gap and its activation by solar energy. Figure 6 represents the self-assembly (a) and layer-by-layer (b) mechanisms of TiO_2-GO on the surfaces of polysulfone membranes.

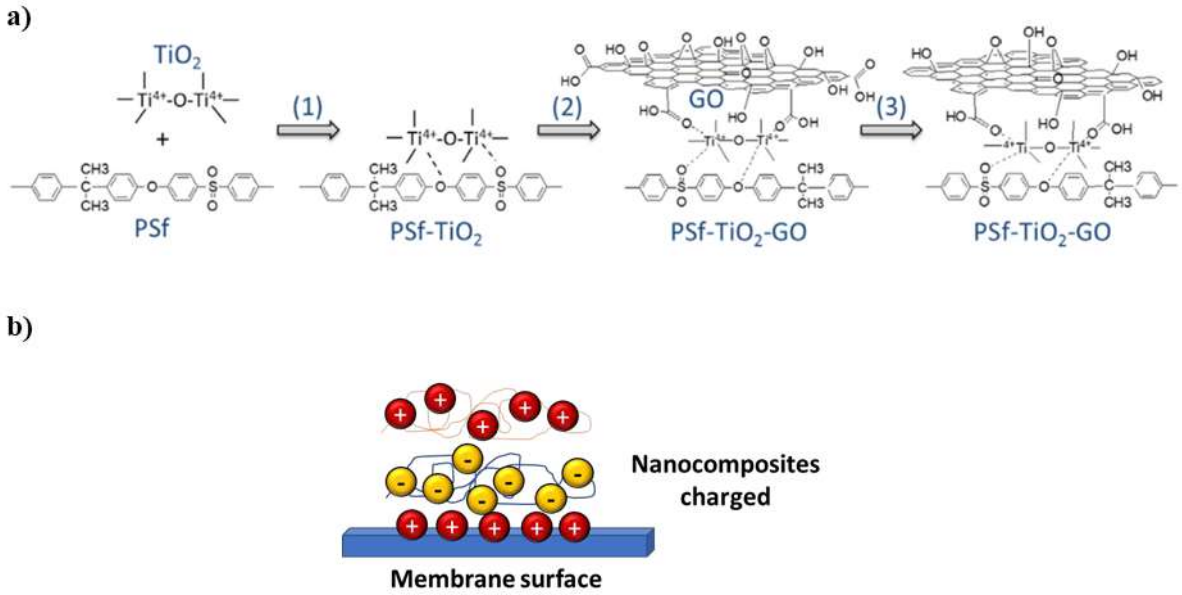

Figure 6 - a) Scheme of the self-assembly mechanism of TiO_2-GO nanocomposites on the surface of polysulfone membranes; adapted from Gao; Hu; Mi, (2014b) with copyright permission. b) Scheme of the layer-by-layer mechanism.

In the surface coating, the assistance of binding agents as an alternative for greater adherence of nanocomposites to the surface of membranes are reported. Zhang *et al.*, (2017) modified TFC polyamide membranes with TiO_2 with the aid of polydopamine. Anti-fouling behavior was observed by filtration tests of bovine serum albumin (BSA) (0.5 g L^{-1}). The flux with the modified membrane remained constant, while the flux of the unmodified membrane declined by 25% both after 8 hours of operation. The tests were performed in the absence of irradiation. The authors attributed the results to the greater hydrophilicity of the surface by modification with the oxide. Zhang *et al.*, (2013) modified the surface of polyamide TFC membranes with TiO_2. Self-assembly modification was compared to surface coating with the assistance of dopamine. To assess the bond strength, the membranes modified by both methods were washed, and subsequently dried with a tissue. SEM analyzes showed adhesion and coverage of the membrane surface with TiO_2 even after washing, while most of the particles had been removed from the modified self-assembly membrane. The authors justify the greater strength of adherence to dopamine, which can polymerize in basic media and connect the materials by long-lasting bonds.

2.5.3 Filtration

The filtration technique consists of filtering the nanocomposites towards the membrane (SALEH; GUPTA, 2016). The nanomaterials enter the pores of the membrane and are bound using connections between the functional groups of the membranes and graphene oxide and titanium dioxide. Under dead-end filtration, GO sheets tend to settle on a lamellar structure.

Gao *et al.*, (2013) modified commercial cellulose acetate MF membranes with TiO_2-GO microspheres. A suspension (2g L^{-1}) of TiO_2-GO was filtered in a dead-end cell pressurized by nitrogen gas. The authors tested the membranes for the degradation of rhodamine B and Acid Orange 7 (AO7). The modified membranes completely removed the dyes in 30 and 20 minutes of UV light irradiation, respectively. The unmodified membrane removed around 40% of the dyes in the same operation times. Also, the steady-state permeate flux in the humic acid (HA) filtration (200 mg L^{-1}) was 9 times higher in the modified membranes than those without modification. Pastrana-Martinez *et al.*, (2015) modified mixed cellulose ester membranes (0.45 μm pore size) with TiO_2-GO (2 g L^{-1}) by means of vacuum filtration of the material suspension. A subsequent drying with N_2 flux was executed for 10 minutes. The modified membranes were used to remove the pharmaceutical compound diphenhydramine (DP) and the organic dye methyl orange (MO). The modified membrane removed 28% of DP under visible irradiation and 73% under close UV-Vis, while the membrane without modification was unable to remove the compound.

Diogo Januário *et al.*, (2020) modified PES MF membranes by filtering individual solutions of TiO_2 and GO in sequence in a dead-end cell. The solutions' pH was adjusted to ensure a positively charged TiO_2 surface (pH adjusted to 2 with nitric acid), and a negatively charged GO surface (pH adjusted to 10 with sodium hydroxide). Before the filtration of the nanomaterial solutions, a sulfuric acid solution (10 % wt) was filtered through the membrane to induce its surface to be negatively charged and favor the interaction with the materials applied thereafter (Fig. 7).

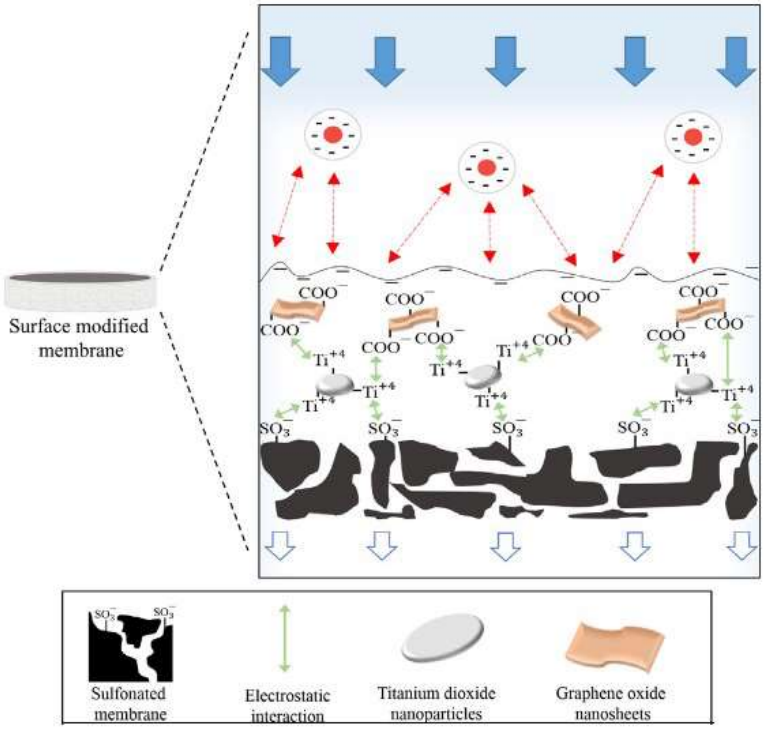

Figure 7 - Interactions between the membrane surface and TiO_2-GO nanocomposites. Adopted from Diogo Januário *et al.*, (2020) with copyright permission.

Although the procedure just described is rather simple, the interactions between the materials can be weak, and the nanocomposites can detach afterwards, generating secondary pollution. Future studies should focus on these modifications of membranes by analyzing their stability under extended periods of operation. Only few studies addressed this type of evaluation so far.

Modifying membranes with nanocomposites other than TiO_2-GO can be performed by techniques different than those mentioned above (QING *et al.*, 2020). For example, in inorganic membranes, chemical vapor deposition (CVD) or sol-gel are also used (LI *et al.*, 2021). However, the need to use higher temperatures or calcination steps limits the use in polymeric membranes.

Although blending, surface coating, and filtration techniques are the most used in modifying polymeric membranes with TiO_2-GO nanocomposites, other variations of less common techniques are reported in some studies (MARINHO; DACHAMIR, 2021; NASEEM *et al.*, 2018). Electrospinning and electrospraying are examples into the blending category. In the first technique, the polymeric solution with the nanocomposites is transferred to a vessel in which, under an electric field, the compound is injected into a conical tip to obtain a fiber membrane.

Electrospraying is also reported as a coating technique by applying a high electrical potential to atomize a solution by forcing it through a metallic capillary. The potential generates shear stress with the formation of a fine dispersion (KORZHOVA *et al.*, 2020). Chen *et al.*, (2018) obtained polyamide and GO nanofiltration membranes with intercalated TiO_2 nanoparticles through electrospinning and electrospraying. The nanofiltration membranes with TiO_2-GO presented pure water flux greater than 13.77 L m^{-2} h^{-1} bar^{-1} at low pressure (1 bar). This water flux value was approximately 80% greater than the membrane modified with GO alone. High rejections of organic dyes (>92% for MB and 99% for MO) were also achieved by the membranes with the nanocomposite. The use of intercalated TiO_2 nanoparticles increased membrane flux while maintaining high rejection capacity. Almeida *et al.*, (2016) also obtained membranes with nanocomposites through electrospinning. Poly(vinylidene difluoride-co-trifluoroethylene) (P(VDF-TrFE)) was used to obtain fibrous membranes. The modified membranes reached approximately 100% MB degradation after 90 minutes of exposure to visible light.

Figure 8 shows the benefits and drawbacks of each fabrication technique.

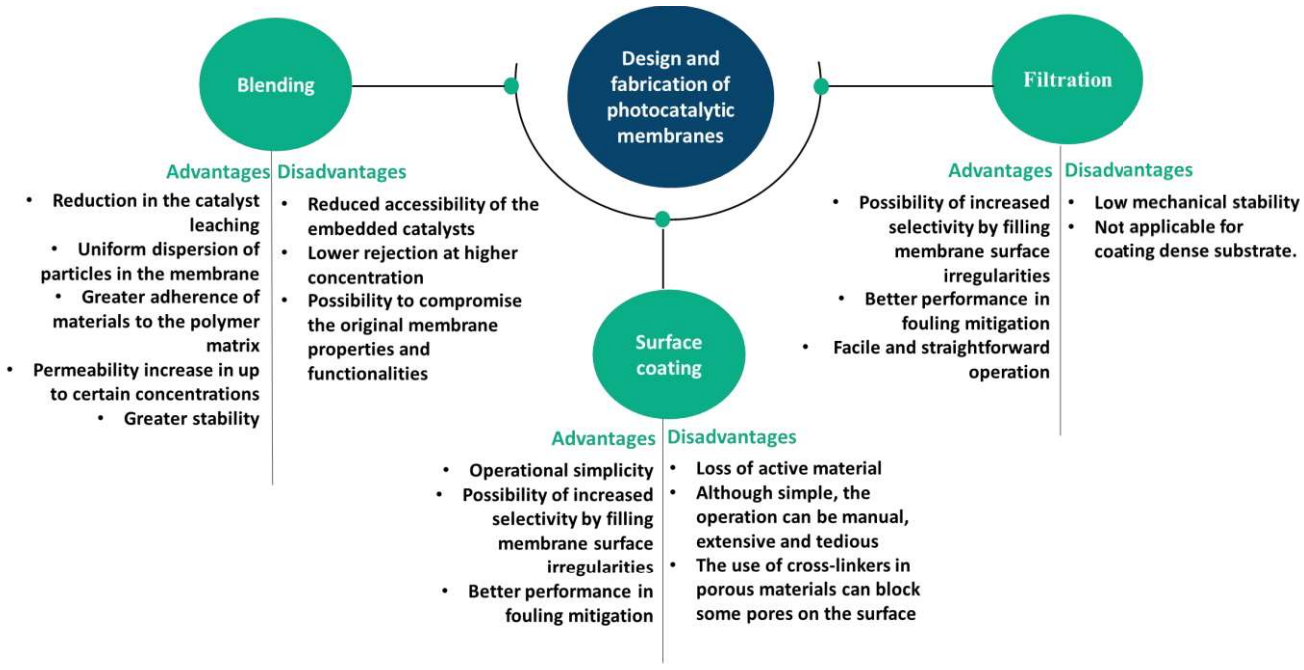

Figure 8 - Benefits and drawbacks of each nanocomposite membrane fabrication technique.

Blending can lead to the formation of pores close to the particles and reduce the rejection by the membranes, whereas filtration and surface coating can fill irregularities in the surface of the membranes and reduce the size of the pores by increasing selectivity.

From the perspective of stability, blending-modified membranes are more advantageous. However, when it comes to the interaction of nanoparticles with the solutes that cause fouling, surface coating and filtration techniques generate greater exposure of these materials and better performance in fouling mitigating.

Although with some promising results, there is a lack of information about the continuous operation of these membranes and about the catalyst lifetime including analysis of a possible detachment of the catalyst. In addition, the toxicity of the permeate has to be evaluated in order to assess the safety of using nanomaterials in the modifications. The stability of nanocomposites and membrane structures separately, as well as the stability of nanocomposites and membranes in combination, should be assessed. A major bottleneck of photocatalytic membranes is the irradiation under the surface of the membranes, which can damage the polymeric structure. The loss of nanomaterials and damage to the structure of the membranes can cause a deterioration of the permeate, secondary pollution, and a reduction of the performance of the treatment system. Detailed assessments in this regard should be carried out in future studies. Further research also needs to study the impact of the formed radicals on the surface of the membranes. Another significant aspect is the cleaning procedure for these membranes, since depending on the modification technique used and cleaning approach applied (backwashing, physical or chemical cleaning), severe changes to the surface modification might appear.

Most studies with different modification techniques use dead-end systems and it is known that the cross-flow system is the most widely used in industrial applications. The assessment of stability in such systems is a gap that needs to be better clarified, with a view to the use of such membranes at full-scale.

2.6 - TIO_2-GO MEMBRANES CHARACTERIZATION TECHNIQUES

In the area of membrane synthesis and modification, characterization techniques play a crucial role. Commonly, modified and unmodified membranes are characterized, and differences in results are evaluated. Several techniques are more common for the characterization of membranes modified with TiO_2-GO nanocomposites being described in the following paragraphs with their respective purposes.

Scanning electron microscopy (SEM) and SEM coupled with elemental analysis by Energy Dispersive X-Ray Analysis (EDX) are the most widely reported characterization techniques in

the studies. Using SEM, the morphologies of the surfaces of the membranes are evaluated before and after modification. On some occasions, the membrane surfaces are also assessed after filtration/degradation tests, and the results are compared between the neat and modified membranes. The study of morphology provides indications of the presence of nanocomposites and their distribution on the surface of the membranes. The cross-sectional morphology analysis also helps verify the thickness of the modifying layer in the case of surface modification techniques. The membrane is immersed in liquid nitrogen and fractured for cross-section analysis.

Atomic force microscopy (AFM) is widely used to verify changes in the roughness and topography of the membrane surface after modification. The images generated by the technique show darker regions representing valleys and pores, and lighter regions that are the highest points on the surface of the membranes. The importance of the technique is associated with the impact of roughness on the anti-fouling behavior of the membranes. In general, the membrane roughness decreases leading to a decrease in fouling, as foulants are less likely to be adsorbed on smoother surfaces. There is no uniqueness in the results regarding the change in roughness by the addition of TiO_2-GO nanocomposites. Some studies report an increase in roughness by its addition (WU *et al.*, 2019b) and others a decrease (XU *et al.*, 2018b). It is worth mentioning that the modification technique employed and the nanocomposite dosage used are preponderant factors in this result.

The contact angle is another technique widely used in the characterizations because it results in the wettability and consequent hydrophilicity of the membrane surface. The membrane is considered hydrophobic if a water drop does not spread over its surface, and the angle between the membrane and the drop is close to 90 °. In contrast, hydrophilic membranes have a much lower angle. This parameter is important concerning the anti-fouling capacity of the modified membranes, as a hydration layer is formed on the surface of hydrophilic membranes during the filtration process that reduces the deposition of fouling agents. The addition of TiO_2-GO nanocomposites increases membrane hydrophilicity due to the oxygenated functional groups of TiO_2 and GO.

Generally attenuated total reflectance - Fourier transform infrared spectroscopy is used (ATR-FTIR) to check for the presence of new functional groups in the modified membranes and analyze the connections involved between polymers and nanocomposites. Similar to FTIR, X-

ray photoelectron spectroscopy (XPS) is used to check the chemical composition of the material's surface. Besides checking the elements present on the membrane surface, the XPS also indicates the electronic state of the elements.

Analyzes are also carried out to check the average pore size of the membrane, usually using molecular weight cut-off (MWCO) measurements by filtering aqueous solutions of compounds of different molecular weights. Porosity is usually measured using the dry-wet method, where the dry and wet membrane weights are measured and compared. Thermogravimetric analysis (TGA) are also reported to verify the alteration of the structural characteristics of the membrane after modification, such as its thermal stability. Such an analysis is especially important for membranes developed for the treatment of high-temperature currents. The mass of the composites in the modified membranes can also be measured by the TGA analysis. The zeta potential of the membranes is measured by a streaming potential analyzer. The antibacterial properties of the modified membranes are assessed using *Escherichia coli* bacteria. The membranes are immersed in a solution with bacteria, and after a specific contact time, alive and dead bacteria are counted with the aid of microscopy and a bacterial viability kit.

Analyzes of nanocomposites are also usually employed, for example, UV/Vis diffuse reflectance measures to assess the band-gap only for TiO_2, only for GO and associated materials in the form of TiO_2-GO nanocomposite. Transmission electron microscopy (TEM) analyses are done to evaluate the size of the nanoparticles, most commonly those of TiO_2, and X-ray diffraction (XRD) analyzes inform about the crystallinity of the materials as well as provids the average crystallite size. Table 3 shows the most common benefits and disadvantages of the modifications detected by the characterization techniques.

Table 3 - Usual characterization techniques for modified membranes with TiO_2-GO nanocomposites.

Characterization technique	Gains	Losses
Scanning Electron Microscopy (SEM) and Energy Dispersive X-Ray Analysis (EDX)	The presence of GO reduces the agglomeration of TiO_2 nanoparticles.	TiO_2-GO nanocomposites increases finger-like pores. The hydrophilic nature of nanocomposites increases the exchange of solvent and non-solvent during phase separation in the blending technique, forming larger pore channels in the underlying layer of the membrane. In the case of surface modification techniques, GO provides wrinkled surface morphology.

Characterization technique	Gains	Losses
Atomic Force Microscopy (AFM)	The use of nanocomposites leads to a reduction in the roughness of the membranes, especially in blending techniques up to specific concentrations.	The use of nanocomposites leads to increased roughness in high concentrations, especially in surface modification techniques.
Contact angle	Modification with TiO_2-GO nanocomposites increases the hydrophilicity of the polymeric membranes.	-
Fourier-transform Infrared Spectroscopy (FTIR)	Detection of characteristic bands of functional groups belonging to nanocomposites with proof of functionalization.	-
X-ray Photoelectron Spectroscopy (XPS)	Identification of modification of the surface of the membranes by the presence of elements of the nanocomposites. Connection confirmation between TiO_2 and GO and between the nanocomposite and the polymeric membrane surface.	
Average pore size and porosity	The use of nanocomposites decreases average pore size and porosity, especially in surface modification techniques.	High doses of nanocomposites increase average pore size and porosity, especially in blending modification techniques.
UV/Vis diffuse reflectance	The use of GO reduces the TiO_2 band-gap in the nanocomposites.	-

2.7 – Impacts of the TiO_2-GO loading in the membrane performance

The dosage of nanocomposites used in the modification of the membranes is a determining factor in the features and performances obtained. In the case of photocatalytic membranes, a higher dosage of catalyst will generate a greater number of active sites available for the formation of radicals which are able to attack pollutants and, consequently, to reduce fouling. However, there is an optimum value that improves performance, above which efficiency decreases again. An excess of catalysts can promote their aggregation, and as a result, part of

the nanoparticles surfaces becomes unavailable. Unlike membrane photocatalytic reactors with suspended catalysts followed by membrane units, the high concentration of catalysts does not reduce the penetration of light into the system, in the case of photocatalytic membranes. It is worth mentioning that the disposition of nanocomposites in surface modification techniques generates more efficient membranes from a photodegradation point of view owing to the direct contact of the catalysts with the compounds to be degraded in the feed. In modification techniques such as blending, pores are generated in the vicinity of nanoparticles and a high dose of nanocomposites can promote the formation of macropores, which, while increasing permeability, may reduce the selectivity of modified membranes.

Tran *et al.*, (2020b) modified PVDF membranes with different proportions of TiO_2 in the TiO_2-GO composite. For TiO_2 percentages up to 50% wt in the composite, SEM micrographs showed that the surface of the membranes resembled the deposited sheets. While above 75% wt, agglomerations, and clusters of TiO_2 particles are observed. Tests of degradation of phenol and m-nitrophenol using the modified membranes were performed under UV irradiation. 70% and 44% removal of phenol and m-nitrophenol was obtained, respectively, with the membrane modified with 25% wt TiO_2 in the composite, while 78% and 48% for the membrane modified with 50% wt TiO_2. This increase in the percentage of removal was attributed to the increase in the number of active sites, which increases the generation of radicals for the degradation of organic compounds. However, by increasing the concentration to 75% wt of TiO_2, the removal reduced to 74% and 48%, of phenol and m-nitrophenol, respectively. The drop in the efficiency was explained with the agglomeration of nanoparticles under high dosages, with a consequent decrease in specific surface area and reduction in photocatalytic activity. Therefore, the GO avoids the agglomeration of the nanoparticles and there is an optimum dosage point of TiO_2 to intensify the photodegradation.

Zhu *et al.*, (2020a) evaluated the performance of polysulfone UF membranes modified with different amounts of TiO_2 and GO. The authors noted an increase in permeability with an increase in the concentration of TiO_2 and GO. However, in terms of rejection of dyes (Chrome Black T, Brilhante Blue, and Congo red), the rejection percentages decreased with increasing concentrations of TiO_2 and GO above 0.125 mg L^{-1} and 125 mg L^{-1}, respectively. The increase in permeability was attributed to the increase in the hydrophilicity of the membranes, confirmed by the reduction of the contact angle. Besides, the space between the GO leaves was increased by the addition of TiO_2 nanoparticles, with a consequent reduction in resistance to water

movement. Simonsen *et al.*, (2020) argue that a higher load of TiO_2 increases the amount of OH groups on the membrane surface, thus the surface energy is enhanced and the contact angle is reduced.

Ngo *et al.*, (2020) modified polyamide membranes through TiO_2-GO nanocomposite suspension filtration. A fixed concentration of TiO_2 (35 mg L^{-1}) was established for modification and different concentrations of GO were used (0.30 mg L^{-1} to 9.33 mg L^{-1}). The TiO_2:GO mass ratio varied from 117:1 to 3.75:1. An increase in the permeabilities of the modified membranes were observed with the increase in the dosage of GO. The authors justified this behavior by the membrane hydrophilicity increase caused by adding higher dosage of hydrophilic groups of GO to the coating. However, the permeability reached a maximum value in the modification with 4 mg L^{-1}. Above this concentration, the permeability was reduced due to the increase in resistance owing to the large number of particles deposited on the surface blocking the pores.

Future studies should be carried out to evaluate the maximum concentration of nanocomposites that increases the performance of the membranes under given conditions while not been leached during operation. The optimal TiO_2:GO mass ratio that cooperates for membrane stability should be better evaluated.

2.8 – Fouling control in TiO_2-GO nanocomposite membranes

The modifications of polymeric membranes with TiO_2-GO aim mainly at reducing fouling propensities and improving the membrane performance by means of permeability enhancement with the maintenance of elevated removal efficiency of contaminants. These nanocomposites reduce the spaces where contaminants could penetrate through the membranes. Also, the nanometric dimensions give them excellent properties owing to the high surface area per volume (LAMBERT *et al.*, 2009; QU *et al.*, 2013). Thus, they are interesting for photocatalysis or increased hydrophilicity. When it comes to the reduction of fouling in modified membranes, this can be due to the degradation of foulants in the feed by photocatalysis, the antibacterial properties of the nanocomposites, or the increased hydrophilicity of the membranes.

2.8.1 Degradation of fouling compounds by photocatalysis

Zhul *et al.*, (2017) modified cellulose membranes (0.45 μm) with TiO_2-GO composites. They observed that membranes modified only with GO have a greater capacity for adsorption of the

methylene blue dye (10 mg L^{-1}) than those modified only with TiO_2. Therefore, the modification of the membranes with TiO_2-GO composites favors the interaction of pollutants with the TiO_2, which increases the photocatalysis. By performing the dye filtration with and without UV light irradiation, the authors observed a stable flux in the absence of irradiation at around 2.5 L m^{-2} h^{-1} and a sharp drop, while under irradiation, the flux stabilized around 7.5 L m^{-2} h^{-1}. Besides, the removal of the dye without irradiation was around 72%, while under irradiation the removals were above 90%. Moreover, the authors observed that the flux recovered to 96% after 100 minutes of dye filtration in pure water, which indicates that the photocatalysis improved membrane performance by reducing fouling and there is a potential for application in wastewater treatment.

Yan *et al.*, (2019) modified PAN membranes with TiO_2-GO and observed a removal of 58.8% of methylene blue dye after 200 minutes of UV irradiation. The unmodified membrane and the modified one without irradiation were unable to remove the dye. Removal was only possible by photocatalysis. The modified membranes showed a recovery of 54% of the flux in water permeation after dye permeation. In contrast, the recovery of the membrane without modification with the nanocomposite was only 30%.

2.8.2 Antibacterial properties

Fouling caused by microorganisms is called biofouling. The biofouling arises by the adhesion of microbial cells to the surface of the membranes, inducing the formation of a biofilm layer that hinders the operational performance by a critical decrease in the flux. These microbial cell generate extracellular polymeric substances (EPS) that accentuate the process and, among the types of fouling, this is one of the most severe (PICHARDO-ROMERO *et al.*, 2020). The phenomenon is especially important in membranes used in bioreactors and desalination processes. The modification of membranes with TiO_2-GO nanocomposites attracts great attention of the scientific community due to the anti-bacterial properties of both materials.

When irradiated, TiO_2 promotes the formation of reactive radical species capable of promoting the death of microorganisms through a lipid peroxidation reaction (VATANPOUR *et al.*, 2012). GO, in addition to having anti-adhesive properties, which reduces the deposition of microorganisms, also promotes the rupture of the bacterial cell membrane, owing to its sharp edges (AKHAVAN; GHADERI, 2010; LIU *et al.*, 2011).

Zhu *et al.*, (2020b) proved the antibacterial capacity of membranes modified with TiO_2-GO testing E. *coli* colonies survival under the membrane surface. The numbers of alive and dead bacteria cells were counted at the beginning of the process and after 6 hours of contact with the membranes. The unmodified membrane showed a 19.7% reduction in the number of living bacteria, whereas the modified membrane showed an 87.8% reduction. The antimicrobial activity of PES membranes modified with TiO_2-GO was also tested by Jiang *et al.*, (2015). An E. *coli* dispersion was placed in contact with the membrane surface without modification and modified with the nanocomposite for 2 hours. Only 3% of viable E. *coli* bacteria remained on the modified membrane surface, while nearly 100% remained on the pristine membrane. Kim *et al.*, (2014) reported the complete sterilization in a film on TiO_2-GO membranes after 15 minutes of test.

2.8.3 Increased hydrophilicity of membranes

The hydrophobicity of most polymeric membranes is one of the main factors that cause fouling. Organic molecules, which make up most of the effluents, adsorb on the surface of the membranes and reduce the permeate flux, as well as increase the operating pressure and operating costs (KOULIVAND *et al.*, 2020; LEE; KIM, 2014). Changing the hydrophobic feature of membranes to hydrophilic can be achieved by the addition of nanocomposites with a large number of oxygenated groups, as it is the case with TiO_2-GO. The increase in hydrophilicity, through modification, therefore promotes the mitigation of fouling (Fig. 9).

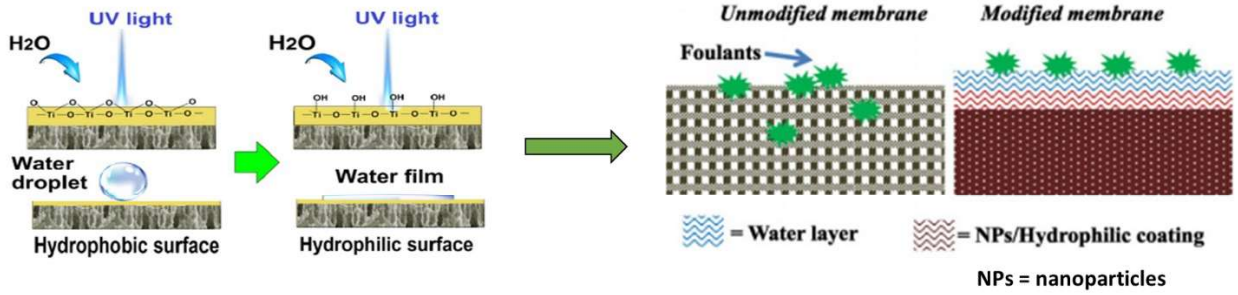

Figure 9 - Surface hydrophilicity of the membranes modified with TiO_2-GO.Adapted from Nasrollahi *et al.* and Jhaveri & Murthy (JHAVERI; MURTHY, 2016a; NASROLLAHI *et al.*, 2021) with copyright permission.

Kumar *et al.*, (2016) observed an increase in the water uptake of polysulfone membranes modified with TiO_2-GO as the load of composite used in the modification increased. The maximum value (70.3%) was reached in the modification using 5% wt TiO_2-GO. For the membrane without modification, this value was just 41.2%. This increase in the water-binding

in the membranes is due to the increase in the hydrophilicity of the structure by the presence of the groups like -COOH, -OH, and Ti-OH of TiO_2-GO. The contact angle of the membrane modified with 5% wt was equal to 50° and that of unmodified equal to approximately 75°. The water flux increased from 105.3 L m^{-2} h^{-1} for the case of the membrane without modification to 135.2 L m^{-2} h^{-1} with the addition of 0.2% wt of TiO_2-GO. Above this percentage, the permeate flux reduced owing to the low porosity of the membranes with a higher load of nanocomposites. Fouling tests showed a considerable reduction in the amount of HA adsorbed on the surface of the modified membranes (15 μg cm^{-2}) compared to those without modification (45 μg cm^{-2}) and a 93% flux recovery, while in the unmodified one the value was 73%. The presence of a hydrated layer on the membrane surface was responsible for reducing the amount of HA adsorbed and, accordingly, the fouling was reduced. (MORALES-TORRES et al., 2016)Morales-Torres *et al.*, (2016) obtained similar results in reducing the contact angle of PSF-PVP membranes from 77° to 61° after modification with TiO_2-GO.

2.9 – TiO_2-GO nanocomposite membranes applications

Membranes modified with TiO_2-GO nanocomposites are very promising for the treatment of wastewater effluents as reported in different studies, in which they have been tested in the recent years in different matrices (LIU *et al.*, 2021; WANG *et al.*, [s.d.]; ZHANG *et al.*, 2021d). Contaminants of emerging concern (i.e., drugs, hormones and herbicides), salts, acids, dyes and hydrocarbons are examples of these matrices. Although promising, such membranes are still mainly tested on laboratory and bench scales, and some details should be better clarified for their implementation on a large, industrial scale. Applications of TiO_2-GO nanocomposite membranes are summarized in Table 4.

Table 4 - Summarization of TiO2-GO nanocomposite membranes applications.

Membrane material	Modifying method	Treated effluent matrix	Main results	References
Celulose	Vacuum filtration	MB solution (10 mg L^{-1})	The TiO_2-GO membrane degraded 92% of the MB after 110 min UV light irradiation and exhibited 96% flux recovery capacity after 100 min when filtrating pure water under UV light.	(ZHUL *et al.*, 2017)
Cellulose acetate	Vacuum filtration	MB, RhB, MO or Congo Red (CR) solutions (50 mg L^{-1})	Membranes modified with TiO_2-GO nanorods significantly increased the water flow compared to some commercial nanofiltration membranes and maintained high dye rejection rates: MB (99.3%), RhB (99.4%), MO (99.3%) and CR (99.5%).	(LIU *et al.*, 2020)
Cellulose acetate	Filtration	CR dye solution (50 mg L^{-1})	There was a gradual increase in the efficiency of dye removal with the mass increase of TNS-GO (TiO_2 nanosheets-GO) in the membrane. However, although the 400 mg TNS-GO membrane could completely remove the dye, it exhibited lower flux and greater dye adsorption. It was concluded that the membrane with 100 mg of TNS-GO was the most efficient by comparing the difference between dye removal in the presence and absence of UV light. In addition, 3 cycles of photocatalyst reuse were performed which revealed that, with the exception of the membrane with 50 mg of TNS-GO, all other membranes evaluated could maintain dye removal capacity since the flux decline provided sufficient time for photocatalytic degradation.	(NAIR; JAGADEESH, 2017)

Membrane material	Modifying method	Treated effluent matrix	Main results	References
Cellulose triacetate (rTAC)	Electrospinning	Oil (n-hexadecane) and water emulsions with and without the addition of sodium dodecyl sulfate (SDS) as a surfactant.	The oil rejection coefficients were higher for emulsions prepared without added surfactant for all samples. The best performance was found in the TiO_2/GO/rTAC-np samples, with an oil rejection coefficient of 98.9% and 88.2% for emulsion prepared without and with the addition of SDS, respectively. The results presented suggest that TiO_2/GO/rTAC-np has a great potential for applications in removing emulsified oil.	(NASEEM *et al.*, 2018)
Polyacrylonitrile (PAN)	Layer-by-layer	MB solution (20 mg L^{-1})	For photocatalytic performance, the TiO_2-GO membrane has a good removal rate of 58.8% under UV, while the virgin PAN-based membrane has failed to remove MB.	(YAN *et al.*, 2019)
Polyamide (PA)	Filtration	MB solution	MB retention of the modified membranes remained high (99%) and equivalent to the base membrane. However, the coated membranes, especially the UV-irradiated PA/TiO_2-GO coated membrane, demonstrated a simultaneous increase in both flux and antifouling properties. As an example, after 120 min of filtration of the MB blue solution, the maintained flux ratio of the uncoated membrane was about 52.9% while the one of the PA/TiO_2-GO coated membranes under UV irradiation was still about 80%.	(NGO *et al.*, 2020).

Membrane material	Modifying method	Treated effluent matrix	Main results	References
Polyamide (PA)	Filtration	NaCl (2000 mg L^{-1}) and Na_2SO_4 (1500 mg L^{-1}) solutions. In order to simulate sea water contaminated with oil and analyze hydrocarbons rejection, the NaCl solution was enriched with toluene, dodecane, isooctane, and tridecane, 500 mg L^{-1} of each	It was observed that the performance of the modified membrane was optimized in terms of salt rejection, hydrocarbons rejection, and water permeability due to the increase in the negative surface charge, hydrophilicity and decrease in the surface roughness of the membranes. The bare membrane had approximately 40 L m^{-2} h^{-1} permeate flux, 81% NaCl rejection and 86% Na_2SO_4 rejection. The best performance was achieved by the membrane with eight layers of TiO_2-GO coating with around 62 L m^{-2} h^{-1} permeate flux, 97% salt rejection, and 100% hydrocarbons rejection.	(AL-GAMAL; FALATH; SALEH, 2021)
Polyamide (PA)	Surface coating (self-assembly)	NaCl aqueous solution (1 g L^{-1}) evaluated before and after exposure of the membrane to chlorine (immersed for 24 hours in NaOCl (2 g L^{-1}))	It was found that salt rejection was greater for modified membranes before and after exposure to chlorine compared to the membrane without changes. As an example, after 20 hours of exposure to chlorine, the unmodified membrane showed a 60% salt rejection rate, while the TiO_2-GO membrane had a 75% rejection rate. In addition, it was observed that the degree of resistance to chlorine increases with higher quantities of TiO_2-GO layers. Membranes with layer numbers less than or equal to 6 also presented increased water flux.	(SHAO *et al.*, 2017b)

Membrane material	Modifying method	Treated effluent matrix	Main results	References
Polyethersulfone (PES)	Blending (Interfacial polymerization)	NaCl, Na_2SO4, $MgCl_2$, or $MgSO_4$ solutions (1 g L^{-1})	Embedded TiO_2-GO membranes showed improvements in the permeate flux of 2 and 5 times compared to pristine membranes and modified GO membranes, respectively.	(WANG *et al.*, 2017a)
Polysulfone (PSF)	Blending (Phase inversion method)	Aqueous solutions containing trifluralin, butachlor, glyphosate or 2,4-Dichlorophenoxyacetic (2,4-D) acid with the initial concentration of 20 mg L^{-1}, each one.	The membranes modified with TiO_2-GO nanocomposites have increased their adsorptive capacity, with a consequent increase in the rejection of pollutants. The membrane having 0.5% wt. of TiO_2-GO (10%) presented the highest efficiency, with a rejection of 73, 69, 61, and 53% for trifluralin, butachlor, 2,4-D and glyphosate, respectively. In addition, the membrane was found to be an herbicide adsorptive filter due to the formation of sponge like structure with interconnected macrovoids in the sub-layer region	(HOSSEINI; TOOSI, 2019)
Polysulfone (PSF)	Blending (Phase inversion method)	Organic contaminants and the ammonia removal in natural rubber industry wastewater (primary treatment effluent).	For PSF-TiO_2/GO membranes under UV irradiation, permeate flux, organic contaminants and ammonia removals of 13.05 L m^{-2} h^{-1}, 60.98% and 91.27% were obtained, respectively. On the other hand, for the pristine PSF membrane the permeate flux, organic and ammonia removal rates were approximately 5 L m^{-2} h^{-1}, 61% and 55%, respectively.	(KUSWORO *et al.*, 2021)
Polysulfone (PSF)	Vacuum filtration	Chrome black T, CR and Brilliant Blue R250 dyes solutions (0.1 g L^{-1}).	After long-term filtration (9 h), the permeability (3.6 L m^{-2} h^{-1} bar^{-1}) and all dye rejection (98%) remained constant, resulting in a stable and robust membrane.	(ZHU *et al.*, 2020a)

Membrane material	Modifying method	Treated effluent matrix	Main results	References
Polysulfone (PSF)	Blending	Humic acid (HA) solutions with concentrations of 10, 20, 40 and 50 mg L^{-1} at pH = 7.	The efficiency of HA removal from hybrid membranes in 10 mg L^{-1} HA solution increased with the amount of TiO_2-GO loading. Membranes with 0 and 5 wt% of GO-TiO_2 (to total wt% of PSf) were able to remove 54.6 and 98.7% HA from the 10 mg L^{-1} solution, respectively. It was observed that the removal efficiency of both membranes for HA decreased with a higher HA concentration.	(KUMAR *et al.*, 2016)
Poly vinyl chloride (PVC)	Blending (Non-solvent induced phase separation (NIPS))	Humic acid aqueous solution (100 mg L^{-1}).	The pure water flow from the membrane increased with the addition of TiO_2-GO nanofilm content in the membrane. The rejection rate of humic acid remained almost equal (above 98%) for samples with and without the addition of GO-TiO_2.	(JHAVERI; PATEL; MURTHY, 2017)
Polyvinylidene fluoride (PVDF)	Vacuum filtration	Oil-in-water (hexadecane and water) emulsion (200 mg L^{-1}).	For both types of membranes, the oil rejection rate was greater than 97.5%, however, with increasing TiO-GO mass ratio, oil rejection ratios of TiO_2-GO membranes gradually increased from 97.5% to 99%. In addition, comparison experiments were carried out between commercial ultrafiltration and TiO_2-GO (with TiO_2-GO mass ratio of 4) membranes. These experiments suggested a greater permeability and better antifouling properties of the TiO_2-GO membrane in addition to presenting a higher oil rejection rate.	(WU *et al.*, 2018)

Membrane material	Modifying method	Treated effluent matrix	Main results	References
Polyvinylidene fluoride (PVDF)	Blending (Phase inversion)	BSA solution (1 g L^{-1}).	All PVDF hybrid membranes containing TiO_2-GO exhibited higher water flux and BSA rejections than the pure PVDF-GO membrane. PVDF/TiO_2 (15%)/GO showed the best performance with a water flux of 158 L m^{-2} h^{-1} and BSA rejection of 89%, while PVDF/GO obtained approximately 40 L m^{-2} h^{-1} and 60%, respectively, for the same parameters. In addition, the authors performed analysis by modifying the compounds of TiO_2(15%)-GO with polyethylene glycol (PEG) with different molecular weights (PEG-600, 1000 or 2000). It was observed that PEG grafted on TiO_2–GO acted as a pore-forming additive in the preparation of PVDF membranes, in addition to increasing the pore structure on the membrane surface. Consequently, membranes with PEG-modified TiO_2–GO composites performed better than those without modifications and the hybrid PVDF membrane containing TiO_2–GO-2000 exhibited the best performance with a water flow of 200 L m^{-2} h^{-1} and a BSA rejection of 91.4%, in addition to better anti-fouling performance	(WU *et al.*, 2019a)
Poly(vinylidene fluoride-trifluoroethylene) [P(VDFTrFE)]	Electrospinning	MB solution (10^{-5} mol L^{-1}).	Even with a low content of TiO_2-GO (3%, w/w), the membranes showed excellent photocatalytic performance with approximately 100% degradation of the MB solution after 90 min of exposure to visible light. In addition, under UV radiation, the membrane with 5% w/w of TiO_2-GO exhibited about 80% greater MB removal compared to the corresponding sample without GO.	(ALMEIDA *et al.*, 2016)

Although many applications of TiO_2-GO nanocomposite modified membranes are being tested, most of the treated matrices are dyes, salts, or synthetic effluents of isolated molecules. The understanding of the operation of such membranes in the treatment of complex matrices, such as real wastewater, is still a gap that needs to be better elucidated.

2.10 - CONCLUSIONS AND PERSPECTIVES

The association of membranes with TiO_2-GO nanocomposites is a promising way in obtaining membranes with better performances. Nanocomposites increase the hydrophilicity of polymeric membranes due to their oxygenated functional groups, consequently increasing the permeate flux and reducing the deposition of organic fouling. Membranes with antimicrobial behavior are obtained by adding nanocomposites. Biofouling is mitigated, and process performance is improved. Photocatalytic activity of the membranes is obtained through modification with the nanocomposites, promoting pollutants attack and organic fouling reduction. Also, the photoactivity of the catalysts allows the removal of organic compounds from effluents such as contaminants of emerging concern.

Different modification techniques have been used. Although nanomaterials are more evenly distributed over the membrane in the blending technique producing more stable membranes, they have less contact with the contaminants. Surface coating and filtration techniques are simpler and promote greater nanomaterials exposure to contaminants; nevertheless, more unstable membranes are obtained. The load of nanomaterials influences the performance of the membranes, and a higher load promotes greater hydrophilicity and greater photocatalytic activity. But high doses can promote the agglomeration of nanomaterials, causing the formation of macropores and efficiency reduction.

The effects of irradiation on the surface of modified membranes should be addressed in future studies. Although one of the main goals of GO associated with TiO_2 is the activation of the catalyst under visible light, most studies still conduct tests with UV irradiation, which can compromise the polymeric structure of membranes and, consequently, their lifespan, limiting scale-up. In this regard, the electronic transfer mechanism between GO and TiO_2 needs to be better evaluated, and the best proportions of materials defined for the optimum performance. It is also necessary to investigate the mitigation of the deposition of inorganic fouling, such as salts, on the surfaces of modified membranes, since the depositions can reduce the permeation

area and the efficiency of the nanocomposites. It is also worth noting that, as this is a hybrid process, the residence times of photocatalysis and membrane separation must be well adjusted.

The technology has the potential to treat complex effluents and ensures highly robust membranes. However, some gaps still need further attention for its application on an industrial scale. Most studies are on a bench scale and focus on the degradation of synthetic matrices and dyes. Further studies should consider the treatment of real matrices, such as industrial and municipal wastewater effluents. Besides, the stability of modified membranes over a practice-relevant period of operation (months, years) is not yet investigated. The estimated lifespan is not known, and this is a critical point that needs to be further clarified. Fouling mitigation strategies should be better evaluated that do not compromise the integrity of the membrane, e.g., what are the effects of backwashing and cleaning on the loss of the catalyst? Studies for establishing cleaning protocols should be carried out, evaluating the effects of chlorinated, acidic, and alkaline solutions and which concentrations are best suited to each membrane. The effluent pH and temperature effects on the performance and integrity of the membranes also need to be analyzed. TiO_2-GO based membranes are a promising technology for water purification, but still many challenges need to be addressed in the future to make that technology ready for prime time.

CHAPTER 3

Converting recycled membranes into photocatalytic membranes using greener TiO_2-Graphene oxide nanomaterials

3.1 INTRODUCTION

Membrane separation processes are widespread technologies effectively applied to water and wastewater treatment (HUANG; SHANG; LI, 2021; JOHARI *et al.*, 2021; NIKBAKHT FINI *et al.*, 2021; ZHANG *et al.*, 2021b). Given their robustness, ease of operation, and modularity, MSPs were also considered in decentralized treatment approaches for water supply, solving different challenges related to water quality and quantity especially in developing and transition countries (CAPODAGLIO *et al.*, 2017; PETER-VARBANETS *et al.*, 2009).

Despite their use and advantages, proper fouling control is a key for achieving a stable performance of most pressure driven membranes. The phenomenon contributes to a decline in flux and physicochemical quality of the permeate. To maintain permeate flux in fouled membranes, higher operating pressures are required, potentially promoting irreversible damage to the membrane, which in turn may require its replacement.

Most membrane modules operate for 2-5 years (DE PAULA; AMARAL, 2017; ZONDERVAN; ROFFEL, 2007) until their replacement. Passed that period, in developing countries membranes are generally discarded in landfills as a secondary pollution source. Grossi *et al.*, (2021) estimated that 900 tons of reverse osmosis (RO) elements waste were generated in Brazil from 2016 – 2019, and predicted that the amount of waste produced would increase to 1,800 tons by 2024. Furthermore, the worldwide amount of RO membranes annually disposed in landfills reached 16.5 tons (equivalent to 37.1 m^3) in 2018 (MORADI *et al.*, 2019). The increased value is directly associated with the growth of membrane market shares in water and wastewater treatment systems. For example, the global desalination capacity increased from 66.4 million m^3/day in 2012 to 99.7 million m^3/day by 2018, and in 2016 RO technology accounts for 65% of the globally installed desalination capacity (MITO *et al.*, 2019). A direct response to the increased demand would be the increase in membrane manufacture, however, that is intrinsically correlated with several environmental impacts (YADAV *et al.*, 2021). Yadav *et al.*, (2021) suggested that replacing fossil-based polymers with bio-based alternatives could reduce the environmental impacts by 35% associated with membranes manufacturing. Furthermore, another approach would be the use of recycled membranes.

De Paula & Amaral, (2017) recommended the conversion of end-of-life reverse osmosis (RO) membrane into ultrafiltration-like membranes through chemical oxidation. Rather than being disposed, end-of-life RO could be recycled by a low-cost oxidative treatment producing a

porous membrane with properties similar to ultrafiltration membranes. Besides the environmental gains, the recycled membranes had also lower acquisition costs (for instance the average costs of commercial membranes are 25.13 US$/m², of recycled membranes 0.22 US$/m² (COUTINHO DE PAULA; SANTOS AMARAL, 2018)), representing additional benefits to their use. Moreira *et al.*, (2021) recently investigated the use of recycled RO membranes for water treatment which apart from the effectiveness in terms of pollutants removal, reported a flux decay greater than 40% due to fouling. To address this issue, recycled RO membranes could be modified by nanocomposites.

Among the materials available for membrane modifications, titanium dioxide (TiO_2) has a superior performance to alleviate fouling and improves membrane rejection efficiency (AYYARU; AHN, 2018; LI *et al.*, 2019a). The material also exhibit photocatalytic characteristics, which would be interesting when considering the removal of chemicals of emerging concern, such as pharmaceutically active compounds (PhACs), increasingly recurrent in aqueous matrices (REIS *et al.*, 2019; SANTOS *et al.*, 2020b). Despite the promising performance of TiO_2 modified membranes shown in recent literature, their performance can be further improved when other nanomaterials, such as graphene oxide (GO), are incorporated, too.

The use of GO associated with TiO_2 aims to increase the performance and reduce certain limitations of the semiconductor such as its quickly electron-hole recombination rate and narrow photoabsorption spectrum (ZHANG *et al.*, 2021e). In turn, the nanocomposite TiO_2-GO increase the performance of the modified membranes. The electrons generated by UV irradiation of TiO_2 can interact with the GO sheets, reducing some groups of its surface, and the remaining electrons are relocated along the basal planes. Such electrons can react with adsorbed O_2 to form $O_2^{\cdot -}$ radicals that can oxidize chemicals in the medium (WILLIAMS; SEGER; KAMT, 2008). This effective charge transfer between TiO_2 and GO increases the photocatalytic activity of TiO_2 in the TiO_2-GO composite. The formation of Ti-O-C bonds can also expand the light absorption to longer wavelengths offering a great opportunity to use the photocatalytic activity driven by visible-light (MORALES-TORRES *et al.*, 2012). GO bandgap values in the range of 2.1-2.2 eV are reported in the literature, which corresponds to an activation at wavelengths around 550 to 560 nm, being in the visible light region of the electromagnetic spectrum (WILLIAMS; SEGER; KAMT, 2008; ZHANG et al., 2021e). Moreover, the GO sheets can avoid the TiO_2 nanoparticles agglomeration and favor the

interaction of some pollutants with the membrane surface by the presence of functional groups able to adsorption. These groups can also increase the membrane hydrophilicity (KUMAR *et al.*, 2016).

There are several methods employed for the fabrication of modified membranes as summarized by Leong *et al.*, (2014). Nevertheless, to the best of our knowledge, none photocatalytic membrane was ever obtained with the use of RO recycled membranes as a support. In addition, the major part of the studies uses commercial TiO_2 in modifications, which is different from the proposal of the present study where we use greener catalyst, synthesized with energy reduction. Thus, the developed membranes are in line with requirements of a circular economy and eco-efficient processes. From the modification techniques available, we decided to investigate and compare the performance of recycled RO membranes modified with TiO_2+GO by self-assembly (1), sonication and further filtration of GO and TiO_2 solutions (2), TiO_2+GO incorporated by dopamine polymerization (3), and TiO_2 incorporated by dopamine polymerization (4). The modified membranes were characterized by their morphology, composition, and film adhesion. Flux, fouling, permeability, and dyes removal efficiencies were evaluated as well, comparing the modified and unmodified RO recycled membranes. The best performing membrane was then finally tested for the removal of seven indicator PhACs commonly present in surface water matrices. The use of photocatalytic membranes to threat complex matrixes, as a mix of emerging pollutants, is also a novelty.

3.2 MATERIALS AND METHODS

3.2.1 Reagents

The reagents used in the present work were dopamine hydrochloride (Merck); eriochrome black T (Synth); hydrogen peroxide (35%) (Sigma-Aldrich), hydrochloric acid (37%) (Sigma-Aldrich); Micrograf HC30 graphite (Nacional de Grafite, Brazil); methylene blue (Exodo Científica); potassium permanganate ($KMnO_4$) (Merck); sodium hydroxide (NaOH) (Dinâmica); sodium nitrate ($NaNO_3$) (Merck); sulfuric acid (95-98% H_2SO_4) (Sigma-Aldrich), and titanium tetrachloride ($TiCl_4$) (Merck). All reagents were analytical grade and all solutions were prepared with Milli Q ultrapure water.

3.2.2 Fabrication of the photocatalytic membranes

The photocatalytic membranes are composed of recycled membranes, titanium dioxide nanoparticles, and graphene oxide. The recycled membranes were obtained by oxidation of end-of-life reverse osmosis membranes, by immersion in a commercial sodium hypochlorite bath, at a contact time intensity of 300,000 ppm·h at room temperature. Details on this methodology can be found elsewhere in our previous work (DE PAULA; GOMES; AMARAL, 2017). The end-of-life membrane sample used in this study was taken from a spiral-wound module, specifically the model FilmTec BW30 of $2.0x10^{-1}$ m in diameter, 1.0 m in length, and an active area of 41 ± 3 m^2. This membrane was used in a desalination plant of the Água Doce Program, Brazil. The program aims to promote sustainable use of groundwater resources and provide potable water for human consumption in areas with critical water scarcity in the Brazilian semiarid region through desalination systems using RO technology. 811 RO plants are in operation serving 320,000 people in the Água Doce Program.

The titanium dioxide used in the synthesis of photocatalytic membranes was obtained through a greener route, with a reduction in the consumption of reagents and energy. Details of the route and characterization of the materials can be found in our previous study (OLIVEIRA; VIANA; AMARAL, 2020). In summary, titanium tetrachloride and water were used as precursors to obtain TiO_2 nanoparticles in the anatase crystallographic phase, with an average crystallite size of 14 nm.

Graphene oxide was prepared from natural graphite powder according to Hummers modified method (PARK *et al.*, 2012). Briefly, the graphite was oxidized by a mixture of $KMnO_4$ and H_2SO_4 under magnetic stirring until homogenization. The mixture was placed in an ultrasonic bath and H_2O_2 was added. The mixture was washed successively with 10% HCl solution, subsequently rinsed with deionized water until pH 7, and then centrifuged. Finally, the dispersion was washed with distilled water until pH ~ 6 and the material obtained was dried by freeze drying. The percentage of oxygen in the GO is 32.4%.

Four different routes for TiO_2-GO incorporation in recycled membrane were evaluated. The membranes were humidified in 200 mL of ethanol (50% v/v) before modification in all routes. This process aimed to swelling the polymeric matrix, increasing the hydrophilicity. Route 1 is described in the literature as self-assembly and is based on the work of Gao; Hu; Mi (2014a). The recycled membrane was immersed in deionized water for 2 hours prior to modification.

Then it was stuck on a glass plate. 0.25 g of TiO_2 was dispersed in deionized water and sonicated during 30 minutes. The suspension was poured over the recycled membrane and constantly stirred in a shaker for 3 hours at room temperature. After this time, the membrane was rinsed to remove any residuals and was dried in an oven at 65 °C. Subsequently, graphene oxide solution (1g L^{-1}) was poured over the membrane, which was soaked with ethanol 95% v/v and exposed to UV light for 15 min to partially reduce the GO and form strong bonds between the GO and TiO_2.

Route 2 was adapted from the work of Zhu *et al.*, (2020a), in which 2.5 mg of GO were dispersed in 100 mL of water and sonicated during 2 hours while a TiO_2 (0.25 mg L^{-1}) suspension was also sonicated separately. The TiO_2 suspension and the GO solution were mixed and sonicated again for 1 hour. The mixture was filtered three times in an Amicon dead-end cell (UFSC20001) fitted with a 28.7 cm^2 recycled membrane and pressurized by compressed air at 2 bar.

Route 3 is based on modifications reported by Zhang *et al.*, (2013) and Zhang *et al.*, (2017), in which a TiO_2 suspension was prepared in a basic medium (pH 12) and sonicated. An aqueous GO solution was mixed with the TiO_2 suspension and subsequently sonicated. A dopamine solution was also prepared in a basic medium. The dopamine solution was transferred to the Amicon cell fitted with a 28.7 cm^2 recycled membrane and kept for a while to promote the dopamine polymerization. The TiO_2-GO suspension was poured over the membrane and kept at rest. The excess was washed with deionized water. The modification was also promoted using only TiO_2 and dopamine (route 4) following the same procedure, except for the addition of GO. Table 5 presents the abbreviations used in the figures regarding the modification routes in the document.

Table 5 - Specifications of the different modification routes.

Route	Components	Abbreviation
1	TiO_2+GO	-
2	TiO_2+GO	Mod. Filtration
3	Dopamine+TiO_2+GO	Dop+TiO_2+GO
4	Dopamine+TiO_2	Dopamine+TiO_2

3.2.3 Photocatalytic membranes characterizations

The photocatalytic membranes were characterized by scanning electron microscopy (SEM) coupled with Energy-dispersive spectroscopy (EDS) (Jeol JSM-IT300 microscope) to verify the morphology of the obtained membranes, as well as to verify the changes in their thickness after modification. The elemental composition of the membranes was also assessed using this technique. Attenuated total reflection Fourier-transform infrared (ATR-FTIR) spectra of the recycled membranes prior to and after modifications were recorded using a FTIR Shimadzu IRAffinity-1 instrument. The samples were analyzed by direct exposure to radiation in the ATR module in the range of 400-4,000 cm^{-1} (resolution: 4 cm^{-1}; number of scans: 20). All the membranes were washed after the modifications and cleaned softly with tissue paper in order to verify the stability of the surface coverage. Visual inspections of the coverage were carried out.

3.2.4 Impact of the modifications in the membrane performances

The performance tests were conducted in an Amicon dead-end bench system (acrylic module, operating pressure of 1 bar, effective permeation area of 28.7 cm^2). Flux normalization to 25 °C was carried out using a correction factor related to the fluid viscosity (Eq. 1),

$$J_N = \frac{\Delta V}{A \Delta t} . \frac{\mu(T)}{\mu(25\ ^\circ C)} \quad (1)$$

where J_N is the normalized permeate flux at 25 °C, is the permeate volume per time, A is the permeation area, μ(T) is the water viscosity at the process temperature, and μ(25 °C) is the water viscosity at 25 °C.

The water permeability at 25 °C was obtained using the linear regression of the pressure versus the normalized flux of distilled water in the recycled membrane at pressures ranging between 0.5 and 3 bar.

In order to investigate the modifications in the rejection capacity of the modified membranes, eriochrome black T dye removal assays were performed. 120 mL of the dye solution (100 mg L^{-1}) were permeated on the synthesized membranes, separately. The permeation occurred in the absence of irradiation. 10 mL of permeate samples were collected sequentially and the time for each ten-milliliter collection measured.

Methylene blue was also used as a model pollutant solute. In this case, the test was conducted without permeation. The recycled membrane modified by the dopamine-TiO_2-GO route was immersed in 300 mL of methylene blue solution (10 mg L^{-1}). Tests with UV irradiation (low pressure (6W) mercury vapor lamp emitting 254 nm radiation) and without irradiation were performed. A control sample of only the dye without membrane was irradiated for comparison. Samples were collected every 20 minutes to assess the reduction in the dye concentration. The tests were performed in a dark box.

The dye concentration of each sample was obtained by UV-Vis spectrophotometer at the maximum absorbance wavelength (525 nm for eriochrome black T and 665 nm for methylene blue, respectively) based in an external calibration curve (R^2>0.99).

3.2.5 Pharmaceutical active compounds removal

Based on the best results found in terms of stabilities of the nanocomposites coverage and the fluxes, observed in the experiments with the dyes, degradation tests with a synthetic matrix composed of six different PhACs (concentration of 1 μg L^{-1} each) simulating wastewater effluent quality after secondary treatment were performed. These PhACs were betamethasone (BET), ketoprofen (KET), fenofibrate (FEN), fluconazole (FLU), loratadine (LOR), and prednisone (PRE), and their main physical-chemical properties are summarized in Table A.2 (Appendix). Their selection is based on their previous detection in surface and groundwater, drinking water, or treated municipal wastewater effluents (JELIC *et al.*, 2011). They have also been detected in Brazilian supply waters, are on the list of the top ten best-sellers or highest sales in 2015 in Brazil, and are provided free of charge by the Brazilian public health system (CAROLINE RICCI *et al.*, 2021). A stock solution with a concentration of 2 mg L^{-1} of each drug in methanol was prepared and stored at –20 °C to avoid degradation. The stock solution was added to a cylindrical reactor to generate a concentration of 1 μg L^{-1} of each PhAC. The tests were performed using a submerged plat and frame module. Modified membranes (Route 3) fragments (12x17 cm) were fitted in both sides of the module (Figure 10). The UV lamp was positioned above the module. The test lasted for about 90 minutes with a 20% recovery rate (operation pressure = 0 bar). According to the methodology described by Faria *et al.*, (2020), the detection of the concentrations of the PhACs after treatment were determined by high-performance liquid chromatography coupled with a quadrupole time-of-flight mass spectrometer.

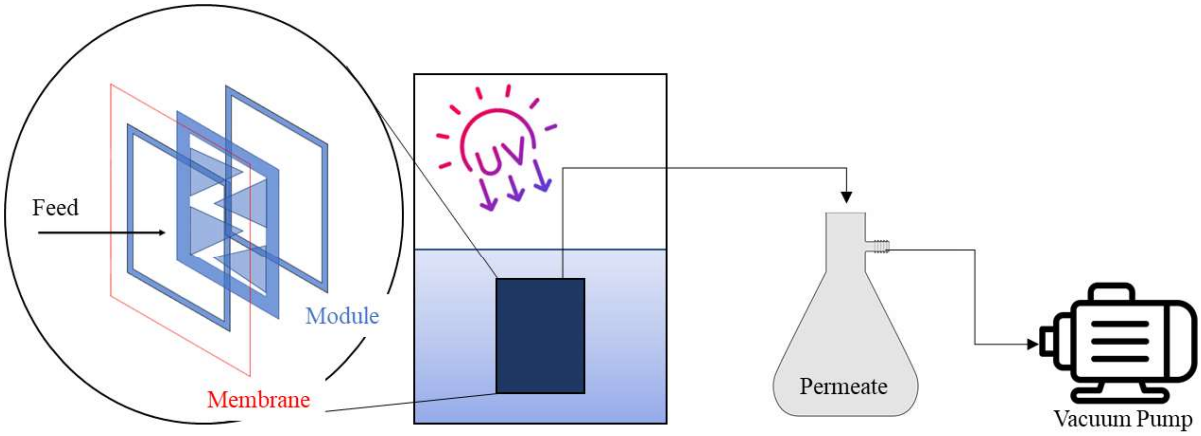

Figure 10 - Schematic design of the experimental apparatus.

3.3 RESULTS AND DISCUSSION

3.3.1 Characterization of the photocatalytic membranes

The original BW30 membrane was characterized by a permeability of 3.0 L h^{-1} m^{-2} bar^{-1} and a rejection of NaCl (2.0 g L^{-1}) of 99.5% (DOW, 2012). The characteristics of the recycled membrane are permeability equal to 86 ± 11.4 L h^{-1} m^{-2} bar^{-1}; 16.7 ± 2.5% of saline rejection (NaCl 2.0 g L^{-1}); contact angle of 75.5 ± 1.7° and roughness of 6.13 ± 0.86 nm. The increase in permeability and loss of saline rejection are associated with changes in the selective layer of the membrane due to the degradation of the aromatic polyamide layer.

A low adhesion of nanoparticulate materials to the recycled membrane surface was verified in depositions by self-assembly type (route 1) as shown in Figure 11(a). When washing was promoted to remove the material in excess, a great portion of the nanoparticulate material detached from the membrane (Fig. 11b). Several studies focus on this modification technique and characterize it as practical and versatile due to its methodological simplicity. However, the main limitation is the weak binding forces between nanomaterials and the surface of the membranes (MANSOURPANAH *et al.*, 2009) rendering it a non-suitable method for this kind of application.

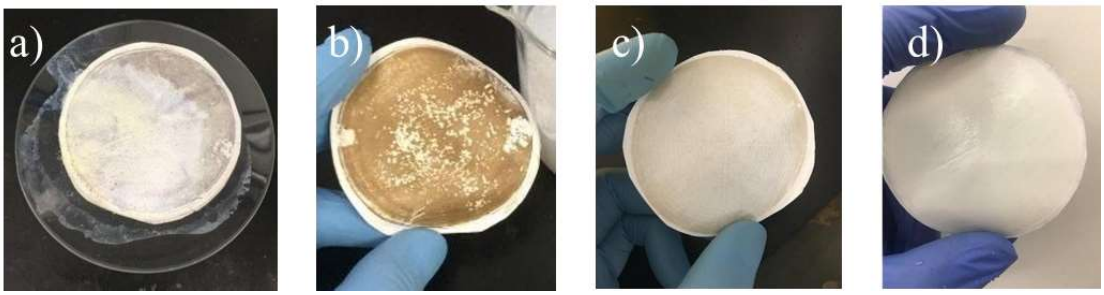

Figure 11 - Samples of membranes modified with TiO_2-GO. a) self-assembly modification; b) washing after self-assembly modification; c) filtration modification of the suspension, and d) modification using dopamine.

For pristine RO membranes, being composed of aromatic polyamide as a selective layer and polysulfone and polyester as support layers, a greater interaction between TiO_2 and GO with the selective layer through hydrogen bonds is expected. In the case of TiO_2, the connection is between the hydroxyl of the oxide and the carbonyl of the polyamide and between the carbonyls of the GO and the hydroxyls of the TiO_2 (SHAO *et al.*, 2017b). When recycled membranes are used, since the selective polyamide layer was partially removed by the oxidative process (Fig. 12), the weak interaction between the materials and the membrane surface may be associated with weak connections between the nanomaterial functional groups and the supporting layers of polysulfone and polyester. Moreover, the non-uniformity of the membrane surface chemical composition after the recycling process could further contribute to this low adhesion.

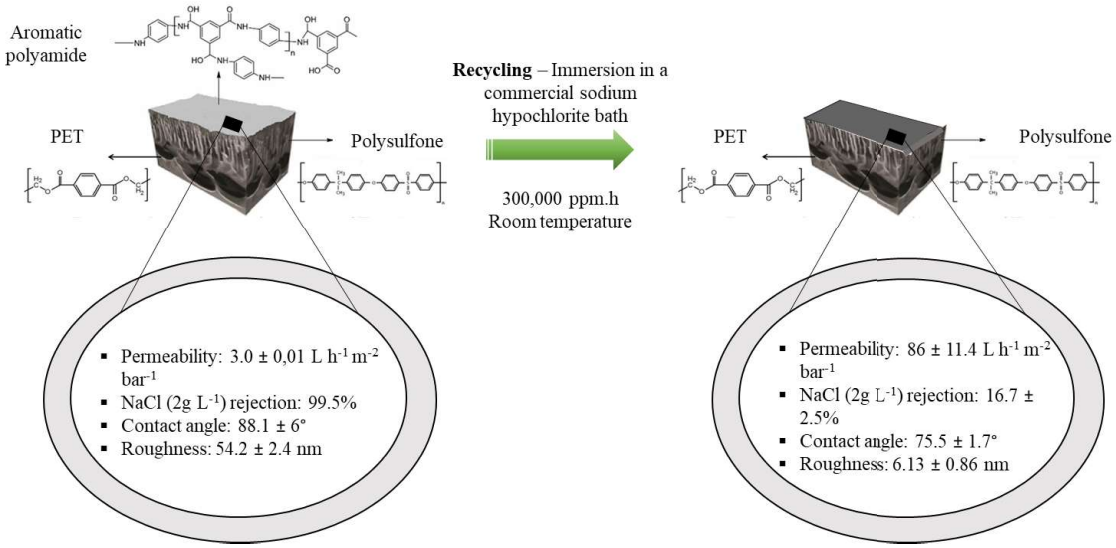

Figure 12 - Schematic representation of the RO membranes characteristics before and after recycling process.

Figure 13 shows the SEM micrographs of the recycled membrane prior to modifications. The surface of the recycled membrane (Fig. 13-a) is predominantly smooth, represented by uniform

coloration throughout the observed area, with few topographical irregularities. This characteristic is caused by the recycling process, where the selective polyamide layer characterized by the finger like structure was removed, leaving the intermediate polysulfone layer. The higher portions in the plane are the remnants of the selective layer. Irregular pores of different dimensions and shapes along the membrane surface can be found. The average pore size is 4.7 ± 2.9 μm, based on the measurement of 170 pores, reaching up to approximately 20 μm. It is worth highlighting that, after the recycling process, the dense reverse osmosis membranes are transformed into porous membranes intermediate between ultra (pore size range: 0.001 – 0.05 μm) and microfiltration (pore size range: 0.05 – 10 μm) (SENÁN-SALINAS *et al.*, 2019). The micrographs in the cross-section (Fig. 13-b) clearly show two layers with different thicknesses and shapes (highlighted with yellow arrow in the figure): the structural polyester, lower and thicker, and the polysulfone, thinner above. Elemental analysis by EDS detected carbon, sulfur, and oxygen, characteristic elements of the mentioned polymers. Depending on the region analyzed (not shown), nitrogen was also detected, showing residual traces of the removed selective layer of the RO membrane.

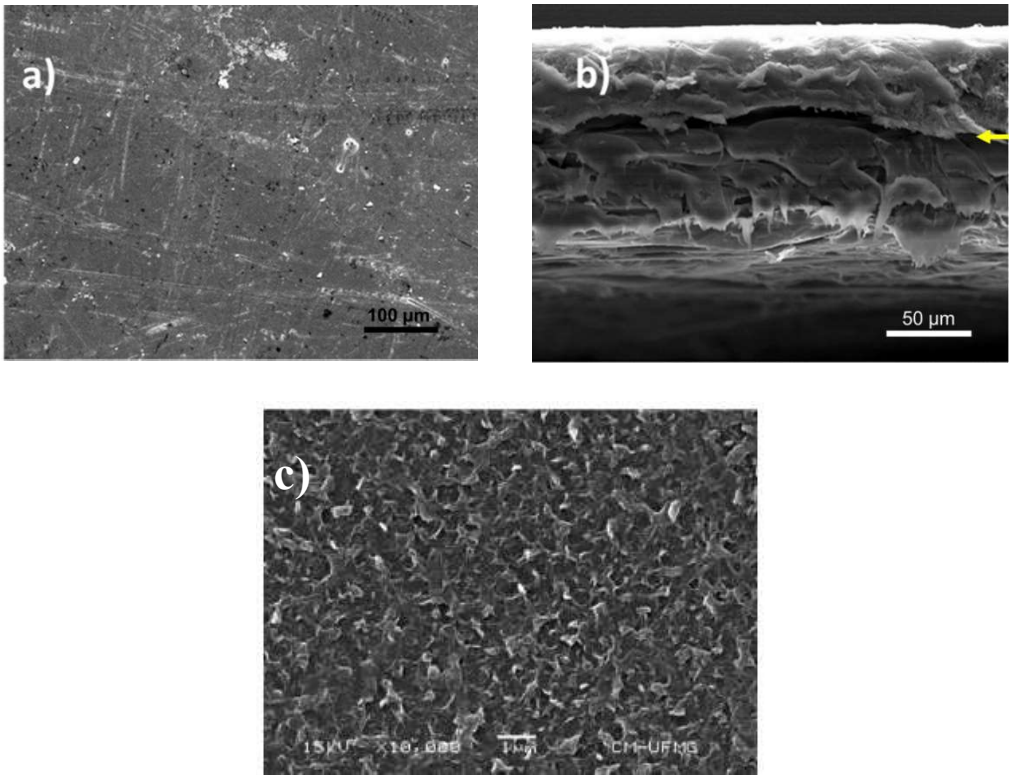

Figure 13 - SEM micrographs of the recycled membrane (a), cross-sectional image of the recycled membrane (b) and micrograph of new RO membrane (c).

A different behavior was obtained when the nanocomposite suspension was filtered after its sonication. As shown in Figure 11-(c), a uniform and well-adhered layer was formed onto the membrane's surface, even after rinsing with water. This behavior has already been detailed by other authors who reported that stable suspensions of graphene oxide sheets could be easily transformed into well-laid films using filtration (XU *et al.*, 2013a).

On the other hand, the dopamine modification method generated a membrane with a homogeneous film on its surface (Fig. 11d) stable even after washing. Mechanical friction was also promoted on the surface of this membrane with a tissue paper, and no alteration or detachment of the formed layer was noticed. This greater stability of the membrane is due to the dopamine, which acted as an adhesion substance for the nanomaterials on the membrane surface. Dopamine can self-polymerize in basic media, promoting the bond between the materials (LEE *et al.*, 2007). Zhang *et al.*, (2013) compared the effectiveness of bonding TiO_2 nanoparticles to the surface of polyamide membranes using self-assembly methods and the application of dopamine. Washings of the obtained membranes and cleaning of its surfaces with a cotton tissue was carried out. Using SEM micrographs, the authors verified the surface coverage by the particles in the method using dopamine, even after washing and cleaning with cotton tissue.

Since the synthesized membranes will be used in environmental applications, it is desirable that they have the stability to treat different water matrices and can withstand severe operational conditions, such as elevated pressure and shear forces created by the flow of fluids. Thus, the most promising modification technique generates the most stable coverage in terms of binding strength of the nanocomposites and better separation/degradation performance.

SEM micrographs with X-ray maps of the modified membranes by routes 2, 3 and 4 are depicted in Figure 14. The membrane modified by route 1 was not evaluated because the nanocomposite coverage completely detached.

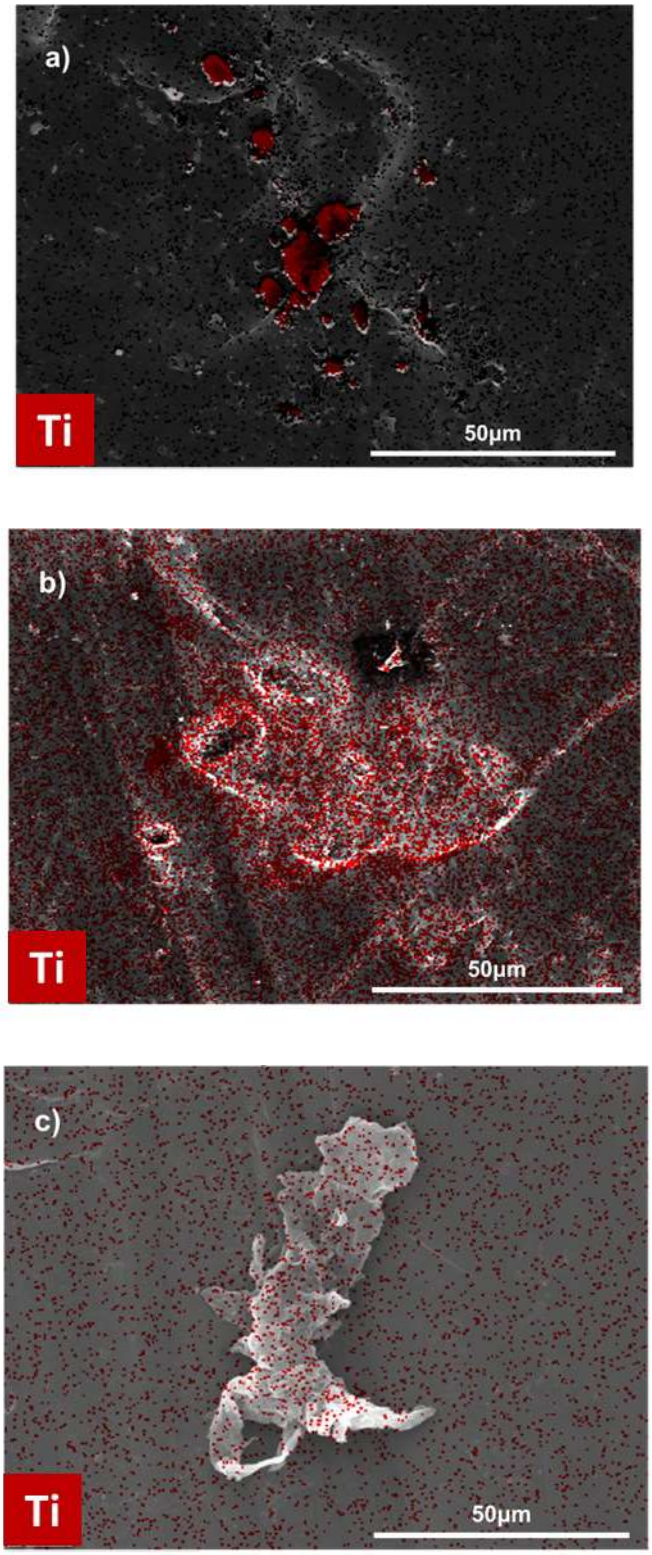

Figure 14 - SEM micrographs of the membrane modified by filtration (a), membrane modified by Dop+TiO_2+GO (b), membrane modified by Dop+TiO_2 (c). Red dots indicate the presence of the element titanium.

The SEM micrographs of the modified membranes confirm the presence of the titanium element, corresponding to the adhesion of TiO_2 nanoparticles to the surface of the membranes. Different particle distributions are observed for the different techniques used. For the modification by filtration (Fig 14a), the nanoparticles were concentrated at specific points, forming clusters. When using dopamine, it is possible to observe that both in modifications with TiO_2-GO (Fig. 14b) as well as with only TiO_2 (Fig. 14c), the particles are dispersed over the entire membrane surface. The suspension of the nanocomposites, upon coming into contact with the surface of the membrane modified with dopamine, is attracted by the catechol and quinone groups of polydopamine. In this way, the nanocomposites, linked by strong coordination bonds, make the nanoparticles remain in their initial position and avoid forming large clusters (ZHANG *et al.*, 2017). For the sample with GO a higher concentration of titanium in the sample is apparent, meaning that a higher concentration of semiconductor nanoparticles adhered to the surface. This behavior can be explained by the ability of GO to act as a binding element between materials, favoring adhesion in the presence of dopamine (Fig. 15). From the photocatalytic activity point of view, more dispersed particles will generate greater specific surface area and, consequently, greater photodegradation activity.

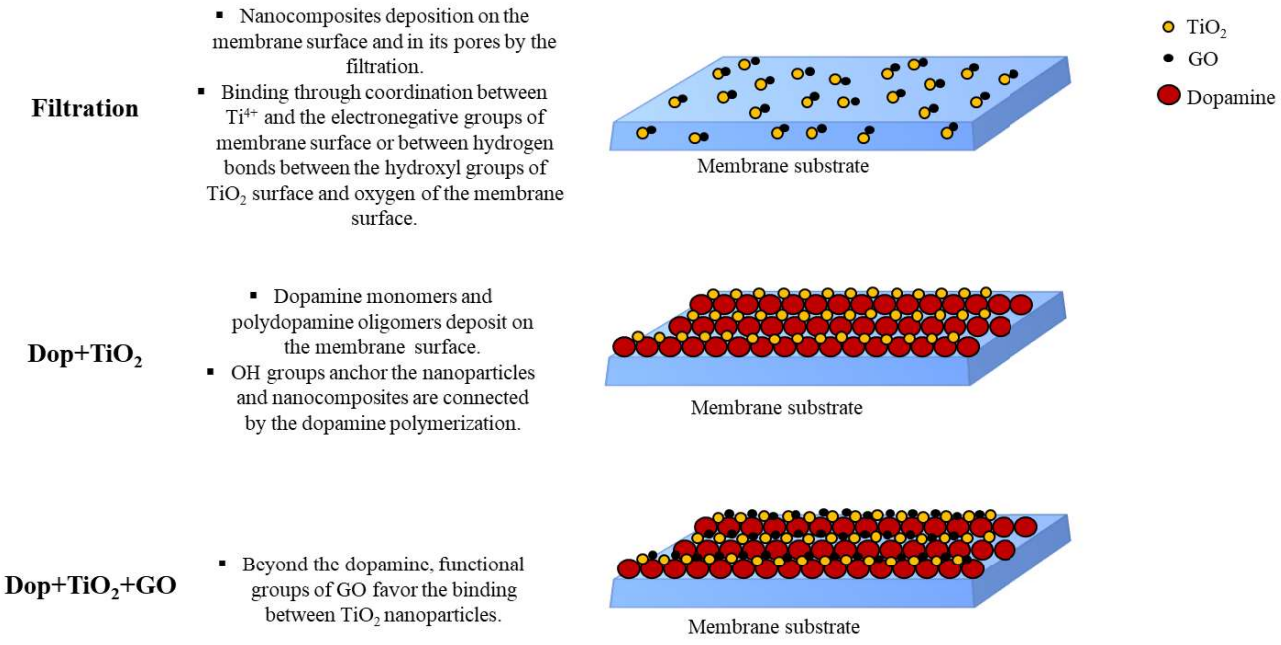

Figure 15 - Schematic representation of the adhesion mechanisms in the filtration, dop+TiO_2 and dop+TiO_2+GO modification routes.

FTIR was used to characterize possible changes in functional groups on the surface of the recycled and the recycled modified membrane with dopamine, TiO_2, and GO (Fig. 16). The

band close to 3,383 cm^{-1} may be related to O-H stretching vibration, while the band close to 2,964 cm^{-1} correspond to aliphatic C-H bonds (*e.g.*: CH_3 and CH_2) characteristic of the membrane polymer matrix. The functional groups NH_2 and NH from the remaining polyamide were responsible for the bands at 1,585 – 1,495 cm^{-1}, whereas aromatic polyamide and polysulfone supports would show no or only very weak IR absorption (SHULTZ *et al.*, 2018). It is known that GO has several functional groups in its structure, which results in a spectrum of greater complexity for the modified membrane, besides peaks of higher intensity and new ones. Examples are the bands observed in 1,741, 1,656, and 1,075 cm^{-1}, attributed to carbonyl (C=O), hydroxyl (OH), and epoxy (C-O) groups (SAFARPOUR; KHATAEE; VATANPOUR, 2014). Peaks at 1,487 and 1,101 cm^{-1} could be induced by C-OH and C-O-C vibrations, respectively (ZHU *et al.*, 2020b). Other peaks, as those observed between 600 - 700 cm^{-1}, can be correlated with the interactions between the species of oxygen-titanium (Ti-O-Ti) and titanium-oxygen-carbon (Ti-O-C) (NGUYEN-PHAN *et al.*, 2011). Other spectral regions that maintained their pattern for pristine and modified membranes reassures that the membrane polymeric matrix was not damaged nor chemically altered during TiO_2 and GO assimilation.

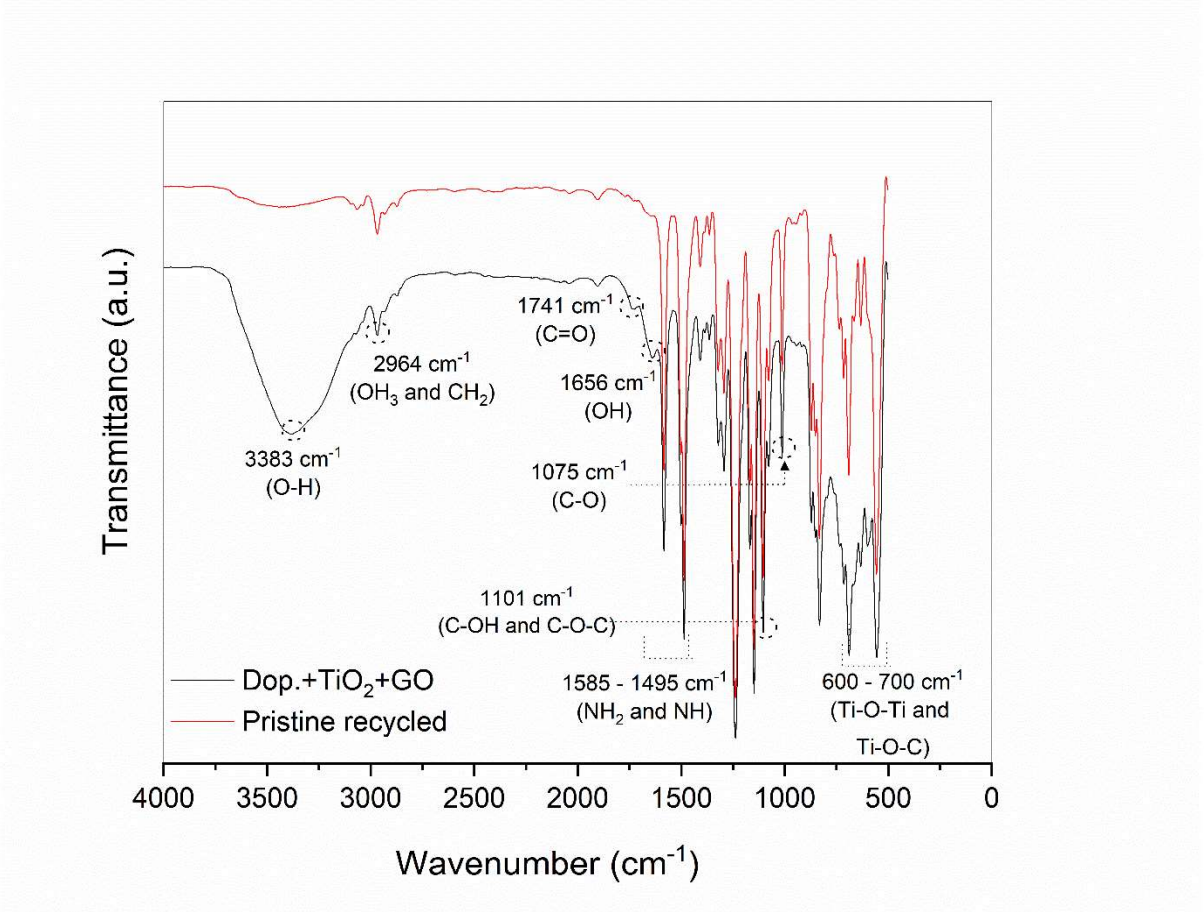

Figure 16 - Fourier infrared spectroscopy of the recycled membrane and recycled modified membrane with dopamine, TiO_2 and GO.

Hydraulic permeability tests were performed to complement the membranes characterization. Fig. 17-(a) shows the permeate flux of deionized water for different membranes and operating pressures, whereas Fig. 17-(b) shows the hydraulic permeability values of the membranes obtained by the different modification techniques.

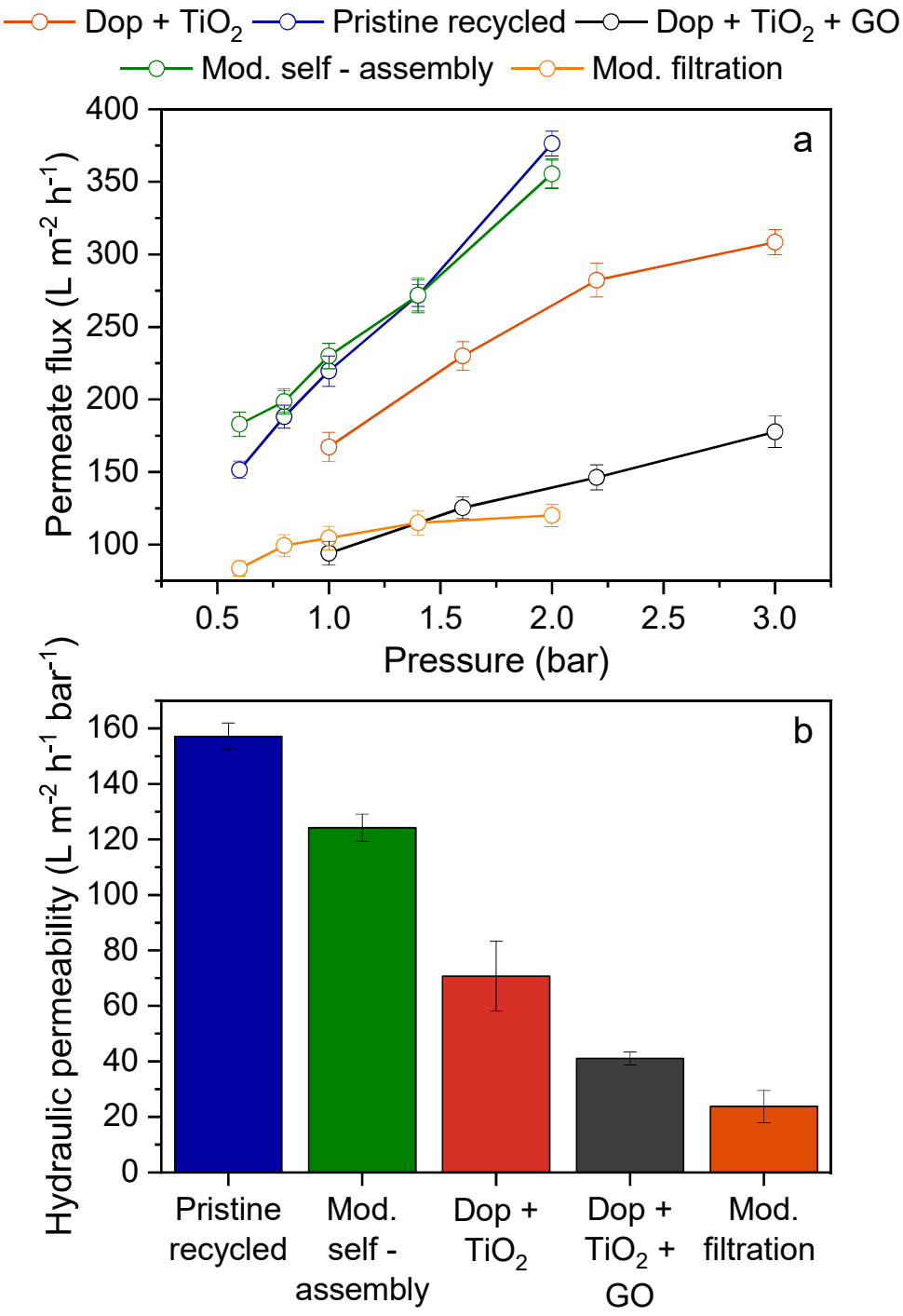

Figure 17 - (a) Water flux under different pressures and (b) hydraulic permeability of the obtained membranes.

For the recycled membrane without surface modification (pristine recycled) and modified in the self-assembly method, the water flux profiles were close to each other and followed a similar pattern. This finding is another evidence of the non-adherence of TiO_2-GO to the membrane surface, what was already apparent during visual inspection (Fig. 11b).

The membrane hydraulic permeability significantly declined when filtration procedures were considered. This indicates that the membrane surface was successful modified since the permeability reduction can be justified by the reduction of the membrane pore size by the deposition of TiO_2-GO nanoparticles. In other studies similar results after modification with TiO_2-GO are reported (ATHANASEKOU *et al.*, 2014; GAO *et al.*, 2013). The authors described the formation of smaller pores (nanometric), capable of retaining a greater number of compounds. It is noteworthy that even after certain pressure increases (from 0.75 to 2 bar), the flow remained stable at around 100 L m^{-2} h^{-1}. As the test was performed at increasing pressures, this result may be associated with coating compaction with the possibility of greater penetration of the coating layer into the pores of the membranes. As a result, there is an enhanced pore reduction and increased transport resistance in the coating, and consequently, lower operational permeability at higher pressures.

A decrease in permeability is also observed for the membranes modified with dopamine. At 2 bar, the membrane modified only with TiO_2 and dopamine showed a permeability around 1.4 fold lower than the membrane without modification, and for the case of that modified with dopamine, TiO_2 and GO, this reduction was even more severe with about 2.9 fold. This decrease in permeability was expected and is confirmed by other studies due to the blockage and reduction of the original pores of the membrane owing to the modification. Zhang *et al.*, (2017) also observed an increase in the hydraulic resistance of membranes modified with TiO_2 and dopamine. The greater decrease in the membrane modified with dopamine, TiO_2, and GO is associated with a greater reduction of the pores due to the GO deposited sheets. Gao *et al.*, (2013), studying the deposition of different masses of GO-TiO_2 under cellulose acetate membranes, found that the greater the deposited mass, the greater the decrease in the permeate flux.

When comparing the permeabilities of membranes modified by dopamine and filtration methods, the membranes obtained in the first method showed greater permeability compared with the second. This behavior is due to the GO sheets orientation and the compacting of the TiO_2 nanoparticles in the different techniques. In the case of the filtration modification, it is usual to layout the GO sheets in a lamellar manner, forming compact films that behave as barriers to permeation (GUO *et al.*, 2012; XU *et al.*, 2013b). In this way, when the stability and permeability of the membranes obtained in the different techniques is evaluated, it is expected that the membranes modified with the aid of dopamine will be the most promising.

Tests for removing the eriochrome black T dye (461.31 Da) without irradiation were conducted with the membrane modified by filtration, modified with dopamine-TiO_2, and dopamine-TiO_2-GO (Fig. 18a). An identical control test was performed with the pristine recycled membrane to compare the results of the modified with the unmodified membranes samples. The membrane modified by the self-assembly method was not used in these tests due to its instability and detachment from the nanomaterials layer.

The modified membranes reached practically 100% rejection of dye compared with 56% for the membrane without modification. This finding aligns well with previously observations in terms of membrane porosity and justifies the greater dye removal (KUMAR *et al.*, 2016). The reduction in pore size has the advantage of increasing the residence time of compounds inside the reactor without impacting the hydraulic residence time, which can be advantageous considering the operation under conditions that contribute to pollutant's reduction, such as irradiation or oxidation. Another factor that increases the rejection of the dye by the membrane is the repulsive effects caused by the negative surface of the membranes modified with TiO_2-GO and the negatively charged molecules of the eriochrome black T dye (SAFARPOUR; VATANPOUR; KHATAEE, 2016).

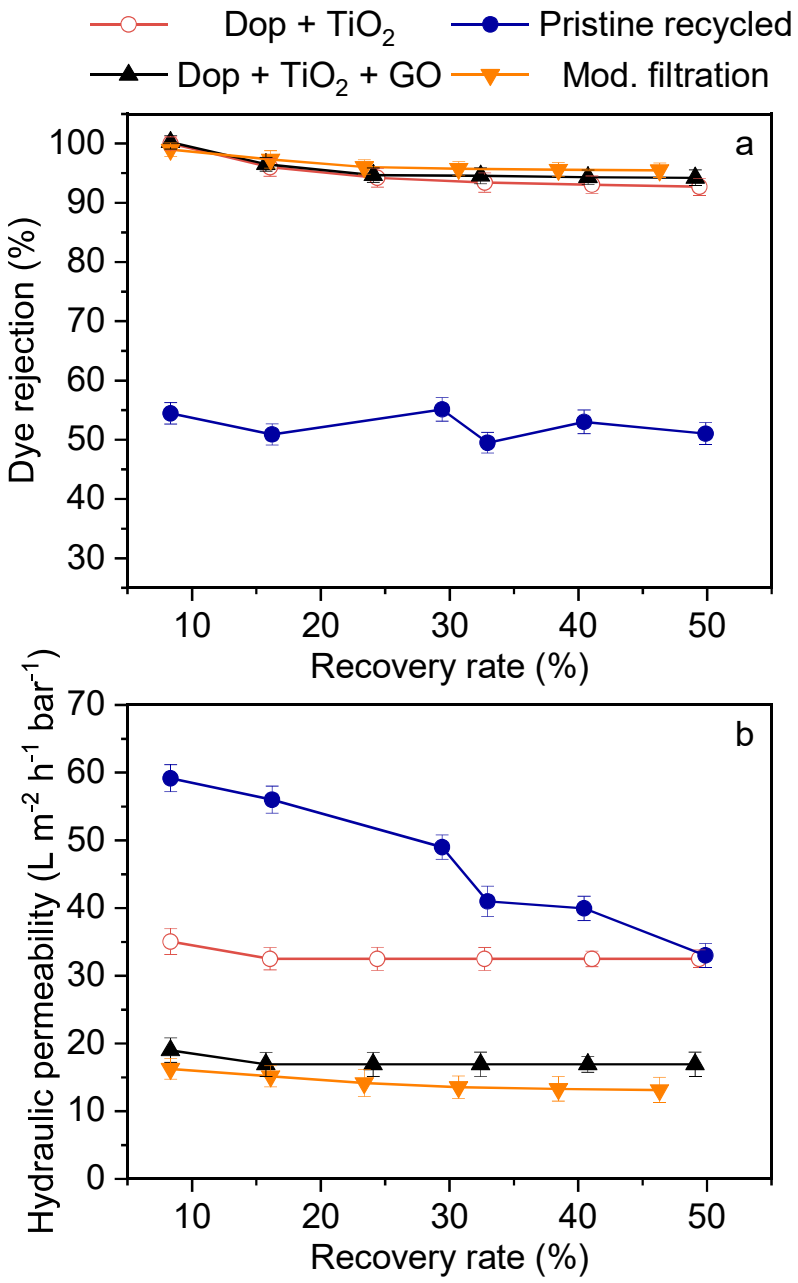

Figure 18 - (a) Rejection efficiency of the eriochrome black dye by the modified membranes, and (b) hydraulic permeability during removal of the eriochrome black T dye.

The fluxes of all modified membranes are smaller than those of the membrane without modification (Fig. 18b). However, a sharp decline (approximately 32%) is observed in the membrane permeability without modification at around 30% recovery rate, whereas the permeability for the modified membranes remained quite stable. This phenomenon in the membrane without modification might be explained by the formation of more severe fouling

and it can be anticipated that the modification of the membrane surface decreases the fouling vulnerability.

The presence of TiO_2-GO convert the membrane surface to ultra-hydrophilicity by forming a hydrated layer that repels organic fouling (DAMODAR; YOU; CHOU, 2009; JHAVERI; MURTHY, 2016a). Furthermore, the surface modification increases the smoothness of the membranes surface and reduces the adsorption of organic molecules, in addition to the fact that the presence of negatively charged functional groups can repel negatively charged fouling agents (URSINO *et al.*, 2018b). Zhu *et al.*, (2020b) tested the potential for removing eriochrome black T dye (0.1 g L^{-1}) by TiO_2-GO modified polysulfone nanofiltration membranes. They performed the membrane stability long tests for 9 hours of operation. It was verified that the dye rejection (97.8% - 98.5%) and the hydraulic permeability (3.6 - 5.8 L m^{-2} h^{-1} bar^{-1}) remained stable during the evaluated time, concluding that the addition of the materials gives resistance to fouling.

In order to assess the adsorption and photocatalytic contribution, tests for the removal of methylene blue were carried out with and without irradiation and permeation with the membrane modified with dopamine-TiO_2-GO. As shown in Figure 19, under irradiation in the absence of the membrane, the concentration of the dye remained practically unchanged, showing the absence of photolysis. Similar results were reported by Zhu *et al.*, (2017a), in which the degradation of methylene blue under UV irradiation was also not observed. During the test with the membrane without irradiation, a slight drop in the dye's concentration was observed, indicating removal by adsorption. During the 90 minutes of the experiment, the dye concentration was reduced by about 10% in the case of the membrane in contact with the dye without irradiation. Studies point to the high adsorptive capacity of GO due to the presence of its oxygenated functional groups that can promote the intimate contact of organic molecules with the membrane surface (ZHANG *et al.*, 2021d). The methylene blue dye can be captured through π-π bonds, hydrogen bonds, and electrostatic interactions (VARAPRASAD; JAYARAMUDU; SADIKU, 2017). Zhang et al., (2021d) observed the removal by adsorption of the methylene blue dye by Polyacrylonitrile (PAN) membranes modified with TiO_2-GO nanocomposites, too. The authors also argue that the GO's negatively charged surface favors the adsorption of cationic dyes, such as methylene blue, in addition to the factors mentioned above. The dye removal by adsorption naturally contributes modestly only when evaluating the

overall membrane removal performance. However, the adsorption favors the interaction of the dye with the catalysts and, therefore, the photocatalytic degradation process.

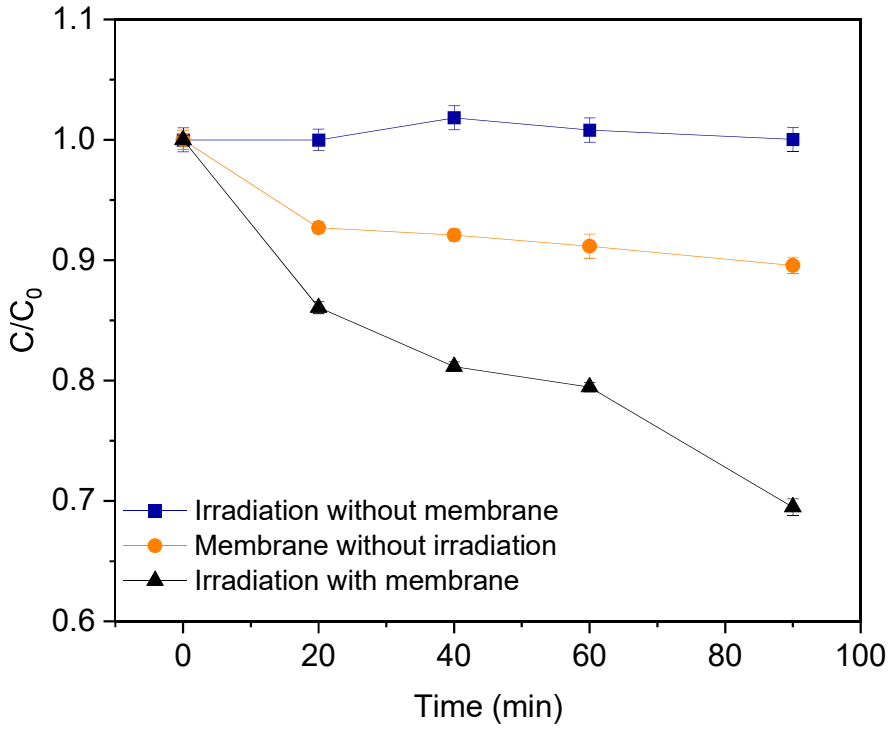

Figure 19 - Methylene blue removal by the Dop+TiO_2+GO membrane under UV irradiation (254 nm) and in the combination of both.

When irradiation is considered, it is possible to notice a more pronounced drop in the concentration of the dye over time, with the removal of approximately 30% being obtained after 90 minutes. It is noteworthy that longer experiment times would probably generate a higher removal efficiency. This is one of the great benefits of the hybrid process. For photocatalysis only, a longer residence time would be needed. However, with the photocatalytic membrane, the membrane instantly retains the dye. Thus, it is possible to operate with a shorter overall hydraulic residence time while guaranteeing a concentrate with better quality. The obtained result reveals the photocatalytic potential of the developed membrane, well in line with other studies also observing degradations of dyes by photocatalysis with membranes modified with TiO_2-GO nanocomposite. Yan *et al.*, (2019) obtained around 45% removal of methylene blue by PAN modified membrane after 90 minutes of UV irradiation. It is important to mention that the degradation efficiency is directly related to the mass of nanocomposite present in the membrane, since photocatalysis is directly proportional to the available surface area of the catalyst (ZHENG *et al.*, 2017), and, for this reason, different photocatalytic degradations are

reported by different studies. The membrane performance is believed to be even improved in solar irradiation tests, since GO has the potential to reduce the TiO_2 bandgap.

Considering the modification stability, nanocomposites distribution on membrane surface, permeability, and rejection efficiency of dyes, the membranes modified with dopamine-TiO_2-GO was considered as the most promising. Besides the high removals of dyes by this membrane (practically 100%), photocatalysis would even reduce the concentration of the rejected pollutants in the concentrate and would reduce membrane fouling. For this reason, the hybrid configuration was considered the most promising and was further tested for PhAC rejection.

3.3.2 Rejection of PhACs

Because the Dop+TiO_2+GO membrane exhibited the best performance in all previous tests, this membrane was further tested for its removal of PhACs (Fig. 20).

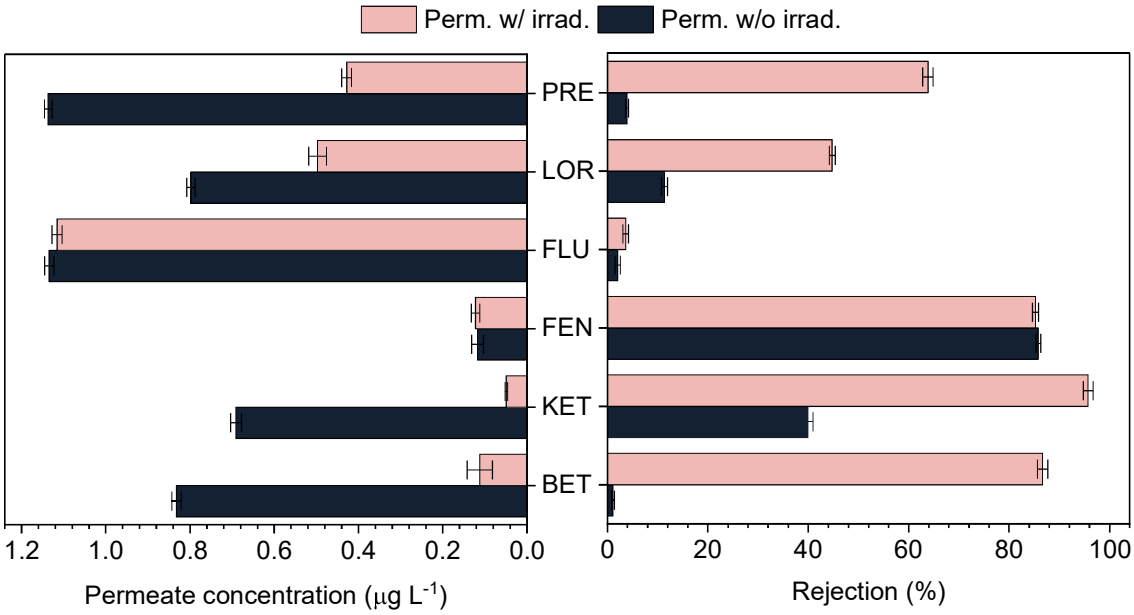

Figure 20 - Concentration of PhACs on the permeate without irradiation, permeate with irradiation, rejection efficiency of the Dop+TiO_2+GO photocatalytic membrane without, and with irradiation at 254 nm.

The rejection efficiency by filtration (rejection w/o irrad.) in the photocatalytic membrane in most cases was low causing a severe breakthrough of several PhACs to the permeate. This indicates that the membrane, even after modification, is still porous. In contrast tight NF and RO membranes, reach a rejection of PhACs of 98.8% (betamethasone rejection by NF) (FOUREAUX *et al.*, 2021) and >99% (fluconazole rejection by RO) (COUTO *et al.*, 2020).

The highest rejection by the membrane was for fenofibrate (FEN, 85.8%), one of the PhACs with the highest molecular weight (361 Da) and log K_{ow} (5.28). Such physical chemical characteristics are known to favor membrane rejection by size exclusion – because of the high molecular weight, and the adsorption onto the membrane surface. On the other hand, fluconazole (FLU) showed one of the lowest rejection efficiencies by the membrane (2.1%). This observation might be explained by the PhAC physical chemical characteristics, with one of the lowest log k_{ow} (0.4). To support that these results are linked to physical chemical properties a moderate and significant correlation between the log k_{ow} and the rejection by the membrane was found ($p<0.05$, $r=0.59$). Furthermore, the pK_a – which can also favor adsorption, exhibited a strong relationship between its value and the rejection efficiency by the membrane ($p<0.05$, $r=-0.92$). These results suggest that adsorption would be the main mechanism responsible for PhACs removal since the relationship between the PhACs molecular weight and their removal efficiency were non-significant ($p=0.76$). The adsorption by the photocatalytic membrane configuration is an interesting outcome since an effective photodegradation relies on effective adsorption of PhACs. Therefore, it would be no limitation on overall efficiency in PhACs removal by the hybrid system.

When the irradiation is applied, the rejection efficiency increases in most cases. Betamethasone (BET) had the highest rejection gain (85.5%) when irradiation was activated, from 1.1 to 86.6%. Nonetheless, fenofibrate (FEN) did not exhibit gains in rejection efficiency, mainly due to its inability to be oxidized. In such cases, the benefits of the photocatalytic membrane are harnessed for fouling mitigation, rather than the photocatalytic activity. Furthermore, the PhAC physical chemical characteristics can also be linked to the photocatalytic efficiency. For example, the log K_{ow} exhibited a moderate and significant correlation between its value and the rejection efficiency with irradiation ($p<0.05$, $r=0.52$). It is known that for the photocatalytic activity take place, the compound needs to be on the catalyst surface, thus, higher log K_{ow} can favor the adsorption and ultimately the photocatalytic activity.

Besides the PhACs content in the permeate, their content in the concentrate is also important. One of the major criticisms against MSPs is the concentrate generation, which usually pose higher risk to the environment (due to the higher concentration) in comparison with the feed. In this context, the application of photocatalytic membranes is also recommended, given that the photocatalytic activity can reduce the content of pollutants in the concentrate stream. Regarding the PhACs, the test without irradiation give rise to a concentrate with higher PhACs

content than the feed. Concentration factor between 1.04 to 1.64 was found for these tests. When the irradiation was turned on, none of the PhACs exhibited concentration factors >1, they ranged from 0.07 to 0.93, confirming that the concentrate had lower PhACs content than the feed. Thus, besides the aforementioned advantages, the use of photocatalytic membranes can also reduce the risks posed by the concentrate, a ubiquitous drawback from MSPs.

3.4 CONCLUSIONS

Different routes for the synthesis of photocatalytic membranes from discarded RO were assessed. The main conclusions are:

- Self-assembly was deemed unsuitable due to the low adhesion of nanoparticulate materials to the recycled membrane surface;
- For the membranes modified by filtration and dopamine aid, a decrease in hydraulic permeability due to the blockage and reduction of the original pores of the membrane owing to the nanocomposite coverage was observed;
- A better distribution and greater number of nanocomposites were observed on the membrane surface modified by dopamine + TiO_2 + GO;
- The rejection of dyes was mainly due to size exclusion and photocatalytic activity;
- The photocatalytic membrane was able to generate a permeate with reduced content of PhACs, and a concentrate that has lower content than the feed.

CHAPTER 4

Use of photocatalytic recycled TiO_2-GO membranes for the removal of TOrCs from wastewaters

4.1 INTRODUCTION

Water scarcity, driven by population growth, urbanization and pollution, has become one of the major problems facing humanity (HE *et al.*, 2021; HUANG *et al.*, 2021). In this context, particular attention has been paid in recent years to the environmental penetration of emerging pollutants, such as pharmaceuticals active compounds (AHMED *et al.*, 2021; VASILACHI *et al.*, 2021). These compounds, even if present at low concentrations, can have adverse effects on human and animal health. Thus, advanced treatment solutions have been explored to remove these contaminants and membrane separation processes, and advanced oxidative processes are promising (EGEA-CORBACHO LOPERA; GUTIÉRREZ RUIZ; QUIROGA ALONSO, 2019; JOURSHABANI *et al.*, 2019; RATHI; KUMAR; SHOW, 2021; ZHANG *et al.*, 2021c).

The association of technologies, such as in photocatalytic membranes, is an improvement in treatment systems aligned with process intensification, as they reduce the size of facilities and resolve or at least mitigate the limitations of technologies if used separately (CAMERA-RODA *et al.*, 2017; IGLESIAS *et al.*, 2016). In the case of membranes, fouling, characterized by the deposition of compounds on its surface throughout the period of operation, increases the energy requirements for maintaining the flux, with consequent increases in costs and a reduction in the quality of the permeate. While the use of nanoscale catalysts for photocatalysis is still limited by the challenges of recovery of the catalysts in these dimensions (KHAN *et al.*, 2015; QING *et al.*, 2019). The combination of the two processes gives the membranes self-cleaning capabilities, as well as reducing the load of the concentrate stream by the degradation of the feed compounds. Furthermore, the maintenance of the catalyst in the operating system is possible (DAROWNA *et al.*, 2017; JIANG; CHOO, 2016).

Titanium dioxide (TiO_2) is one of the most common nanomaterials used in photocatalytic membranes because of its low cost, non-toxicity, high stability and high hydrophilicity (BOBIRICĂ *et al.*, 2021; JIANG *et al.*, 2015; ZHANG *et al.*, 2020; ZHOU *et al.*, 2021). When irradiated by irradiation below 320 nm, electrons from the valence band of the oxide are migrated to the conduction band leaving holes in the valence band. The electron-hole pair forms radicals with species present in the medium, initiating a series of oxidation-reduction reactions with the resulting degradation of pollutants (LEONG *et al.*, 2014). However, high energies are necessary to activate the semiconductor and electron-hole recombination occurs easily. Strategies such as doping with metals or sensitization with organic molecules aim to circumvent

this problem, and the association with graphene oxide shows to be very promising, as the oxide has interesting electronic properties, with the potential to reduce the TiO_2 band-gap and decrease the rate of electron-hole recombination, in addition to having several functional groups capable of promoting the adsorption of pollutants for their subsequent degradation (DE OLIVEIRA *et al.*, 2022a; GAO; HU; MI, 2014a; YAN *et al.*, 2019).

Li *et al.*, (2022) evaluated the removal of three pharmaceuticals (naproxen, carbamazepine and diclofenac) by TiO2-GO photocatalytic membranes. Under UV-LED irradiation, removals of 100% of diclofenac and naproxen and 90% of carbamazepine were obtained, while 80%, 70% and 13% of rejection of the same compounds, respectively, were obtained in the absence of irradiation only by the membrane filtration. In addition, degradation tests of the compounds were performed by the membrane being irradiated with and without filtration and the degradation efficiency increased four times for the case of the system with filtration. Chakraborty *et al.*, (2017) obtained the degradation of approximately 40% of the Chlorhexidine digluconate antiseptic in 280 minutes of operation by using PES hollow fiber photocatalytic membranes, while the membranes without modification showed removals of only 15%. Singh *et al.*, (2021) noticed greater removals of the antibiotic chloramphenicol through photocatalytic membranes as the concentration of TiO_2 increased (around 25% without the oxide and around 62% with the oxide, both in 120 minutes of operation). Moreover, the fluxes were higher in the modified membranes (21.2 L m^{-2} h^{-1}) compared to the pristines (5.7 L m^{-2} h^{-1}), due to the increase in the hydrophilicity of the membrane surface by the addition of the semiconductor. In addition to better contaminant removal efficiency, photocatalytic membranes also have lower electrical energy per order, as well as lower energy consumption due to reduced fouling and concentrated loads.

Several factors impact the efficiency of the pollutant's degradation process through photocatalysis in photocatalytic membranes, such as catalyst dose, substrate concentration, pH, system temperature, light intensity, among others (KOE *et al.*, 2020). To activate the catalyst and carry out photodegradation reactions, light irradiation must be used. And this parameter is one of special relevance, quite elucidated for the case of applications of suspended catalysts (UNG-MEDINA *et al.*, 2015), but little discussed in the context of photocatalytic membranes. Koe *et al.* (2019) reports that the reaction rate is directly proportional to the square root of the light intensity, wherein low intensities are insufficient for the migration of electrons from the conduction band to the valence band of the catalyst, and high intensities can increase electron-

hole recombination, with a consequent reduction in the pollutant degradation reaction speed (KUMAR; PANDEY, 2017). In this way, optimized intensity is desirable with the aim of improving the performance of the process. Guozheng *et al.*, (2010) studied the relationship between phenol degradation and light intensity using TiO_2/activated carbon under 254 nm irradiation. Intensities ranged from 0.875 to 2.625 W L^{-1} and higher degradation was achieved at higher intensities up to the limit of 1.75 W L^{-1}. Beyond this value, intensity was no longer a constraining factor. Wang; Fane; Lim, (2013) compared the degradation of carbamazepine in a membrane photocatalytic reactor and observed greater removals when the system was subjected to irradiation of higher intensities (68% removal) compared to lower intensities (28% removal). Especially in the context of photocatalytic membranes, the use of optimized light intensity, in addition to promoting greater catalyst efficiency, can also reduce energy consumption, as well as decrease the degradation of the polymeric chains of the membranes.

Although photocatalytic membranes have notable advantages, the stability of nanocomposites within their structure or on their surface, and the degradation of polymer chains by long-term UV-C irradiation on them are still drawbacks that need to be better elucidated (MUCHTAR *et al.*, 2019). One of the solutions to overcome such limitations is the use of compounds that promote greater adhesion of nanocomposites to the surface of membranes and provide protection to polymeric chains by absorbing the radicals generated by irradiation. One of the recently used for these purposes is polydopamine (PDA) (WU *et al.*, 2017; ZHU *et al.*, 2017b). PDA, a mussel-inspired polymer, has the ability to adhere and form stable layers on most material surfaces and, consequently, promote the adhesion of nanocomposites to membrane surfaces. Furthermore, it acts as a free radical scavenger, as it is a catechol-bearing compound rich in electron-donating hydroxyls and amine groups, which provides protection to the polymeric structure of the membrane (FENG *et al.*, 2015).

Therefore, the present work aims to evaluate the removal of emerging contaminants from wastewater after biological treatment using photocatalytic membranes based on titanium dioxide, graphene oxide and dopamine. Recycled reverse osmosis membranes converted to porous membranes, after their lifespan, are used as support membranes. The effects of different sources of irradiation (UV-C and LED) are assessed and the impacts of the position of the lamp inside the reactor are discussed. As far as we are aware, with the exception of the work developed by our group (DE OLIVEIRA *et al.*, 2022b), recycled photocatalytic membranes have not been identified in the literature. There are also very few studies that evaluate the layout

of the system where photocatalytic membranes are used and consider the effects of the irradiation intensity that reaches the membrane surface as a function of position. More than that, most studies test the efficiency of photocatalytic membranes in the removal of isolated compounds, such as dyes and drugs in synthetic effluent, which greatly compromises the evaluation of the effectiveness of this technology in the treatment of real effluents, which differs from the performed in the present study.

4.2MATERIALS AND METHODS

4.2.1 Materials

The reagents used in the present work were dopamine hydrochloride (Merck); hydrogen peroxide (35%) (Sigma-Aldrich), hydrochloric acid (37%) (Sigma-Aldrich); graphite Micrograf HC30 (Nacional de Grafite, Brazil); potassium iodide (KI)(Merck); potassium iodate (KIO_3) (VWR); potassium permanganate ($KMnO_4$) (Merck); sodium borate ($Na_2B_4O_7.10H_2O$) (J.T. Baker); sodium hydroxide (NaOH) (Dinâmica); sodium nitrate ($NaNO_3$) (Merck); sulfuric acid (95-98% H_2SO_4) (Sigma-Aldrich), and titanium tetrachloride ($TiCl_4$) (Merck). All reagents were analytical grade and all solutions were prepared with Milli Q ultrapure water. End-of-life membrane sample used in this study was taken from a spiral-wound module, specifically the model FilmTec BW30 of $2.0x10^{-1}$ m in diameter, 1.0 m in length, and an active area of 41 ± 3 m^2. This membrane was used in a desalination plant of the Água Doce Program, Brazil.

4.2.2 Modified membrane preparation

First, post-lifespan reverse osmosis thin-film composite membranes were recycled to act as support membranes for the modification process with nanocomposites. The recycled membranes were obtained by oxidation of end-of-life reverse osmosis membranes by immersion in a commercial sodium hypochlorite bath, at a contact time intensity of 300,000 ppm·h at room temperature. Details of this methodology can be found elsewhere in our previous work (DE PAULA; GOMES; AMARAL, 2017). TiO_2 was prepared using a pathway with lower reagent consumption and microwave use, by means of titanium tetrachloride and water as precursors. The methodological details can be found in our work (OLIVEIRA; VIANA; AMARAL, 2020). GO was prepared using the modified Hummers method from natural graphite powder (ALAM; SHARMA; KUMAR, 2017). TiO_2 suspension (0.5 g L^{-1}) in pH 12 buffer solution was sonicated for 1 hour in a beaker. At the same time, GO suspension (25 mg

L^{-1}) were also prepared in pH 12 buffer solution and sonicated for one hour. The suspensions were mixed and sonicated for 2 hours. A solution of dopamine (2 mg mL^{-1}) in pH 12 buffer solution was prepared and poured over the membrane and kept resting to polymerize for one hour. After this period, excess dopamine was removed with deionized water and the suspension of TiO_2-GO nanocomposites poured over the membrane and allowed to rest for one and a half hours. After this period, the excess was gently washed off with deionized water.

4.2.3 Photocatalytic reactor design

A rectangular (12x17 cm) flat metal module was built to support the produced photocatalytic membrane. The module was designed to operate submerged in the reaction tank and the permeate flow occurred inward of the module, as shown in Figure 21. A source of aeration, made of a perforated sphere has been placed inside the reactor to reduce fouling and improve the number of potential species to form reactive radicals. A chiller has also been integrated to the reactor to maintain the temperature of the medium. A pressure gauge, flowmeter and peristaltic pump were connected to the module.

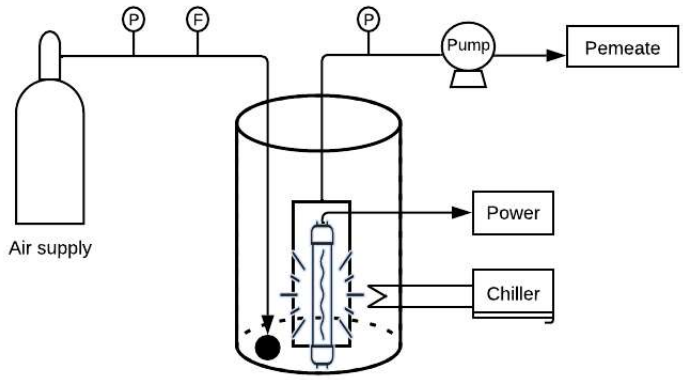

Figure 21 - Schematic representation of the experimental apparatus.

The reactor layout was optimized through actinometric tests with iodide/potassium iodate (SPERLE *et al.*, 2022) to determine the position of the lamp inside the reactor that generated greater efficiency in terms of light intensity reaching the membrane surface. The concentrations of the actinometric solution were determined with the aid of the DR 6000 UV/Vis Spectrophotometer (HACH, Germany). For the actinometric tests, a module was developed with the same geometric characteristics of the module that supported the membrane, except for being massive and not hollow, with only a hole in its center with the dimensions of a quartz

cuvette (1,3x1,3x4,5 cm), in which the cuvette was inserted with the actinometric solution in the light intensity tests. The cuvette simulated the location of the center of the membrane receiving the light irradiation. The lamp (UV-C, 9W) was fixed inside the reactor at a distance of 3.5 cm from the membrane surface. Supports have been created inside the reactor to ensure that the membrane, lamp and aeration source (7,5 cm distant from the lamp) always remain in the same position in all tests carried out. Comparative tests were also carried out with an LED lamp (Grow Light Bulb Sun-Like Full Spectrum LED, 20W), this turn outside the reactor at a distance of 12 cm from the surface of the liquid inside the reactor.

4.2.4 Photocatalytic and filtration tests

The tests with photocatalytic membranes were performed in batches in a cylindrical reactor (diameter 27,5 cm, height 25 cm) (Figure A.6). 12 liters of wastewater after treatment from the wastewater treatment plant (WWTP) located in Garching, Germany were used as process feed. The WWTP mainly treats domestic effluent from a population of approximately 31,000 inhabitants. The plant, in addition to secondary biological treatment, also has stages of nitrogen, phosphorus and disinfection removal. First, tests were carried out with only UV-C irradiation on the effluent for 90 minutes to determine the effect of photolysis on the removal of Trace Organic Chemicals (TOrCs). Subsequently, the membranes were moistened in 50% v/v ethanol for 15 minutes and after that, immersed inside the reactor, which was again fed with new 12 liters of Garching effluent for a new batch of tests. These first membrane tests lasted 90 minutes and were conducted in the absence of irradiation to detect the membrane rejection potential without considering the photocatalytic effect. Operating pressure was -0,9 bar, aeration at a pressure of 0,4 bar and flow rate of 225 qnL h^{-1}, and temperature inside the reactor maintained at 17 °C. Following this, tests were carried out with the system in operation with membrane filtration during irradiation. The operating conditions were similar to the membrane test with no irradiation. The same test was carried out changing the pH of the wastewater to 9 using sodium hydroxide (NaOH). Similar experiments were carried out with the system by switching the irradiation source to LEDs. All tests were conducted in triplicate and at the end of each batch, permeate and concentrate samples were collected for characterization. All samples for TOrCs measurements were collected in 20 mL prewashed amber glass vials and sealed with PTFE caps. When quantification measures could not be taken within 3 days of sampling, samples were stored at 4°C.

4.2.5 Analytical methods

The wastewater before and after treatment with the membranes were characterized in terms of pH, Conductivity, UV absorbance at 254 nm (UVA_{254}) with the aid of a DR 6000 UV/vis Spectrophotometer (HACH, Germany), total organic carbon (TOC) (Vario TOC cube analyzer (Elementary Analysensyteme, Langenselbold, Germany) and total nitrogen (TN) (LCK 138, HACH-Lange, Germany).

The concentrations of trace organic chemicals were measured using liquid chromatography coupled with direct injection tandem mass spectrometry (LC-MS/MS PLATINblue UHPLC – Knauer, Germany, ABSciex TQUAD 6500 – SCIEX, USA) by the method established and described by Müller; Drewes; Hübner, (2017). Quantification was performed in positive mode.

Prior to the measurements, 1900 µL of the sample was spiked with 100 µL of a 10 ppb isotope-labeled aqueous standard mixture. Filtration was performed using 0.22 µm PVDF membrane filters and stored in 2 mL amber glass vials. For chromatographic separation of the analytes, a XSelect HSS T3 column (particle size 2.5 mm; 2.1 x 100 mm) (Waters, Germany) was used. For component separation, a binary gradient method was developed using A: water containing 0.2% formic acid and B: acetonitrile. Data exploration and peak integration was performed using Analyst 1.6.2 and Multiquant software (ABSciex – SCIEX – USA).

To better elucidate the results of removing TOrCs with respect to the membrane properties, the membranes were characterized by measuring the zeta potential of their surfaces (SurPASS 3, Anton Paar), thermal analysis (alumina melting pot, gas flow of 100 mL min^{-1}, nitrogen atmosphere) (DTG-60H, Shimadzu), contact angle (goniometer, 2x2 cm samples, average droplet volume 17 µL) and scanning electron microscopy (SEM) (FEI Quanta 3D FEG). Samples for microscopy were metallized with gold/palladium. Recycled membranes and membranes recycled and modified with nanocomposites were characterized.

4.2.6 Calculation

The removal values for UVA_{254}, TOC, TN, conductivity and concentration of each of the evaluated TOrCs were calculated using generic equation 2:

$$R_J = \frac{J}{J_0} x100 \quad (2)$$

Where R is the removal, J can represent each of the evaluated parameters (UVA_{254}, TOC, TN, electrical conductivity and concentration of each of the TOrCs) and J_0 the initial values of the evaluated parameters.

The fluence radiation incident on the cuvette inserted in the module simulating the center of the membrane was calculated using equation 3, described by Sperle *et al.* (2022):

$$UV\ fluence\left[\frac{mW}{cm^2}\right] = \frac{(a_{352}(t) - a_{352}(t=0))\cdot V}{\varepsilon_{352}\cdot \Phi_{254}\cdot t\cdot A}\cdot U \quad (3)$$

Where: ε_{352} = 27636 M^{-1} cm^{-1} is the molar absorption coefficient of the formed I_3, U is the photon energy at 254 nm, V is the sample volume, A is the irradiated area, $\frac{a_{352(t)} - a_{352(t=0)}}{t}$ is obtained by the slope of the linear regression of the decay of the absorption coefficients of the actinometric solution as a function of time, Φ_{254} represents the quantum yield of the actinometric solution at 254 nm equal to 0.71 mol $Einstein^{-1}$. The quantum yield was adjusted based on the temperature of the experiment.

The fluence at the lamp output was calculated based on the fluence value reaching the membrane surface, with the aid of the Lambert-Beer Law (4)

$$\frac{I_1}{I_0} = 10^{-\alpha l c} \quad (4)$$

Where I_0 is the light intensity that leaves the lamp, I is the intensity of the light that reaches the membrane surface after passing through the medium, α is the molar absorptivity of the substance, l is the distance that the light travels through the medium, c is the concentration of adsorbing substance in the medium. α*l*c was calculated using effluent absorbance and the resulting value was 0.195. With the calculated value of the fluence that leaves the lamp, equal to 1.97 mW cm^{-2}, it was also possible to calculate, by the Lambert-Beer law, the fluence in other positions of the membrane, considering the distance of the traveled path, from the lamp to a point on the surface. To stipulate the distances traveled by light, they were considered to be the hypotenuse of different right triangles (Fig. 22) formed when moving in different points parallel to the surface of the membrane starting from the center of the membrane, from where the measurements were made.

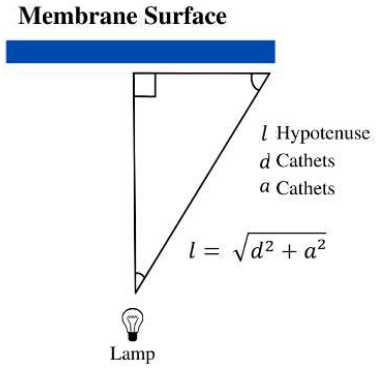

Figure 22 - Geometrical calculation strategy for the light fluence.

Multivariate statistical analyzes were carried out in Jamovi Software 2.2.5

4.3 RESULTS AND DISCUSSION

4.3.1 Membrane characterization

The modified and unmodified membranes were characterized by different techniques to elucidate the removal of emerging contaminants regarding the membrane's properties and characteristics. Zeta potential measurements (Fig. 23) of the modified membrane reveal that the membrane surface charge is positive at acidic pHs up to neutral pH. Above neutral pH, the membrane surface becomes negative. The isoelectric point occurs around pH 7, which means that operating with effluents at this pH value, the membrane surface will have no charge. When observing the unmodified membrane, it is possible to notice a change in the behavior of the formed curve when varying the pHs, in which the membrane surface has negative zeta potential for the entire pH range analyzed. It is important to mention that it is also much more negative than in the regions where the modified membrane is. The same behavior was found by Ji *et al.*, (2019) who found negative zeta potentials on the surface of polysulfone membranes in the pH range from 3 to 10. It is important to mention that the recycled membranes were obtained by chemical attack on post-lifespan reverse osmosis membranes. In this process, the selective layer of aromatic polyamide was removed, leaving the intermediate layer of polysulfone. On the other hand, the zeta potential differences for the modified membrane are due to the presence of nanocomposites on the membrane surface after modification. The presence of a large number of functional groups of GO gives it an expressive electrical character that can facilitate adsorptive processes and, consequently, increase the photodegradation process by TiO_2. In addition, TiO_2 presents ionizable groups on its surface, such as Ti-OH, and can adsorb ions

from the bulk solution, causing its surface to be electrically charged, favoring electrostatic removal mechanisms (ZIMMERMANN *et al.*, 2010). For P25 titanium dioxide, the isoelectric point is 6.8 (SZYMAŃSKI; MORAWSKI; MOZIA, 2016), which agrees with the values obtained from the membrane surface. Thus, at values lower than this, the membrane surface is positively charged and the opposite happens at pHs greater than 6.8. Darowna *et al.*, (2017) also obtained a similar curve for the zeta potential analysis of commercial TiO_2 P25 Aeroxide, with an inflection point at pH 6.3. The performance of membranes concerning to the zeta potential will largely depend on the characteristics of the feed components. For example, Szymański; Morawski; Mozia, (2016) observed higher humic acid removals at acidic pHs (3 and 6.5), compared to basic pH (9) using TiO_2-based photocatalytic membranes, and justified the results by the negative charge of the molecules of humic acid that increases the compound attraction by the TiO_2 particles on the membrane surface at lower pHs, where the nanoparticles will be positively charged, increasing, consequently, the removal. Mendret *et al.*, (2013) reported greater removal of AO7 dye by TiO_2-modified membranes also at acidic pH and observed that the adsorption mechanism was favored under these conditions because the dye is anionic, and negatively charged at pHs lower than 11. However, the authors point out that under these pH conditions, an expressive drop in flux occurred faster than at basic pHs due to dye deposition and reduction of photocatalytic activity. Therefore, in the study, the reduction of fouling was obtained at alkaline pHs where greater amounts of hydroxyl radicals can be formed on the surface of the catalyst, increasing the efficiency of the photocatalytic process. On the other hand, Singh; Sinha; Purkait, (2020) obtained greater removals of methylene blue dye by photocatalytic membranes with TiO_2 at basic pH compared to acid pH. This is because the dye at basic pHs has a positive charge and the membrane is negative, causing the opposite charges to favor the electrostatic attraction between membrane and dye, with consequent adsorption and, subsequently, photodegradation in the case of operation using sufficiently energetic irradiation. Therefore, the definition of the best operating pH will be associated with the characteristics of the compounds present in the process feed.

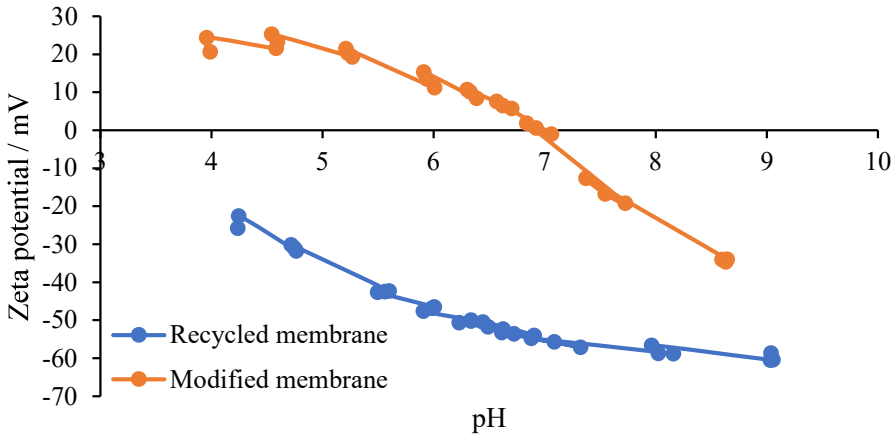

Figure 23 - Zeta potential versus pH for the recycled and modified membrane.

It is possible to observe in the thermal analysis of the membranes in Figure 24, that the mass loss profiles are very similar for the modified and unmodified membranes, which is coherent since the highest mass composition of the membrane comes from the polymeric matrix. Only a smaller percentage constitutes the surface modification with nanocomposites. The beginning of mass loss occurs close to 400°C and for the unmodified membrane a loss of about 92% is observed, while for the modified one, about 89%. Muhulet *et al.*, (2020) obtained a 75.03% mass loss of polysulfone membrane when evaluating temperatures from 100 to 800 °C. The authors also found small differences in mass losses with membranes modified with nanocomposites and without modification. Between approximately 550 and 600 °C, it is possible to notice a detachment of the mass loss curves of the modified and unmodified membrane. In the modified ones, a lower mass loss occurs in this temperature range, probably due to the non-degradation of some portion of the nanocomposites. Alaoui *et al.*, (2009) evaluated the mass loss of PVDF membranes modified with different percentages of TiO_2 (0 to 1 TiO_2/PVDF wt. ratio) and noticed in the ranges between 430° and 600° lower mass losses in membranes modified with a greater amount of nanomaterial, justifying the behavior in their presence. Therefore, the values found in the present study confirm the modification of membranes by nanomaterials.

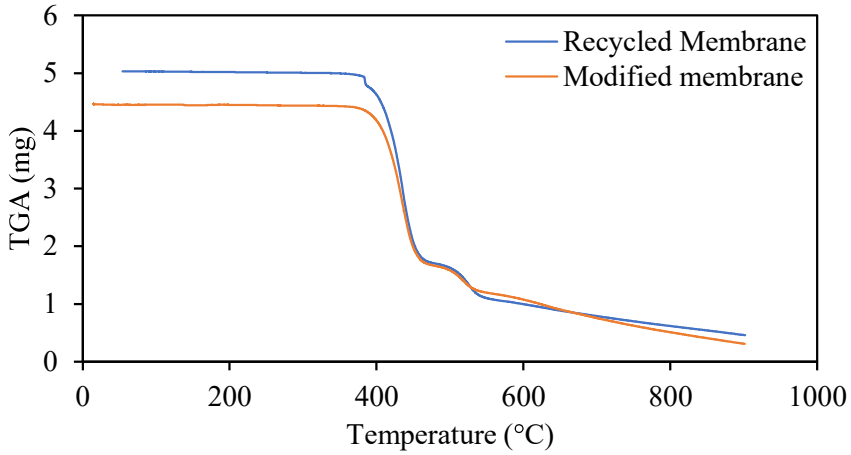

Figure 24 - Thermogravimetric analysis of the recycled and modified membranes.

Contact angle measurements of modified and unmodified membranes were performed, since this analysis gives an indication of the hydrophobic or hydrophilic character of a surface and is associated with which extent the membrane is prone to fouling by nonpolar organic compounds. The measured contact angle value of the unmodified membrane was 59.85±4.83° with an upper value of 66.28° and a lower value of 53.79°, depending on the portion of the membrane surface evaluated. The variation is justified by the chemical recycling process where different regions of the polyamide layer may have been attacked with greater or lesser intensity, generating a heterogeneous surface. As for the membranes modified with nanocomposites, a value of 55.54±2.11° was obtained, with a maximum value of 57.4° and a minimum value of 53.24°. There is a reduction in the average contact angle value after the modification process, which denotes an increase in the hydrophilicity of the membrane by the modification with the nanocomposites. This is a beneficial effect because, in addition to reducing the tendency to fouling, it can also increase the permeate flux. The presence of TiO_2 on the membrane surface increases its hydrophilicity due to its high affinity for water, and the hydrolysis of its surface hydroxyl groups. Moreover that, there is a large amount of oxygenated functional groups, such as carboxyl and hydroxyl on the surface of GO, promoting interaction with water molecules through hydrogen bonds with increased hydrophilicity. Penboon; Khrueakham; Sairiam (2019) also observed a reduction in the contact angle value when modifying PVDF membranes with TiO_2 nanoparticles and the values decreased even more as the mass of nanoparticles in the composition increased. The original value for the unmodified membrane was 128.1° and dropped to 114.3° for the modified membrane with 1 g L^{-1}. Vatanpour *et al.*, (2022) also obtained similar contact angle reduction results when modifying polymeric polyamide

membranes with TiO_2 and carbon dots. The values reduced more as the load of added nanocomposites increased.

AFM was used to probe the surface changes of the membranes in the modification process. The characterization analysis by AFM (Fig. 25) showed that the reverse osmosis membrane after its lifespan, having gone only through a cleaning process, presents a topography of ridges and valleys that are characteristic of the selective layer of aromatic polyamide formed in the interfacial polymerization process characteristic of these thin film membranes. By promoting recycling, it is possible to observe a considerable reduction in the surface roughness of the membrane, as also reported in Table 6, resulting in a more homogeneous layer, which is justified by the removal of the aromatic polyamide layer and exposure of the intermediate layer of polysulfone. It is possible to notice the presence of elevations that are characteristic of the nanomaterials deposited in the modification process on the modified membranes. It is possible to observe well-defined peaks that are associated with TiO_2 particles, dispersed in a partially uniform way over the membrane surface. As for the micrograph of the membrane after use, it is possible to notice a very irregular relief with not very uniform geometric formations associated with the deposition of incrustations during the operation with the membrane. It is important to mention that for the membranes used, the value of the height difference of the highest peak and lowest valley (Rz) was the most prominent, denoting a very irregular topography surface. The roughness of the photocatalytic membrane with nanocomposites will depend, in addition to the nanomaterials used, also on the process of obtaining them. Techniques such as blending, filtration, and surface coating are used in the photocatalytic membranes fabrication, and, depending on the technique, different authors report different surface roughness (DE OLIVEIRA *et al.*, 2022a). For example, in promoting the modification by blending, in the phase inversion method, Xu *et al.*, (2016b) observed a decrease in the roughness of membranes modified with nanocomposites TiO_2-GO compared to PVDF pristine and explained the phenomenon by the filling of the membrane concavities by the inorganic material. The reduction in roughness was associated with a better antifouling capacity of the membranes obtained. When promoting the modification of porous cellulose membranes with TiO_2-GO through filtration, Zhul *et al.*, (2017) observed an increase in roughness by the addition of nanomaterials in the modification process. For the case of the present study, it is worth mentioning that, after the recycling process, the roughness of the membrane obtained was already very low and the modification with nanocomposites only contributed to a slight

increase in this parameter.

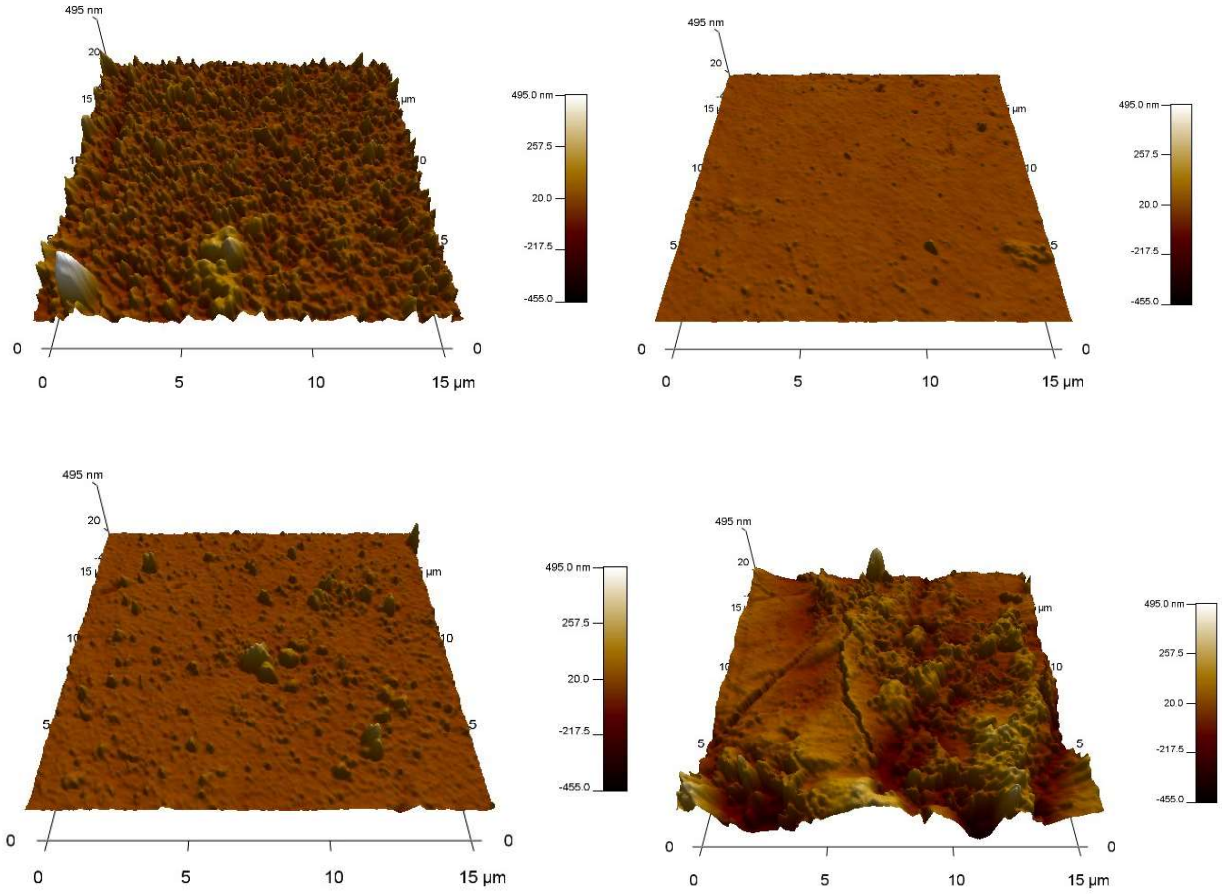

Figure 25 - AFM micrographs of the (a) RO membrane after cleaning process, (b) recycled membrane, (c) Modified membrane with TiO_2-GO, (d) modified membrane after use.

Table 6 - Roughness parameters of the different membranes.

Membranes	Roughness parameters (nm)		
	Ra	Rq	Rz
RO membrane after lifespan	17.9±4.8	50.4±2.5	522.9±156.7
RO recycled membrane	2.8±0.8	13.5±5.9	283.7±131.0
RO modified membrane	4.8±2.1	26.7±11.5	425.2±175.5
RO modified membrane after use	-0.4±0.7	88.3±48.8	818.6±288.5

Scanning Electronic Microscopy of the modified membranes after six months of use was carried out to verify the modifications in the surface composition or the detachment of the nanocomposites. The micrographs (Fig. 26) of the modified membrane after its use in the different batches of treatment show the presence of compounds deposited on its surface, with certain species with the appearance of crystals. The EDS analysis (not shown) and elemental map confirmed the presence of the titanium element uniformly spread over the membrane surface. This is a very interesting result, since one of the main concerns with the application of modified membranes is the stability of nanostructured coatings. The evaluated membrane was used in batches of treatment for 10 months and, even after this period, titanium oxide remained present on the surface, confirming the validity of dopamine as a binding element between the materials and a promoter of the stability of the formed membrane. Zhang *et al.*, (2017) point out that when in contact with the TiO_2 suspension, the catechol and quinone groups of dopamine attract the TiO_2 particles, and residual dopamine monomers can polymerize between the nanoparticles and the membrane surface.

It is worth to mention that it can be observed, also by the micrographs, that there are pores on the membrane surface after modification, but the surface is not completely porous, and different rejections mechanisms can take place as size exclusion or electrostatic adsorption-repulsion, as occurs in ultrafiltration or nanofiltration membranes.

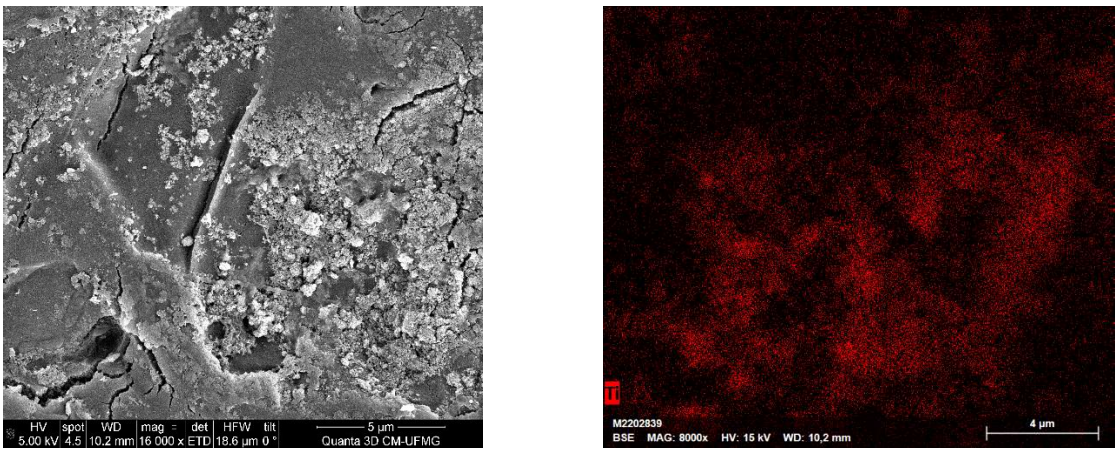

Figure 26 - (a) SEM micrograph of the modified membrane after use and (b) SEM micrograph with elemental map indicating the presence of titanium element.

4.3.2 The impact of light position on the fluence radiation incident on membrane surface

For the activation of TiO_2 and the start of the photodegradation process, it needs to be irradiated

by irradiation with an energy greater than its band gap (3.2 eV). Therefore, the fluence of incident radiation at the membrane surface is one of the most relevant aspects in the construction and functioning of photocatalytic membranes. For this study, the lamp was placed at a fixed distance from the center of the membrane and actinometric tests were performed. Based on the value of the luminous fluency that reached the center of the cuvette, the fluence rate leaving the lamp was determined with the aid of the Lambert-Beer law, and based on the fluence leaving the lamp, the fluence in different points of the membrane of rectangular structure of 12x17 cm, were calculated, also by the Lambert-Beer law.

The distances were estimated using the hypotenuse, assuming that the perpendicular distance from the center of the lamp to the surface of the membrane and the plane parallel to the membrane are cathets (Fig. 22). For instance, for arbitrary values of cathets in the plane parallel to the membrane surface, different values of hypotenuse were obtained for different points on the surface.

It can be seen from the results presented in Figure 27 that the closer to the center of the membrane, the greater the luminous fluency and, consequently, the greater energy use is obtained. While in the right and left extremities the fluencies are lower. An approximate fluence rate of 1.97 mW cm^{-2} was detected on the lamp surface, while approximately 0.29 ± 0.10 mW cm^{-2} at the center of the membrane and 0.07 ± 0.03 mW cm^{-2} at the right and left extremities. Such results can be used as tags to define the spacing between lamps in a full-scale facility.

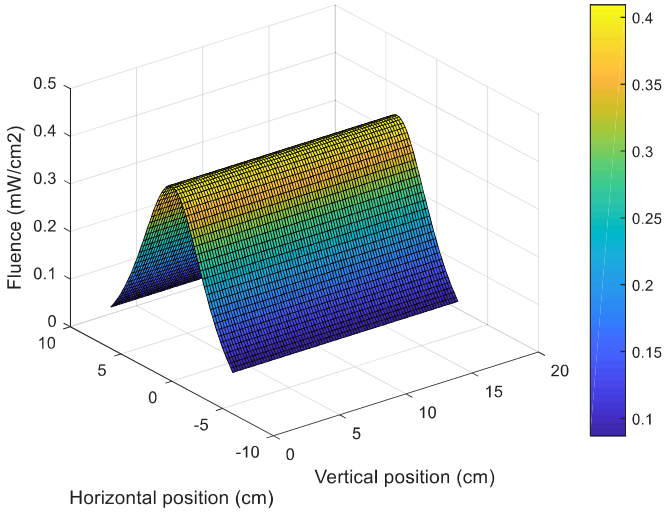

Figure 27 - Light fluence as a function of the position on the membrane surface.

Energy losses occur depending on the environment in which the light moves. And the greater the distances traveled, the greater the losses. With the submerged lamp arrangement layout as planned, these losses were in the order of 85% to 96%, which is already quite expressive. Many studies use lamps external to the reaction medium, so the losses are even greater and there is great energy waste, given that in addition to the path in the air to be covered, the radiation will also travel through the fluid in the reaction medium. Thus, designing membrane photocatalytic reactors and thinking about the position of the irradiation source and reactor geometry is an important aspect in the sustainability and efficiency of the project. Wang; Fane; Lim (2013) compared the degradation of carbamazepine in a membrane photocatalytic reactor and observed greater removals when the system was subjected to irradiation of higher intensities (68%) compared to lower intensities (28%). Kertèsz; Cakl; Jiránková, (2014) also found the same in the decolorization of dyes.

An optimized layout can improve energy use and, consequently, reduce energy consumption and waste generation from its production. From the results obtained, it is concluded that the best strategy is the use of lamps submerged in the reaction medium and, if possible, not only one, but a set of lamps aligned in parallel and of lower power, so that the irradiation reaches perpendicularly to the complete membrane surface traveling the same distances. One of the limitations of irradiation on the surface of membranes is the degradation of polymer chains. Therefore, thinking strategies that guarantee greater energy use and greater photocatalytic performance, but also less damage to the membrane must be evaluated.

4.3.3 Membrane performance on the wastewater treatment

Different treatment alternatives were approached and their efficiencies were evaluated in the removal of conductivity, TOC, and UVA_{254} parameters from wastewater after tertiary treatment. As can be seen from the Figure 28, the electrical conductivity removals were low in all the studied treatment systems, which is consistent since the membranes used are porous, as they had their selective layer removed in the chemical recycling process. The systems that use only irradiation, whether UV-C or LED, did not present practically any removal of conductivity, which was already expected, since this process is not capable of precipitating ions and or retaining them, as done by membranes. The highest conductivity removal, around 20%, was obtained with the entire system operating with UV-C irradiation. This is attributed to the removal of multivalent ions by the membranes, which can be considered in low concentration

compared to other species that confer high conductivity to the effluent. The UVA_{254} parameter was monitored to evaluate the attenuation of the presence of compounds with double and triple bonds present in the effluent and, it can be observed that all treatment processes were effective in this removal, with a minimum value of 5% by irradiation UV-C alone up to approximately 38% for systems with irradiation and filtration operating at basic pH (9). In the case of TOC removal, in systems where only irradiation was used, whether UV-C or LED, there was an increase in the parameter value. The same occurred in the entire system being irradiated with UV-C. It is suspected that there may have been a degradation of the polymeric structures of the reactor by UV-C irradiation. In the entire system with LED and the entire system with UV-C at pH 9, the removals were positive.

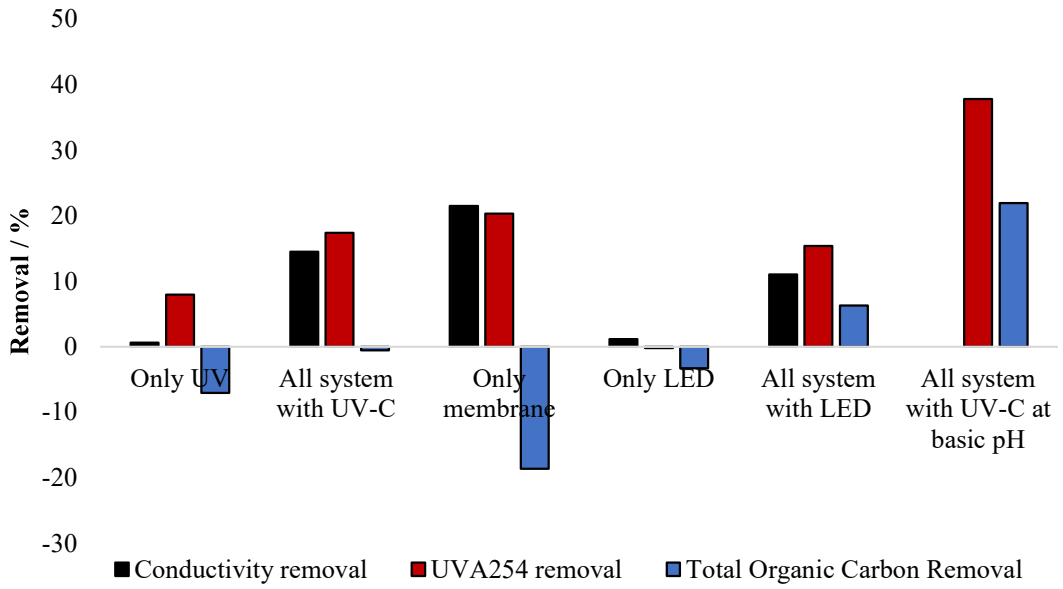

Figure 28 - Parameters removals by different treatment techniques.

4.3.4 Removal of emerging contaminants

The attenuation of nineteen TOrCs with different characteristics present in the wastewater from the Garching treatment plant after tertiary treatment were evaluated. Their main characteristics are presented in the table 7.

Table 7 - TOrCs main characteristics.

Compound	Molecular Weight	Log Kow	pKa_1; pKa_2; pKa_3
3-OH Carbamazepine	252,27	-	-
Methylbenzotriazol	133,15	-	1,4

Compound	Molecular Weight	Log Kow	pKa_1; pKa_2; pKa_3
Amisulpride	369,5	1,1	9,37
Antipyrine	188,23	0,38	1,4
Atenolol	266,34	0,16	9,60; 14,08; 15,95
Benzotriazol	119,12	1,44	8,37
Caffeine	194,19	-0,07	14
Candassartan	440,5	4,79	2,45; 6,70
Carbamazepine	236,27	2,45	13,9
Citalopram	324,4	1,39	9,78
Diclofenac	296,1	4,51	4,15
Fluconazol	306,27	0,5	1,76
Gabapentin	171,24	-1,1	3,7; 10,70
Metoprolol	267,36	1,88	9,56
Sulfamethoxazol	253,28	0,89	1,60; 5,70
Tramadol	263,37	2,4	9,41; 13,08
Trimethoprin	290,32	0,91	7,12
Valsartansaeure	435,5	4	4,73
Venlafaxin	277,4	3,2	8,91; 14,42

TOrCs removals were quantified by different treatment strategies and the results are shown in Figure 29.

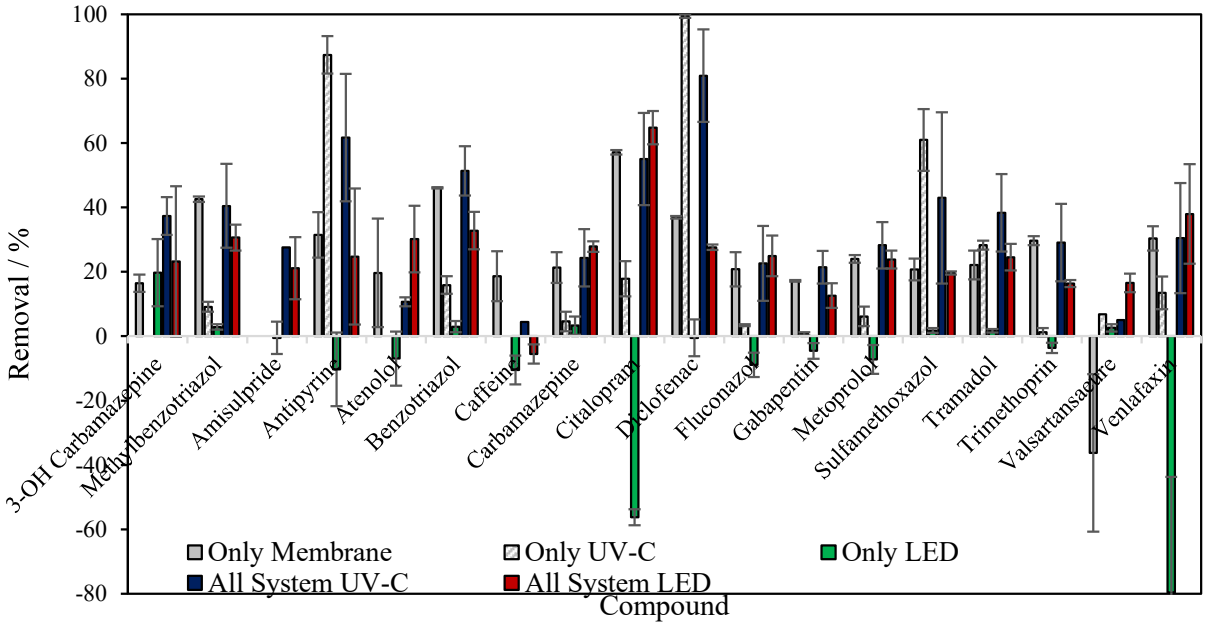

Figure 29 - TOrCs removals by different treatment techniques.

When observing the attenuations of the compounds, it is noted that antipyrine, diclofenac and sulfamethoxazole are the components with the highest removal percentages only by UV-C irradiation, which has also been confirmed in other studies (MULLER, et al, 2017), while carbamazepine, fluconazole and trimethoprim were the lowest. In the case of these last compounds, in the operation with the entire system and only with the membrane, it is possible to observe very close attenuations, indicating that the removal mechanism occurred through size exclusion or electrostatic repulsion and not by photocatalysis mechanisms. Phototransformation is therefore component dependent and the component structure has great relevance in the efficiency of direct photolysis (PAREDES *et al.*, 2019).

Statistical analysis showed that for compounds with molecular weights above 200 g mol^{-1}, there is a statistically significant positive correlation between removal by the system operated only by membrane filtration and molecular weight ($p=0.007<0.05$). The justification for this fact may lie in the irregularity of the surface of the membrane formed after the recycling process and subsequent modification with dopamine-TiO_2-GO. Although the formed membrane has some pores, its behavior seems to resemble membranes between ultrafiltration or nanofiltration, as ultrafiltration membranes have a molecular weight cutoff of around 100 KDa (SHENG *et al.*, 2016), and all trace compounds investigated have masses smaller than that.

The removal only through the membrane can also occur by adsorption or rejection by electrostatic mechanisms. For the evaluation of the first mechanism, the Kow log is a widely used parameter. When this value is low (<2.6), the compounds have low lipophilicity and high hydrophilicity, while for high log Kow values (>4.5), the characteristic is the opposite. The components with the highest removals in the membrane-only treatment system were citalopram and benzotriazole and all of them have low log Kow values: 1.39, 1.44, respectively, which denotes hydrophilic character. It is important to note that although the membrane is polymeric, in the surface modification process with the nanocomposites there was an increase in its hydrophilicity, as confirmed by the contact angle results, due to the presence of the functional groups of GO and hydroxyls of TiO_2. Therefore, the attenuation may have occurred by adsorption or electrostatic attraction. For compounds with high log Kow values that are still attenuated through the membrane, even on a small scale, the justification may be their deprotonations with a consequent reduction in their hydrophobicity, as in the case of diclofenac. Similar results were also reported by (SNYDER *et al.*, 2007).

In the case of integrated membrane UV-C system, the correlation value for the removal values and molecular weight presents p-value equal to 0.637 denoting that the irradiation causes a distinct mechanism of removal of the drugs that there is no exclusion by size, which was already expected because in this case, removal by photocatalysis also occurs. Moreover, there is a statistically significant positive correlation between log Kow and TOrCs attenuation ($p = 0.026 < 0.05$). The justification lies in the fact that photocatalytic reactions take place on the surface of the catalyst. Thus, the adsorption step is important in the mechanism. The higher the log Kow, the more lipophilic the compound and the removal mechanism may have been by adsorption on the surface of the polymeric membrane.

For the case of the operation of the integrated membrane - UV-C system, the analysis is complex, because in addition to the mechanisms of rejection only by the membrane, there are also the mechanisms of removal by photocatalysis, making it difficult to consider the impact of each happening simultaneously. What may have justified greater or lesser removals of certain compounds are the charge characteristics of the compounds, since photocatalysis with TiO_2 is non-selective, since hydroxyl radicals and other reactive substances are non-selective in nature. The average pH of the process feed effluent is around 7.5 and under these conditions, as observed in the zeta potential results, the membrane surface is negatively charged. Therefore, cationic compounds such as venlafaxine, carbamazepine and tramadol will have a favored

interaction with the nanocomposites and consequently the photocatalytic process will be benefited. Arlos *et al.*, (2016) reported this behavior with the use of TiO_2. However, this rule cannot be affirmed for the present system studied since compounds such as caffeine and atelonol, also cationic, had a reduction in removal when evaluating the integrated membrane UV-C system in operation compared to only membrane filtration.

In general, the performances of the systems where LED was used were lower than the complete systems where UV-C irradiation was used, which was to be expected since the wavelengths in the case of LED were longer, with consequent lower energies. The lower energies, in addition to not promoting the photolysis of TOrCs, were also unable to activate the nanocomposites on the membrane surface. Surprisingly, for some compounds, there was an increase in concentration after LED irradiation, which can be explained by the release of certain compounds present in suspended solids in the irradiation process or even the synthesis of new compounds by smaller precursors molecules. Valsartansaeure and venlafaxine do not follow this profile and were more attenuated throughout the system being irradiated by LEDs. This mechanism cannot be very well explained, as venlafaxine, for example, is not photosensitive (SANTOKE *et al.*, 2012). However, a hypothesis for the values found is indirect photolysis due to the presence of dissolved organic matter. The treated wastewater had total organic carbon values around 7 mg L^{-1} and UVA_{254} around 0.150. This organic matter, when irradiated, can have its singlet state excited, which can return to the ground state or transit via intersystem crossing to the excited triplet state. In this way, energy transfer occurs between the excited organic matter and the molecule of interest or oxygen, returning to the ground state. Excited oxygen decomposes into reactive species. These reactive species, in turn, react with the trace organic compounds causing their degradation (TRAWIŃSKI; SKIBIŃSKI, 2017). Other studies also mentioned the increase in the photodegradation rate (8-fold) of venlafaxine by the presence of organic matter in a study with river water and ultrapure water being irradiated by sunlight (RÚA-GÓMEZ; PÜTTMANN, 2013). For comparative purposes, interesting results were found by Wawryniuk; Pietrzak; Nałęcz-Jawecki (2015) when evaluating the decomposition of mianserin. The drug is not degraded by visible irradiation directly, but when humic acid was added to its solution, rapid decomposition was observed under visible irradiation.

Through the analysis of principal components using multivariate statistics (Fig. 30), a greater positive correlation can be observed between the removal by integrated membrane LED system

and log Kow, and a completely different behavior of the system operating only with LED irradiation from the other treatment systems evaluated. The systems of UV-C irradiation only, membrane only and membrane UV-C system showed positive correlations.

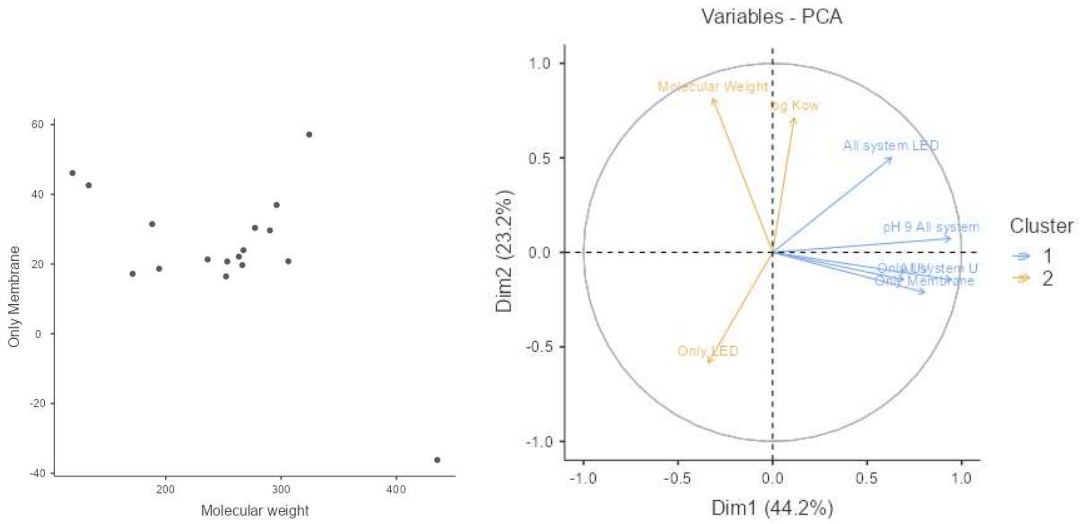

Figure 30 - Principal components analysis of the different techniques and evaluated parameters.

Experiments were performed with the membrane UV-C system with correction of the wastewater pH to 9 and the results are shown in Figure 31. Except for caffeine, the removal of all other 18 trace organic chemicals was superior in the higher pH operation. Removal values are associated with compound speciation, membrane surface charge, and feed solution pH (HUANG *et al.*, 2015). As evidenced in the zeta potential tests, the higher the pH, the more electronegative the membrane surface due to graphene oxide and TiO_2, consequently, in addition to the adsorption and photocatalysis, electrostatic repulsion mechanisms can play a relevant role, making the rejection of the evaluated contaminants greater. In the case of diclofenac, for example, removal of 92% was achieved in the operation of the entire system in pH 9. Expressive results were also obtained for antipyrine (~87% attenuation). In terms of percentage gains, the removals of atenolol and amisulpride increased considerably in the operation at higher pH.

All 18 compounds, with the except caffeine and carbamazepine, will be negatively charged at pH 9 or with pKas close to 9. Therefore, since the membrane surface is negatively charged, the main mechanism of interaction is electrostatic repulsion. Huang *et al.* (2015) when evaluating

the rejection of sulfamethoxazole by membranes modified with TiO_2, observed that higher pHs increased the removal efficiency through electrostatic repulsion.

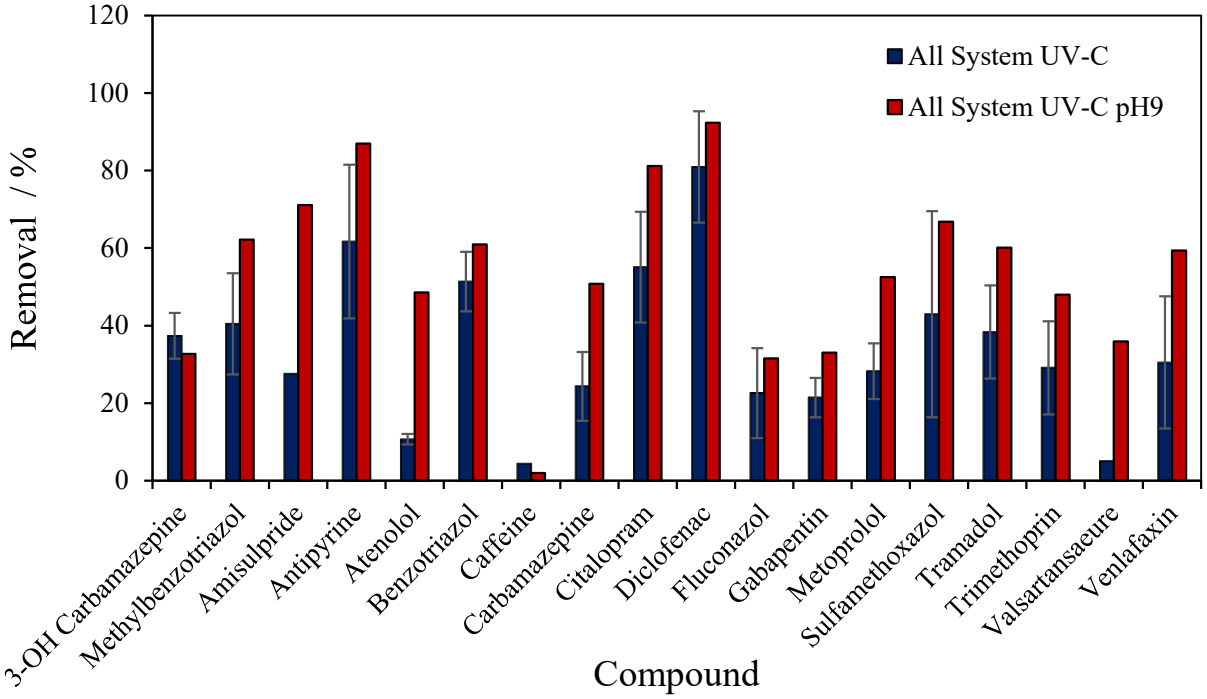

Figure 31 - TOrCs removals in different pHs.

4.5 CONCLUSIONS

Membranes modified with TiO_2-GO nanocomposites with the aid of dopamine proved to be stable in successive batches of operation. Micrographs showed the presence of TiO_2 in the membranes after use. The improvement of membrane characteristics such as increased hydrophilicity and greater electronegativity on the surface contributed to better performances in the removal TOrCs. The system operating in conjunction with filtration and photocatalysis obtained more satisfactory results in terms of removal of trace organic chemicals. Better performances were observed with pH elevation, which may justify an electrostatic rejection mechanism. Statistical analyzes showed a positive correlation between the molecular mass of the components and removal, as well as with log Kow and removal. Outstanding attenuation of TOrCs were achieved as for the case of diclofenac (92%) and antipyrine (87%). Thus, the photocatalytic membranes are a promising technology to generate safe water and even produce reuse water.

CHAPTER 5

Photocatalytic recycled membranes for municipal wastewater treatment: economical evaluation

5.1 INTRODUCTION

Compared to some years ago, the outlook for wastewater treatment has changed. In addition to decreased water availability and increased demand for water, global awareness of the presence of contaminants in low concentrations with potential adverse effects on human health and other organisms, such as trace organic compounds (TOrCs), has grown. Furthermore, laws in various parts of the world are becoming more restrictive, and the costs of obtaining clean water are rising. As a result, reuse is viewed as a viable option with both economic and environmental advantages (HUNTER *et al.*, 2019).

Conventional treatment plants are inefficient in the removal of TOrCs and do not even meet the standards for the generation of reuse water, requiring the use of advanced techniques for this purpose. Coagulation, sedimentation, ozonation, membrane separation processes, disinfection, and other tertiary treatments are commonly used in this context (WANG *et al.*, 2018). And, while each has advantages and disadvantages and produces satisfactory results in terms of technical effectiveness, their use is limited by an economic criterion that renders the process unfeasible. For example, Remy *et al.* (2014) concluded that membrane bioreactors were the best in terms of effluent quality when evaluating the environmental impacts of five tertiary treatment processes using life cycle analysis. However, the costs of electricity and chemical consumption were prohibitively expensive. As a result, the process's efficiency must be considered alongside economic criteria.

Wastewater treatment plants have two types of costs: capital and operating. The first is related to the costs of equipment, construction, land, and permits. The second is about the costs of energy, maintenance and repairs, chemical consumption, and labor, among others. The type of technology used in the plant, as well as its size, will have a direct impact on costs, and evaluating these parameters serves as a management tool for decision makers (OZGUN *et al.*, 2021).

Among the available tertiary treatment processes, membrane separation processes receive special attention (QING *et al.*, 2019; WANG *et al.*, 2022). However, while they reduce the polluting load, they involve a phase transfer process that generates a concentrate stream with a higher charge than the process feed that must be treated and disposed of, incurring additional costs and steps (CHELME-AYALA; SMITH; EL-DIN, 2013). Associating membranes with advanced oxidative processes is a promising alternative not only for improving performance,

but also for cost reduction in concentrate treatment steps, because mineralization of polluting compounds in effluents is possible (SINGH *et al.*, 2021).

Photocatalytic membranes, which act through separation mechanisms as well as photocatalysis, are being studied extensively as a technological alternative for producing high-quality water. However, most of the research is still in its early stages, taking place on a laboratory scale and focusing on the removal of isolated compounds, primarily in synthetic matrices. There are few studies that evaluate the treatment of complex real matrices, and to the best of our knowledge, no studies that make the economic evaluation of the process taking into account the treatment compatible with the capacity of a plant that serves the population of a city or region. As a result, the current study assesses the CapEX and OpEX of an advanced treatment system comprised of photocatalytic membranes based on recycled post-life reverse osmosis membrane, TiO_2 nanoparticles, graphene oxide and dopamine. The use of recycled membranes and a catalyst produced in a more environmentally friendly manner are both novelties that help to reduce the overall cost of the treatment process.

5.2 MATERIAL AND METHODS

5.2.1 Photocatalytic membrane preparation

The preparation route of the photocatalytic membranes was reported in our previous studies and more details can be found in De Oliveira *et al.*, (2022). In general, after-lifespan reverse osmosis membrane is recycled and transformed into an ultrafiltration membrane, greener titanium dioxide (TiO_2) nanoparticles, graphene oxide (GO), and dopamine are used as precursors. The membranes obtained demonstrated high rejection of trace organic compounds in wastewater treatment after tertiary treatment and were stable in operation for 10 months. Each synthesis method produced membranes with a surface area of 0.0204 m^2 and a permeate flux of 20 L m^{-2} h^{-1} bar^{-1}. These values were used in process costing and scaling.

5.2.2 Wastewater treatment plant

Garching wastewater treatment plant in Germany was used as a data reference for calculating the costs of using photocatalytic membranes in the advanced treatment of municipal wastewater. The treatment flow at the station is 1,812,859 m^3 $year^{-1}$, and it primarily treats domestic effluent from a population of approximately 31,000 inhabitants. In addition to secondary biological treatment, the station includes nitrogen, phosphorus, and disinfection

steps. The use of photocatalytic membranes as an advanced treatment step to remove trace organic compounds was considered, and calculations were performed based on the plant's treatment capacity.

5.2.3 Data collection, Capex and Opex calculation

First, the equipment and chemicals required to fabricate the photocatalytic membrane were evaluated. At this point, in addition to the costs of chemical precursors, the operating costs of the used equipment were considered, depending on the time required for each manufacture and the power of the equipment. With the membrane values, the acquisition costs (CapEX) and operating costs (OpEX) of the treatment system were calculated. The treatment system was based on the treatment performed on a bench scale (Fig. 32), followed by scaling factor corrections. In this system configuration, permeation occurs in the direction of the membrane's surface towards its interior, and the membrane used was flat.

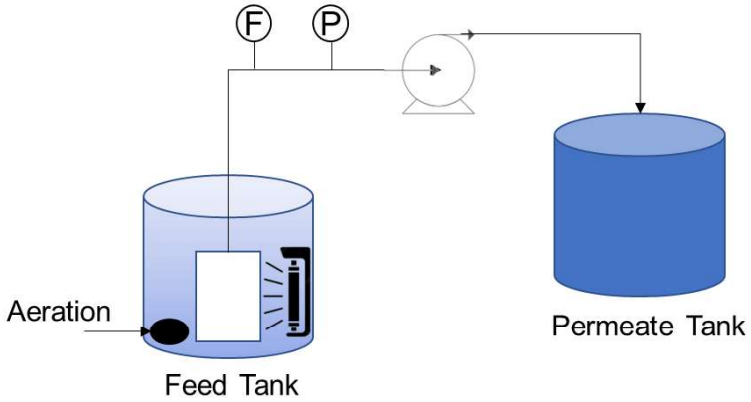

Figure 32 - Schematic representation of the treatment system.

The capital (CapEX) and operational (OpEX) costs were calculated taking into account a flow of 207 m^3 h^{-1}, which concerns the treatment flow of the Garching wastewater treatment plant. For the cost of equipment (Cb), estimates were made with the base variable (Sa), costs in the base variable (Ca, taking into account the equipment acquisition and installation costs) and an exponent factor (n), according to equation 5.

$$C_b = C_a \left({}^{S_b}/_{S_a} \right)^n \quad (5)$$

For CapEX, the initial costs of acquiring the membranes to start the treatment process were also considered. The membranes were estimated to have a useful life of 5 years. In terms of operating

costs, we considered the energy required by the lamps to activate the photocatalytic membranes, the energy required for pressurizing and pumping, the energy required for the aeration system, maintenance costs, and membrane replacement costs. The value of 5% of Capex was considered for maintenance, and since the useful life of the membranes was assumed to be 5 years, the total value of the acquisition of the membranes was calculated and divided by 5 to generate the annual cost. It is important to note that this contribution will become valid after the first five years of plant operation, because the acquisition of membranes was already considered in CapEX during the initial stage.

5.3 RESULTS AND DISCUSSION

5.3.1 Photocatalytic membrane fabrication costs

The costs of chemicals, materials and operation of equipment used to manufacture photocatalytic membranes are shown in Table 8.

Table 8 - Summary of cost variables considered for estimation of photocatalytic membrane production. *Values were based on the most recent Chemicals Market Report provided by the Independent Commodity Intelligence Service (ICIS)

Process Step	Chemicals and utilities for membrane costs estimation	Base variable (Sa)	Bare cost (US$; Ca)	Real variable (Sb)	Cost (US$; Cb)
TiO_2 synthesis	$TiCl_4$	1000 mL	251,34	6 mL	1.51
	NH_4OH	1000 mL	5,75	15 mL	0.09
	Synthesis Microwave	1 KWh	0.11	0.13 KWh	0.014
	Centrifuge	1 KWh	0.11	0.07 KWh	0.0077
	Kiln	1 KWh	0.11	8 KWh	0.88
	Muffle	1 KWh	0.11	7 KWh	0.77
	Total cost to produce 2.5 g of TiO_2 (US$)		3.27		

Process Step	Chemicals and utilities for membrane costs estimation	Base variable (Sa)	Bare cost (US$; Ca)	Real variable (Sb)	Cost (US$; Cb)
Photocatalytic membrane fabrication	Total cost to produce TiO_2 (US$ g^{-1})		1.31		
	TiO_2 used in the membrane preparation	2.5 g	3.27	0.02 g	0.026
	GO costs	1 g	0.5	0.001 g	0.0001
	Dopamine	1 g	11.34	0.08 g	0.91
	Buffer solution	1 L	13.79	0.12 L	1.65
	Ultrasound	1 KWh	0.11	0.48 KWh	0.0528
	UF recycled membrane	1 m^2	0.208	0.0204	0.00424
Total cost for the photocatalytic membrane	*Total cost to produce one photocatalytic membrane of 0.0204 m^2(US$)*		*2.64*		
	Total cost to produce one photocatalytic membrane (US$ m^{-2})		*129.41*		

The cost to produce each photocatalytic membrane is approximately US$ 2.64. However, the membranes produced are laboratory scale with an area of 0.024 m^2 and a permeate flow of 20 L m^2 h^{-1} bar^{-1}. If considering the area of membrane produced, the cost for production was approximately 129.41 US$ m^{-2}. These are values higher than those reported for commercial ultrafiltration membranes, whose price would be close to 25 US$ m^{-2} (COUTINHO DE PAULA; SANTOS AMARAL, 2018). On the other hand, if compared to emerging technologies such as membrane distillation and direct osmosis, which still depend on greater technological maturity for large-scale implementation, prices would be comparable. LI *et al.* (2020b) presented costs close to 100 US$ m^{-2} for the combined system of membrane distillation and direct osmosis when applied for the treatment of industrial effluent. The authors also

worked with the synthesis of membranes and considered expenses with chemicals, solvents, purification processes, among others, emphasizing the need for technological advances that were capable of simplifying the presented production costs. In all cases, the trend to be observed is lower costs of obtaining these membranes as one advances in the production scale.

It is worth mentioning the advantage of using recycled membranes, both in economic and environmental aspects. The costs for obtaining photocatalytic membranes based on recycled membranes were lower due to the lower acquisition costs of these membranes. The cost expectation for photocatalytic membranes obtained by commercial ultrafiltration membranes (25 US$ m^{-2}) is 153.92 US$ m^{-2}, with greater contribution from ultrafiltration membranes (16%; Figure 33). The expectation is that the amount of end-of-life reverse osmosis membranes disposed of in landfills in 2018 has reached values close to 16,500 tons (MORADI *et al.*, 2019), value that tends to grow with the spread of reverse osmosis technology. On the other hand, they are membranes that can be recycled even at the end of their lifespan, producing membranes similar to the ultrafiltration membranes that would act as a support for the photocatalytic membranes. Due to the simplicity of obtaining, they are low cost membranes with values close to 0.208 US$ m^{-2}, as shown in Table 33 (COUTINHO DE PAULA; SANTOS AMARAL, 2018).

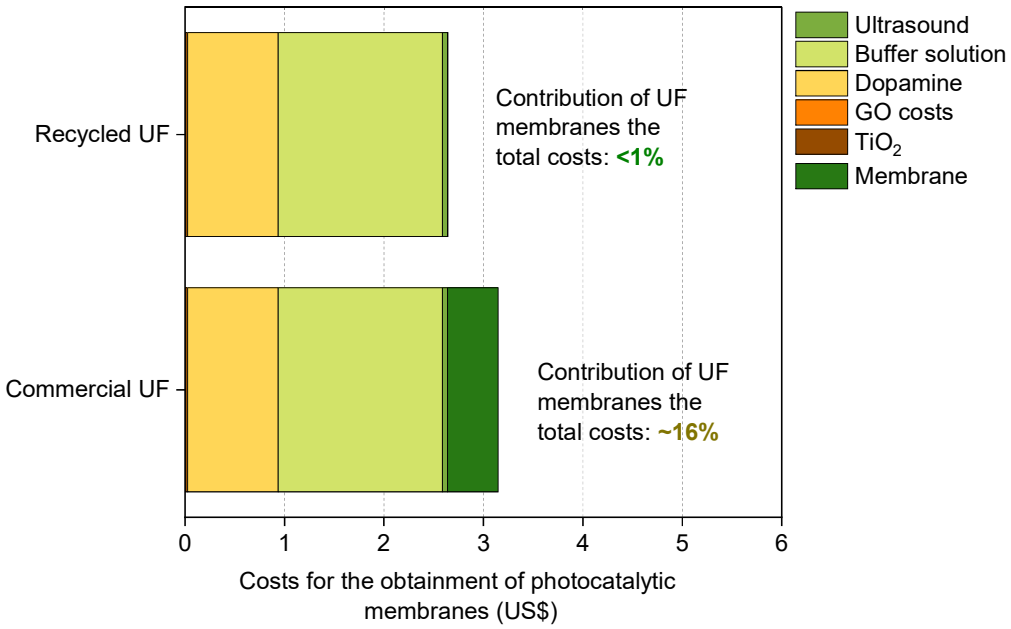

Figure 33 - Costs comparison between photocatalytic membranes obtained by commercial and recycled UF.

5.3.2 CapEX

Since the cost calculations are performed to evaluate the process in the tertiary treatment of wastewater in a given region, the treatment flow of the ETE Garching in Germany was taken into account. At this station, the treated flow is 207 $m^3 h^{-1}$. With the flow rate of the obtained photocatalytic membrane, a membrane area of 11500 m^2 would be required to meet the flow rate. Thus, the scale factor used to scale the values was based on dividing the required membrane area by the produced membrane area (scale factor = 563,725.50), generating a membrane cost equal to US$ 1488235.32.

The other values of the treatment system are described in table 9 and refer to the equipment and accessories for the tertiary treatment using the photocatalytic membrane.

Table 9 – Summary of cost variables considered for estimation of capital expenses (Capex) of the tertiary treatment unit.

Equipment Description for Capex estimation	Base variable (Sa)	Bare cost (US$; Ca)	n*	Real variable (Sb)	Equipment Cost (US$; Cb)
Feed tank	90 m^3	63524	0.6	207 m^3	104706,716
Permeate tank	90 m^3	63524	0.6	207 m^3	104706,716
Peristaltic pump	5.5 KWh	20026	0.7	-	20026
Multiple pipe – carbon steel	5% of all costs of installation	104563,75	-	-	104563,75
Membrane module	0.0204 m^2	0.57	0.6	11500 m^2	1614,943774
Rotameter	-	1012	-	-	1012
Manometer	-	20	-	-	20
Aerator	18 $m^3 h^{-1}$	207.50	0.7	126823.24 $m^3 h^{-1}$	102471,3568
UV-C Lamp	0.0204 m^2 (irradiated area)	28	0.7	11500 (irradiated area)	297101,8817

Adding the values of the photocatalytic membranes with the treatment system, the Capex of the process is US$ 2224458.68, that is, approximately 1.23 US$ m^{-3}. The highest values are associated with photocatalytic membranes with a contribution of 67% to the total acquisition value of the system (Figure 34). Then, acquisition of UV-C lamps, with a contribution of 13% to the total value of the system. Following these are the feed and permeate tanks, which due to the high volume also had considerable costs with a contribution of 5% each. In the case of combination with an existing wastewater treatment plant, the feed tanks could be replaced by direct connection of the system to the secondary effluent network, while the permeate tank could be replaced by direct integration of the photocatalytic system into the discharge network of the treated effluent.

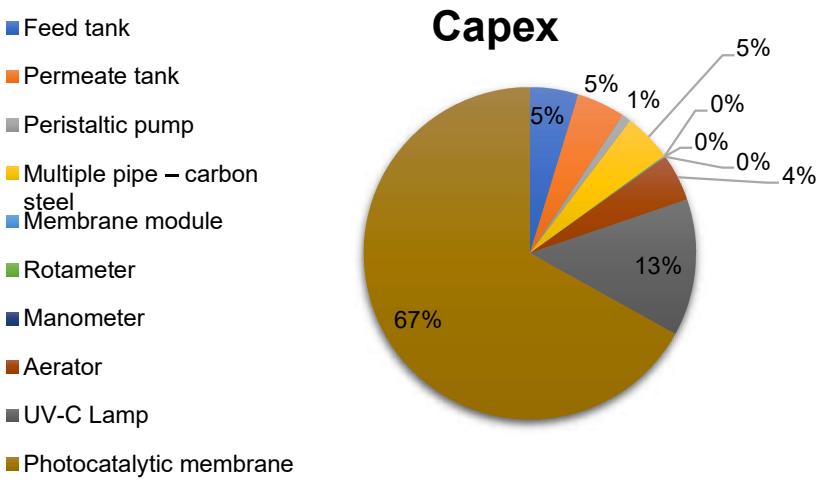

Figure 34 - Percentage impact of each equipment on Capex.

The investment to be made to implement the photocatalytic process is higher than those obtained by Ozgun *et al.* (2021) for the same treatment capacity. The authors evaluated the use of anaerobic-anoxic-aerobic (A^2O) systems, with and without integrated digesters, as a tertiary treatment technology, reporting implementation costs ranging from US$ 212923.75 - 542554.35. When comparing the capital costs for different treatment plants in different countries with different capacities, the authors found that, as expected, the larger the size, the greater the Capex and that for a small capacity plant (<100000 m^3 day^{-1}), Capex is 0.056±0.009 US$ m^{-3}. This value is much lower than that found in the present study, since it takes into account the capital for installing an entire treatment plant from preliminary to tertiary treatment and, in this type of approach, the previous processes, as they require less sophisticated equipment, such as tanks and other physical mechanisms, it ends up diluting the cost to the

treatment capacity. Unlike the analysis carried out in the present study, where only the value per m^3 is considered for only the tertiary treatment.

Knowing that the greatest impact on Capex is due to the acquisition of photocatalytic membranes, it is interesting to verify the cost portions of its production process. And observing Figure 33, it can be noted that the highest costs of the produced membranes relate to the expenses with the tris buffer solution (62% of the total cost of the membrane) for basifying the medium and polymerizing the polydopamine. An alternative to reduce costs would be the use of sodium hydroxide to adjust the pH in the synthesis. This alternative has already been tested by our research group and the membranes obtained had performances comparable to those synthesized with a tris buffer solution in terms of stability and rejection. Therefore, this may be a promising modification for process scaling. It is interesting to note that for the synthesis of the photocatalytic membrane, the TiO_2 used was obtained by a greener route with reduced consumption of chemicals and energy, produced by our group. This route reduced the costs of such a nanomaterial to manufacture the membrane, since commercial TiO_2 (Degussa P25) has a higher cost (3.35 US$ g^{-1}) (MERCK, 2022) than that synthesized in the present work (1.308 US$ g^{-1}).

5.3.3 OpEX

In order to calculate the operating costs of the process, it was taken into account that the lifespan of the membranes is 5 years (ZHANG *et al.*, 2021a), therefore, the production value of the membrane area that meets the treatment capacity was divided by 5. In addition, there are costs associated with the consumption of electricity for pressurizing the system and pumping wastewater, as well as for operating the lamps and aeration (Table 10). The maintenance cost was defined as 5% of Capex (MOREIRA *et al.*, 2022). The total calculated cost of Opex is 6803249 US$ $year^{-1}$. Since the total flow treated per year is 1812859 m^3, this value corresponds to approximately 3.75 US$ m^{-3} (Table 3). Regarding operating costs, it is possible to observe that the energy requirement for irradiation of the membrane by means of a UV-C lamp represents the greatest preponderance (75% of Opex) and this is one of the factors that most limit the use of large-scale technologies that use photocatalysis with TiO_2. This finding is in agreement with other authors who reported energy consumption as the one with the greatest impact on tertiary treatment of wastewaters (TSAGARAKIS; MARA; ANGELAKIS, 2003). However, if the material could be activated by irradiation of shorter wavelengths,

corresponding to the visible region of the electromagnetic spectrum, the use of solar irradiation could be a promising alternative in terms of cost reduction. The data obtained in the present study show membrane activation by LED irradiation at shorter wavelengths, thanks to the use of graphene oxide. If the use of lamps were removed, the Opex cost would be reduced to approximately 0.93 US$ m^{-3}. There are still other simplifications that can be made in the treatment, such as the removal of the aeration system. This system was used in order to reduce incrustations on the surface of the membrane during the period of operation. However, although it is an item for improving performance, this is not a fundamental criterion for its operation. Thus, if it were disregarded in the cost analysis, the new OpEX would be approximately 0.23 US$ m^{-3}. Mulder; Antakyali; Ante (2015) compared the costs of different tertiary treatment techniques for removing micropollutants in the planning of wastewater treatment plants in the Netherlands, based on the values of tertiary treatments already implemented in Germany and Switzerland. For ozonation, the Opex value found was 0.105 US$ m^{-3}, while 0.116 US$ m^{-3} for powdered activated carbon and 0.231 US$ m^{-3} for granular activated carbon. When comparing these values, it is possible to observe that the photocatalytic membrane has a higher cost than the other techniques. However, it must be considered that for other advanced techniques, such as activated carbon, there are still costs for treatment and disposal of the sludge that must be taken into account. In addition, the replacement of the material must take place at certain intervals (6 months in the case of granular activated carbon) due to the saturation of the active sites over the operating period. Moral *et al.* (2019) when carrying out the analysis of operational costs of tertiary treatment in Spain in 2017, found values between 0.147 and 0.284 US$ m^{-3}. Close values, 0.286 US$ m^{-3}, were also calculated by Gallego Valero *et al.*, (2018) in the year of 2014. Therefore, if it is possible to operate the membrane in a scenario of solar irradiation, in addition to being technically, the technology is also economically viable.

From the results obtained, it is possible to observe that adding both costs (CapEX and OpEX) the cost of Opex is more prevalent than Capex, representing approximately 75% of the total. Ozgun *et al.* (2021) also noted that Opex is more relevant (58%) in tertiary treatment.

Table 10. Operational costs for the tertiary treatment of secondary wastewater by photocatalytic membranes.

Chemicals, materials and utilities considered for OpEx estimation	Bare Cost	Real variable	Real Cost
Energy for the lamp (9W)	0.115 US$ kWh^{-1}	$4.44x10^7$ KWh $year^{-1}$	5111073.62 US$
Energy for the pump (5.5 KW)	0.115 US$ kWh^{-1}	48180 KWh $year^{-1}$	5540.7 US$
Energy for the aeration system (180 W)	0.115 US$ kWh^{-1}	1.11 $x10^7$ KWh $year^{-1}$	1277768.73 US$
Membrane replacement	129.41 US$ m^{-2}	2300 m^2 ano^{-1}	297643 US$
Maintenance	-	5% Capex	111222.94 US$

The consideration of the tertiary treatment process would imply an increase of 3.75 US$ m^{-3} for the wastewater treatment plants. However, the additional cost must be evaluated from a broader perspective, considering the advantages of the photocatalytic process. In the study presented by Garcia-Ivars *et al.*, (2017), nanofiltration membranes were evaluated as a tertiary process for the removal of eight trace organic compounds. Removals ranged from 30 - 40% for acetaminophen and caffeine to values close to 80% for triclosan. Variability is expected when dealing with compounds with different molecular weights and hydrophobicity, characteristics considered essential when dealing with the mechanisms involved in the removal of organic compounds by nanofiltration membranes. In addition to the variability in removal capacity, they are processes incapable of completely destroying the pollutant, transferring it from one phase (feed) to another (concentrate).

The system evaluated by Foureaux *et al.* (2021) also considered the use of nanofiltration membranes for betamethasone removal, also classified as a trace organic compound. High rejection values (>98.8%) were observed up to a recovery rate of 60%. Values higher than this resulted in the transfer of the compound to the permeate, compromising its quality. The study

suggests that of the total volume fed to the system, 40% would be converted into a concentrate stream, requiring additional treatment steps with direct implications for operating costs. Thus, the costs presented by the authors of 0.434 US$ m^{-3} would certainly be higher since the costs of treatment and disposal of the concentrate were not considered.

Some alternatives for managing the concentrate generated in these processes are disposal in surface water, disposal in the sewage collection network, injection into underground wells, evaporation ponds and soil application. The decision for the best strategy must consider, however, the impacts associated with each of the mentioned practices and the legal aspects involved. In addition, they are practices whose associated cost may even be higher than the total cost of treatment, ranging from 0.69 – 3 US$ m^{-3} (VERGILI et al., 2012). Thus, considering the treatment costs reported by Foureaux *et al.* (2021), associated to the concentrate disposal costs, the processes become equivalent in economic terms. Figure 35 shows the comparison of the two processes.

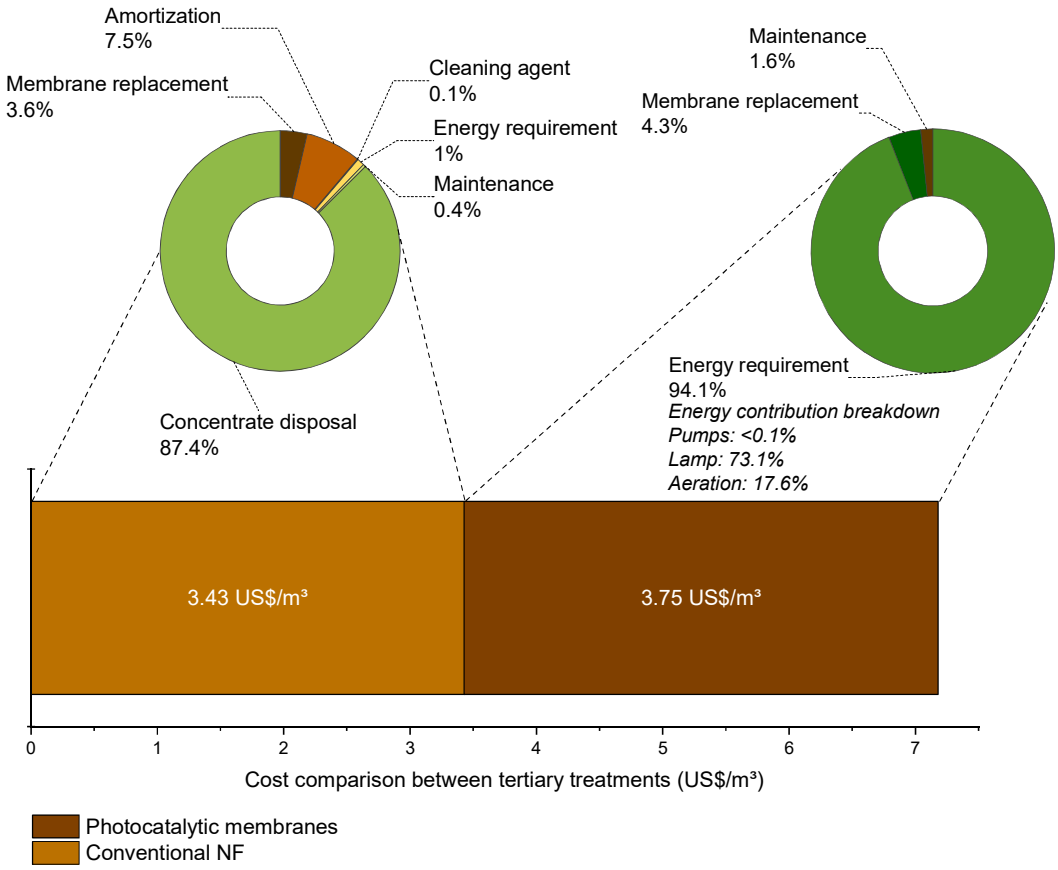

Figure 35 – Comparison between the operational costs obtained for photocatalytic membranes and the costs reported by Foureaux *et al.* (2020) for conventional membrane separation processes.

If considering the disposal costs of the concentrate, the nanofiltration treatment presented by Foureaux *et al.* (2020) would have a final operating cost close to 3.434 US$ m^{-3}, compared to 3.75 US$ m^{-3} for the photocatalytic system. However, the photocatalytic system would have advantages of not generating concentrate and greater treatment efficiency, after all, trace organic compounds would be degraded regardless of their molecular weight or hydrophobicity. Thus, the expectation is for a concentrate stream even free of these compounds if their complete mineralization by the photocatalytic process is proven. Studies that evaluated the photocatalytic process for the mineralization of trace organic compounds reported efficiencies that ranged from 94.52% to values close to 100% (XU et al., 2020), reinforcing the advantages associated with the greater efficiency of the process when compared to conventional ones.

5.4 CONCLUSIONS

The investigation of technological alternatives for wastewater treatment should be based not only on technical efficiency and performance criteria, but also on economic feasibility. The cost variables of system implementation and operation serve as a tool for decision makers in selecting the best option for a given situation and as a tool for comparing different technologies. In the case of the photocatalytic membranes, the implementation of a system for the tertiary treatment of wastewater from a population of approximately 31,000 people was considered. The calculated CapEX was US$ 1.23 per cubic meter, and the Opex was US$ 3.75 per cubic meter. Such values are higher than the costs of conventional processes and even some advanced processes, and the majority of the Opex costs were associated with electricity consumption. If the system was simplified by using natural irradiation such as sunlight and removing the aeration system, the new Opex would be US$ 0.23 per cubic meter, which is comparable to other advanced techniques such as granular activated carbon. It is worth noting that photocatalytic membranes have the advantage of not producing sludge and the generation of concentrate with less load, with consequent lower cost to be treated, aside from not being an environmental liability. As a result, all of these variables must be considered, and the technology shows promise for future scalability.

CHAPTER 6

Final considerations and suggestions for future works

- Among the techniques for modifying recycled membranes with TiO_2-GO, the one based on dopamine as a binding agent showed the best results. Dopamine acts as a "glue" between the materials and, therefore, the membranes generated in this route showed greater stability, even after being physically cleaned with water and tissue paper; Moreover, even after 10 months of operation, the presence of nanoparticles on the membrane surface was detected. A better distribution and greater number of nanocomposites were also observed on the membrane surface modified by this route.

- The self-assembly modification route did not generate satisfactory results, which may be associated with the weak interactions of nanomaterials with the remaining polymeric structure (polysulfone and polyester) in the membrane after the oxidation process;

- The modification route by filtration generated a membrane with a high capacity to reject the black eriochrome black dye (around 95%). However, it was the membrane with the lowest permeate flux among the evaluated, in addition to having presented instability as the detachment of the nanomaterials;

- High rejection of the eriochrome black dye was achieved by the membrane modified with the aid of dopamine (around 96%). Furthermore, the permeate flux during dye filtration remained practically unchanged, evidencing the anti-fouling capacity of the membrane;

- The increased rejection of eriochrome black dye by modified membranes compared to pristine is attributed to the decrease in pore size caused by the modification with the materials, as well as the electrostatic repulsion promoted by the functional groups of nanomaterials;

- Photocatalytic tests showed the photocatalytic activity of the membrane modified with TiO_2-GO reaching 30% degradation of the methylene blue dye in 90 minutes of UV-C irradiation. These results are promising since the combined operation of the filtration/photocatalysis system will promote the retention/degradation of pollutant compounds without affecting the overall residence time. Thus, in addition to guaranteeing

its removal, it will also guarantee a concentrate with a lower load, and the fouling will be mitigated.

- By the results of the system being irradiated by LED, there are great prospects for the TiO_2-GO nanocomposite to be activated by solar irradiation due to the presence of GO. This is a promising perspective, especially when thinking about scaling and reducing the process's costs and this alternative must be investigated.

- One of the biggest bottlenecks in the use of photocatalytic membranes is their stability. The route with dopamine is as a promising alternative and long-term tests (years) need to be performed to evaluate its performance and prove its stability.

- Eco-friendly and cost-effective photocatalytic membranes were developed.

- Fouling mitigation and enhanced rejection were found for photocatalytic membranes.

- Effective rejections of dyes (~100%) and PhACs (up to 95.7%) were achieved.

- Concentration of PhACs was clearly reduced in the feed solution under permeation with UV-C irradiation.

- In addition to producing a permeate with a lower concentration than the feed, the photocatalytic membrane produced a concentrate with a lower charge, which helps to solve a problem in membrane separation processes: the treatment and disposal of the concentrate.

- The photocatalytic membranes have demonstrated promise in removing TOrCs from domestic wastewater after secondary treatment.

- The inclusion of dopamine throughout the fabrication process allowed the membranes to demonstrate stability after 10 months of use.

- By modifying membranes with nanocomposites, an increase in membrane hydrophilicity and increased surface electronegativity was demonstrated which contributed to better performances in the removal TOrCs.

- The effect of the lamp position on the light fluence that reaches the membrane was assessed, and greater values were found in the middle of the membrane, providing parameters for process optimization.

- It was examined wastewater treatments with the photocatalytic membranes by complete UV-C system (irradiation and filtration), full LED system (irradiation and filtration), only the filtration system, the UV-C system alone and LED system alone. In general, the best results were obtained with all UV-C system.

- Outstandig reductions in the concentrations of diclofenac (92%) and antipyrine (87%) were achieved in 90 minutes of the system operation.

- Changes in effluent pH demonstrated an improved trend in the attenuation of TOrCS concentration at higher pHs.

- The implementation of a photocatalytic membrane system for wastewater treatment at a flow rate of 207 $m^3 h^{-1}$, serving a population of approximately 31,000 people, will result in a Capex of 1.23 US$ m^{-3} and an Opex of 3.75 US$ m^{-3}. These values are higher than conventional and advanced techniques that have been on the market for a longer period of time. However, such costs can be reduced by adaptations as using solar irradiation or removing the aeration system. As a result, photocatalytic membranes show technical and economic promise.

- To maintain the process's efficiency, it is suggested that cleaning processes for membranes be evaluated, as well as the frequency of this procedure. Furthermore, the maintenance of the nanoparticles on the membranes' surface after cleaning should be assessed.

REFERENCES

REFERENCES

ABADIKHAH, H. *et al.* High flux thin film nanocomposite membrane incorporated with functionalized TiO_2@reduced graphene oxide nanohybrids for organic solvent nanofiltration. **Chemical Engineering Science**, v. 204, p. 99–109, 2019b.

AHMED, S. et al. Emerging pollutants and their removal using visible-light responsive photocatalysis – A comprehensive review. **Journal of environmental chemical engineering**, v. 9, n. 6, p. 106643, 2021.

AKBARI, M. *et al.* Janus graphene oxide nanosheet: A promising additive for enhancement of polymeric membranes performance prepared via phase inversion. **Journal of colloid and interface science**, v. 527, p. 10–24, 2018.

AKHAVAN, O.; GHADERI, E. Toxicity of graphene and graphene oxide nanowalls against bacteria. **ACS Nano**, v. 4, n. 10, p. 5731–5736, 2010.

AL-GAMAL, A. Q.; FALATH, W. S.; SALEH, T. A. Enhanced efficiency of polyamide membranes by incorporating TiO2-Graphene oxide for water purification. **Journal of Molecular Liquids**, v. 323, p. 114922, 2021.

ALAM, S. N.; SHARMA, N.; KUMAR, L. Synthesis of graphene oxide (GO) by modified hummers method and its thermal reduction to obtain reduced graphene oxide (rGO). **Graphene**, v. 6, n. 1, p. 1–18, 2017.

ALAOUI, O. T. et al. Elaboration and study of poly (vinylidene fluoride)–anatase TiO2 composite membranes in photocatalytic degradation of dyes. **Applied Catalysis A: General**, v. 358, n. 1, p. 13–20, 2009.

ALMEIDA, N. A. *et al.* TiO_2/graphene oxide immobilized in P(VDF-TrFE) electrospun membranes with enhanced visible-light-induced photocatalytic performance. **Journal Of Materials Science**, v. 51, n. 14, p. 6974–6986, jul. 2016.

AMANIPOUR, M. *et al.* Effect of CVD parameters on hydrogen permeation properties in a nano-composite SiO2–Al2O3 membrane. **Journal of Membrane Science**, v. 423–424, p. 530–535, 2012.

ANTONY, A.; BRANCH, A.; LESLIE, G.; LE-CLECH, P. Impact of Membrane Ageing on Reverse Osmosis Performance – Implications on Validation Protocol. **Journal of Membrane Science**, v. 520, p. 37-44, 2016.

APHA - Standard Methods for the Examination of Water and Wastewater, 20th Edition. **American Public Health Association**, Washington, DC, 2005.

ARLOS, M. J. et al. Photocatalytic decomposition of organic micropollutants using immobilized TiO2 having different isoelectric points. **Water research**, v. 101, p. 351–361, 2016.

ATHANASEKOU, C. P. *et al.* Prototype composite membranes of partially reduced graphene oxide/TiO2 for photocatalytic ultrafiltration water treatment under visible light. **Applied Catalysis B: Environmental**, v. 158–159, p. 361–372, 2014.

ATHANASEKOU, C.P. *et al.*. Ceramic Photocatalytic Membranes for Water Filtration Under UV and Visible Light. **Appl. Catal. B Environ**. 2015, 178, 12–19.

AYYARU, S.; AHN, Y. H. Fabrication and separation performance of polyethersulfone/sulfonated TiO2 (PES–STiO2) ultrafiltration membranes for fouling mitigation. **Journal of Industrial and Engineering Chemistry**, v. 67, p. 199–209, 25 nov. 2018.

BAEK, Y. *et al.* High performance and antifouling vertically aligned carbon nanotube membrane for water purification. **Journal of membrane science**, v. 460, p. 171–177, 2014.

BAI, H.; LIU, Z.; SUN, D. D. Hierarchical ZnO nanostructured membrane for multifunctional environmental applications. **Colloids and surfaces. A, Physicochemical and engineering aspects**, v. 410, p. 11–17, 2012.

BAIG, M. I. *et al.* Water vapor transport properties of interfacially polymerized thin film nanocomposite membranes modified with graphene oxide and GO-TiO2 nanofillers. **Chemical engineering journal** (Lausanne, Switzerland : 1996), v. 373, p. 1190–1202, 2019.

BAILLY, E.; LEVI, Y.; KAROLAK, S.; Calibration and field evaluation of polar organic chemical integrative sampler (POCIS) for monitoring pharmaceuticals in hospital wastewater. **Environmental Pollution**, 174, pp. 100–105, 2013.

BAKER, R. W. Membranes and Modules. In: **Membrane Technology and Applications**. [s.l.] John Wiley & Sons, Ltd, 2004. p. 89–160.

BAO, Z. *et al.* Superamphiphilic and underwater superoleophobic membrane for oil/water emulsion separation and organic dye degradation. **Journal Of Membrane Science**, v. 598, mar. 2020.

BET-MOUSHOUL, E. *et al.* TiO_2 nanocomposite based polymeric membranes: A review on performance improvement for various applications in chemical engineering processes. **Chemical Engineering Journal**, v. 283, p. 29–46, jan. 2016.

BHANDARI, A. *et al.* Contaminants of emerging environmental concern. **American Society of Civil Engineers (ASCE).** 2009. https://doi.org/10.1061/9780784410141

BOBIRICĂ, L. et al. Influence of Operating Parameters on Photocatalytic Oxidation of 2,4-Dichlorofenol in Aqueous Solution by TiO2/Stainless Steel Photocatalytic Membrane. **Applied sciences**, v. 11, n. 24, p. 11664, 2021.

BRASIL, **Diagnósticos dos Serviços de Água e Esgoto**, Ministério do desenvolvimento Regional – Secretaria Nacional de Saneamento, 2019.

CAI, Z. *et al.* Application of nanotechnologies for removing pharmaceutically active compounds from water: development and future trends. **Environmental Science-Nano,** v. 5, n. 1, p. 27–47, jan. 2018.

CAMERA-RODA, G. et al. Process intensification in a photocatalytic membrane reactor: Analysis of the techniques to integrate reaction and separation. **Chemical engineering journal (Lausanne, Switzerland : 1996)**, v. 310, p. 352–359, 2017.

CAO, X.-L. *et al.* Tailoring nanofiltration membranes for effective removing dye intermediates in complex dye-wastewater**. Journal of membrane science**, v. 595, 2020.

CAPODAGLIO, A. G. et al. Sustainability of decentralized wastewater treatment technologies. **Water Practice and Technology**, v. 12, n. 2, p. 463–477, 1 jun. 2017.

CAROLINE RICCI, B. et al. A novel submerged anaerobic osmotic membrane bioreactor coupled to membrane distillation for water reclamation from municipal wastewater. **Chemical Engineering Journal**, v. 414, p. 128645, 2021.

CHAKRABORTY, S. et al. Photocatalytic hollow fiber membranes for the degradation of pharmaceutical compounds in wastewater. **Journal of environmental chemical engineering**, v. 5, n. 5, p. 5014–5024, 2017.

CHELME-AYALA, P.; SMITH, D. W.; EL-DIN, M. G. Membrane concentrate management options: a comprehensive critical review. **Journal of Environmental Engineering and Science**, v. 8, n. 3, p. 326–339, 2013.

CHEN, L. *et al.* Graphene oxide based membrane intercalated by nanoparticles for high performance nanofiltration application. **Chemical engineering journal** (Lausanne, Switzerland : 1996), v. 347, p. 12–18, 2018.

CHEN, P. C.; CHEN, C. C.; CHEN, S. H. A Review on Production, Characterization, and Photocatalytic Applications of TiO2 Nanoparticles and Nanotubes. **Current Nanoscience**, v. 13, n. 4, p. 373–393, 2017.

CHEN, X.; MAO, S. S. Titanium dioxide nanomaterials: Synthesis, properties, modifications, and applications. **Chemical Reviews**, v. 107, n. 7, p. 2891–2959, 2007.

CHI-JUNG, C. *et al.* Polymer/BiOBr-Modified Gauze as a Dual-Functional Membrane for Heavy Metal Removal and Photocatalytic Dye Decolorization. **Polymers**, v. 12, n. 9, p. 2082, 2020.

CHOUDHURY, P. *et al.* Preparation of ceramic ultrafiltration membrane using green synthesized CuO nanoparticles for chromium (VI) removal and optimization by response surface methodology**. Journal of cleaner production**, v. 203, p. 511–520, 2018.

CORREA, C. *et al.* Antimicrobial activity from polymeric composites-based polydimethylsiloxane/TiO_2/GO: evaluation of filler synthesis and surface morphology. **Polymer Bulletin**, v. 74, n. 6, p. 2379–2390, 2017.

COUTINHO DE PAULA, E.; SANTOS AMARAL, M. C. Environmental and economic evaluation of end-of-life reverse osmosis membranes recycling by means of chemical conversion. **Journal of Cleaner Production**, v. 194, p. 85–93, 2018.

COUTO, C. F. et al. Assessing potential of nanofiltration, reverse osmosis and membrane distillation drinking water treatment for pharmaceutically active compounds (PhACs) removal. **Journal of Water Process Engineering**, v. 33, p. 101029, 2020.

DADVAR, E. *et al.* Efficiency of Polymeric Membrane Graphene Oxide-TiO2 for Removal of Azo Dye. **Journal of Chemistry**, v. 2017, 2017.

DAMODAR, R. A.; YOU, S.-J.; CHOU, H.-H. Study the self cleaning, antibacterial and photocatalytic properties of TiO 2 entrapped PVDF membranes. **Journal of hazardous materials**, v. 172, n. 2–3, p. 1321–1328, 2009.

DAROWNA, D. et al. The influence of feed composition on fouling and stability of a polyethersulfone ultrafiltration membrane in a photocatalytic membrane reactor. **Chemical Engineering Journal**, v. 310, p. 360–367, 2017.

DE OLIVEIRA, C. P. M. *et al.* Potential use of green TiO_2 and recycled membrane in a photocatalytic membrane reactor for oil refinery wastewater polishing. **Journal of Cleaner Production**, v. 257, p. 120526, 2020a.

DE OLIVEIRA, C. P. M. et al. Converting recycled membranes into photocatalytic membranes using greener TiO2-GRAPHENE oxide nanomaterials. **Chemosphere**, v. 306, p. 135591, 2022b.

DE OLIVEIRA, C. P. M. et al. TiO2-Graphene oxide nanocomposite membranes: A review. **Separation and Purification Technology**, v. 280, p. 119836, 2022a.

DE OLIVEIRA, M. et al. Pharmaceuticals residues and xenobiotics contaminants: Occurrence, analytical techniques and sustainable alternatives for wastewater treatment. **The Science of the total environment**, v. 705, 2020b.

DE PAULA, E. C.; GOMES, J. C. L.; AMARAL, M. C. S. Recycling of end-of-life reverse osmosis membranes by oxidative treatment: A technical evaluation. **Water Science and Technology**, v. 76, n. 3, p. 605–622, jul. 2017.

DE PAULA, E.; AMARAL, M. C. S. Extending the life-cycle of reverse osmosis membranes: A review. **Waste Management & Research**, v. 35, n. 5, p. 456–470, 2017.

DE PAULA, Eduardo Coutinho; AMARAL, Míriam Cristina Santos. Environmental and economic evaluation of end-of-life reverse osmosis membranes recycling by means of chemical conversion. **Journal of Cleaner Production**, v. 194, p. 85-93, 2018.

DHARUPANEEDI, S. P. *et al.* Membrane-based separation of potential emerging pollutants. **Separation and Purification Technology**, 2019.

DIOGO JANUÁRIO, E. F. *et al.* Functionalization of membrane surface by layer-by-layer self-assembly method for dyes removal. **Process safety and environmental protection**, v. 134, p. 140–148, 2020.

DOW. Reverse Osmosis Membranes Technical Manual. DOW FILMTEC™, 2012. Available in:<http://msdssearch.dow.com/PublishedLiteratureDOWCOM/dh_095b/0901b8038095b91d.pdf?filepath=liquidseps/pdfs/noreg/609-00071.pdf>. Acess in: May, 8 2019.

DUONG, H. C. *et al.* Membrane scaling and prevention techniques during seawater desalination by air gap membrane distillation. **Desalination**, v. 397, n. C, p. 92–100, 2016.

EGEA-CORBACHO LOPERA, A.; GUTIÉRREZ RUIZ, S.; QUIROGA ALONSO, J. M. Removal of emerging contaminants from wastewater using reverse osmosis for its subsequent reuse: Pilot plant. **Journal of Water Process Engineering**, v. 29, p. 100800, 2019.

ENICK, O. V; MOORE, M. M. Assessing the assessments: Pharmaceuticals in the environment. **Environmental impact assessment review**, v. 27, n. 8, p. 707–729, 2007.

FARALDOS, Marisol; BAHAMONDE, Ana. Environmental applications of titania-graphene photocatalysts. **Catalysis Today**, [s.l.], v. 285, p.13-28, maio 2017. Elsevier BV.

FARIA, C. V et al. Removal of micropollutants in domestic wastewater by expanded granular sludge bed membrane bioreactor. **Process safety and environmental protection**, v. 136, p. 223–233, 2020.

FENG, K. et al. A self-protected self-cleaning ultrafiltration membrane by using polydopamine as a free-radical scavenger. **Journal of Membrane Science**, v. 490, p. 120–128, 2015.

FISCHER, K.; GRIMM, M.; MEYERS, J.; DIETRICH, C.; GLÄSER, R.; SCHULZE, A. Photoactive Microfiltration Membranes via Directed Synthesis of TiO_2 Nanoparticles on the Polymer Surface for Removal of Drugs From Water. **J. Membr. Sci**. 2015, 478, 49–57

FOUREAUX, A. F. S. et al. Insights into the retention behavior of betamethasone by nanofiltration – An alternative for decentralized drinking water treatment. **Journal of Water Process Engineering**, v. 40, p. 101792, 2021.

FRYE, C. *et al.* Endocrine Disrupters: A Review of Some Sources, Effects, and Mechanisms of Actions on Behaviour and Neuroendocrine Systems. **Journal of Neuroendocrinology**, v. 24, n. 1, p. 144–159, 2012.

GALLEGO VALERO, L. et al. Analysis of environmental taxes to finance wastewater treatment in Spain: an opportunity for regeneration? **Water**, v. 10, n. 2, p. 226, 2018.

GAO, P. *et al.* Multifunctional graphene oxide-TiO_2 microsphere hierarchical membrane for clean water production. **Applied Catalysis B-Environmental**, v. 138, p. 17–25, jul. 2013b.

GAO, P. *et al.* High quality graphene oxide-CdS-Pt nanocomposites for efficient photocatalytic hydrogen evolution. **Journal of Materials Chemistry**, v. 22, n. 5, p. 2292–2298, 2012.

GAO, Y.; HU, M.; MI, B. Membrane surface modification with TiO2-graphene oxide for enhanced photocatalytic performance. **Journal of Membrane Science**, v. 455, p. 349–356, 2014a.

GARCIA-IVARS, J. et al. Nanofiltration as tertiary treatment method for removing trace pharmaceutically active compounds in wastewater from wastewater treatment plants. **Water research**, v. 125, p. 360–373, 2017.

GARCÍA-PACHECO, R.*; et al.* Transformation of end-of-life RO membranes into NF and UF membranes: Evaluation of membrane performance. **Journal of Membrane Science**, v. 495, p. 305-315, 2015.

GROSSI, L. B. et al. Reverse osmosis elements waste assessment: Screening and forecasting of emerging waste in Brazil. **Desalination**, v. 517, p. 115245, 1 dez. 2021.

GUO, F. et al. Graphene-Based Environmental Barriers. **Environmental Science & Technology**, v. 46, n. 14, p. 7717, 2012.

GUO, W.; NGO, H.-H.; LI, J. A mini-review on membrane fouling. **Bioresource technology**, v. 122, p. 27–34, 2012.

GUOZHENG, J. et al. **Effects of light intensity and H2O2 on photocatalytic degradation of phenol in wastewater using TiO2/ACF**. 2010 international conference on digital manufacturing & automation. **Anais**...IEEE, 2010

HASAN, M. T. *et al.* Optical Band Gap Alteration of Graphene Oxide via Ozone Treatment. **Scientific reports**, v. 7, n. 1, p. 1–8, 2017.

HE, C. et al. Future global urban water scarcity and potential solutions. **Nature communications**, v. 12, n. 1, p. 1–11, 2021.

HENRIQUES, J.; CATARINO, J. Sustainable Value and Cleaner Production – research and application in 19 Portuguese SME. **Journal of cleaner production**, v. 96, n. C, p. 379–386, 2015.

HORIKOSHI, S.; SERPONE, N. Can the photocatalyst TiO2 be incorporated into a wastewater treatment method? Background and prospects. **Catalysis today**, v. 340, p. 334–346, 2020.

HOSSEINI, N.; TOOSI, M. R. Removal of 2,4-D, glyphosate, trifluralin, and butachlor herbicides from water by polysulfone membranes mixed by graphene oxide/TiO2

nanocomposite: study of filtration and batch adsorption. **Journal of Environmental Health Science and Engineering**, v. 17, n. 1, 2019.

HOSSEINI, S. M. *et al.* Tailoring the electrochemical properties of ED ion exchange membranes based on the synergism of TiO_2 nanoparticles-co-GO nanoplates. **Journal of colloid and interface science**, v. 505, p. 763–775, 2017.

HUANG, M. et al. Rejection and adsorption of trace pharmaceuticals by coating a forward osmosis membrane with TiO2. **Chemical Engineering Journal**, v. 279, p. 904–911, 2015.

HUANG, Y.; SHANG, C.; LI, L. Novel N-doped graphene enhanced ultrafiltration nano-porous polyvinylidene fluoride membrane with high permeability and stability for water treatment. **Separation and Purification Technology**, v. 267, p. 118622, 2021.

HUANG, Z. et al. Global assessment of future sectoral water scarcity under adaptive inner-basin water allocation measures. **The Science of the total environment**, v. 783, p. 146973, 2021.

HUANG, Z.-Q. *et al.* The performance of the PVDF-Fe_3O_4 ultrafiltration membrane and the effect of a parallel magnetic field used during the membrane formation. **Desalination**, v. 292, p. 64–72, 2012.

HUNTER, R. G. et al. Municipal wastewater treatment costs with an emphasis on assimilation wetlands in the Louisiana coastal zone. **Ecological Engineering**, v. 137, p. 21–25, 2019.

IGBINIGUN, E. *et al.* Graphene oxide functionalized polyethersulfone membrane to reduce organic fouling. **Journal of membrane science**, v. 514, p. 518–526, 2016.

IGLESIAS, O. *et al.* Membrane-based photocatalytic systems for process intensification. **Chemical Engineering Journal**, v. 305, p. 136–148, 2016.

JELIC, A. et al. Occurrence, partition and removal of pharmaceuticals in sewage water and sludge during wastewater treatment. **Water research (Oxford)**, v. 45, n. 3, p. 1165–1176, 2011.

JHAVERI, J. H.; MURTHY, Z. V. P. A comprehensive review on anti-fouling nanocomposite membranes for pressure driven membrane separation processes. **Desalination,** v. 379, p. 137–154, 2016.

JHAVERI, J. H.; MURTHY, Z. V. P. Nanocomposite membranes. **Desalination and water treatment**, v. 57, n. 55, p. 26803–26819, nov. 2016b.

JHAVERI, J. H.; PATEL, C. M.; MURTHY, Z. V. P. Preparation, characterization and application of GO-TiO2/PVC mixed matrix membranes for improvement in performance. **Journal of industrial and engineering chemistry (Seoul, Korea)**, v. 52, p. 138–146, 2017.

JI, M. et al. Improved blood compatibility of polysulfone membrane by anticoagulant protein immobilization. **Colloids and Surfaces B: Biointerfaces**, v. 175, p. 586–595, 2019.

JIA, Z.; SHI, W. Tailoring permeation channels of graphene oxide membranes for precise ion separation. **Carbon (New York)**, v. 101, p. 290–295, 2016.

JIANG, L.; CHOO, K.-H. Photocatalytic mineralization of secondary effluent organic matter with mitigating fouling propensity in a submerged membrane photoreactor. **Chemical engineering journal (Lausanne, Switzerland : 1996)**, v. 288, p. 798–805, 2016.

JIANG, Y. *et al.* Engineered Crumpled Graphene Oxide Nanocomposite Membrane Assemblies for Advanced Water Treatment Processes. **Environmental Science & Technology**, v. 49, n. 11, p. 6846–6854, jun. 2015.

JIN, L. M. *et al.* Synthesis of a novel composite nanofiltration membrane incorporated SiO2 nanoparticles for oily wastewater desalination. **Polymer (Guilford),** v. 53, n. 23, p. 5295–5303, 2012.

JOHARI, N. A. et al. Polyethersulfone ultrafiltration membrane incorporated with ferric-based metal-organic framework for textile wastewater treatment. **Separation and Purification Technology**, v. 270, p. 118819, 2021.

JOO, S. H.; TANSEL, B. Novel technologies for reverse osmosis concentrate treatment: A review. **Journal of environmental management**, v. 150, n. C, p. 322–335, 2015.

JOURSHABANI, M. et al. Synergetic photocatalytic ozonation using modified graphitic carbon nitride for treatment of emerging contaminants under UVC, UVA and visible irradiation. **Chemical engineering science**, v. 209, p. 115181, 2019.

JUKOSKY, J. A.; WATZIN, M. C.; LEITER, J. C. The effects of environmentally relevant mixtures of estrogens on Japanese medaka (Oryzias latipes) reproduction. **Aquatic toxicology**, v. 86, n. 2, p. 323–331, 2008.

KASPRZYK-HORDERN, B.; DINSDALE, R. M.; GUWY, A. J. The removal of pharmaceuticals, personal care products, endocrine disruptors and illicit drugs during wastewater treatment and its impact on the quality of receiving waters. **Water research (Oxford),** v. 43, n. 2, p. 363–380, 2009.

KERTÈSZ, S.; CAKL, J.; JIRÁNKOVÁ, H. Submerged hollow fiber microfiltration as a part of hybrid photocatalytic process for dye wastewater treatment. **Desalination**, v. 343, p. 106–112, 2014.

KHAN, S. et al. Humic acid fouling in a submerged photocatalytic membrane reactor with binary TiO2–ZrO2 particles. **Journal of industrial and engineering chemistry (Seoul, Korea)**, v. 21, n. 1, p. 779–786, 2015.

KIM, I. Y. *et al.* Strongly-Coupled Freestanding Hybrid Films of Graphene and Layered Titanate Nanosheets: An Effective Way to Tailor the Physicochemical and Antibacterial Properties of Graphene Film. **Advanced Functional Materials**, v. 24, n. 16, p. 2288–2294, 2014.

KLAVARIOTI, M.; MANTZAVINOS, D.; KASSINOS, D. Removal of residual pharmaceuticals from aqueous systems by advanced oxidation processes. **Environment international**, v. 35, n. 2, p. 402–417, 2009.

KOE, W. S. et al. An overview of photocatalytic degradation: photocatalysts, mechanisms, and development of photocatalytic membrane. **Environmental science and pollution research international**, v. 27, n. 3, p. 2522–2565, 2020.

KORZHOVA, E. et al. Modification of commercial UF membranes by electrospray deposition of polymers for tailoring physicochemical properties and enhancing filtration performances. **Journal of membrane science**, v. 598, 2020.

KOULIVAND, H. *et al.* Development of carbon dot-modified polyethersulfone membranes for enhancement of nanofiltration, permeation and antifouling performance. **Separation and Purification Technology**, v. 230, p. 115895, 2020.

KUMAR, A.; PANDEY, G. A review on the factors affecting the photocatalytic degradation of hazardous materials. **Mater. Sci. Eng. Int. J**, v. 1, n. 3, p. 1–10, 2017.

KUMAR, M. *et al.* Preparation and characterization of low fouling novel hybrid ultrafiltration membranes based on the blends of GO−TiO_2 nanocomposite and polysulfone for humic acid removal. **Journal of Membrane Science**, v. 506, p. 38–49, 2016.

KURDVE, M. *et al.* Waste flow mapping to improve sustainability of waste management: a case study approach. **Journal of cleaner production**, v. 98, n. Special Volume: Support your future today! Turn environmental challenges into opportunities, p. 304–315, 2015.

KUSWORO, T. D. *et al.* Preparation and characterization of photocatalytic PSf-TiO2/GO nanohybrid membrane for the degradation of organic contaminants in natural rubber wastewater. **Journal of Environmental Chemical Engineering**, v. 9, n. 2, p. 105066, 2021.

LAMBERT, T. N. *et al.* Synthesis and characterization of titania-graphene nanocomposites. **Journal of Physical Chemistry C**, v. 113, n. 46, p. 19812–19823, 2009.

LAWLER, W.; ANTONY, A.; CRAN, M.; DUKE, M.; LESLIE, G.; LE-CLECH, P. Production and characterization of UF membranes by chemical conversion of used RO membranes. **Journal of Membrane Science**, v. 447, p. 203–211, 2013.

LEE, H. et al. Mussel-inspired surface chemistry for multifunctional coatings. **Science**, v. 318, n. 5849, p. 426–430, 2007.

LEE, S.-J.; KIM, J.-H. Differential natural organic matter fouling of ceramic versus polymeric ultrafiltration membranes. **Water research (Oxford)**, v. 48, n. 1, p. 43–51, 2014.

LEONG, S. et al. TiO_2 based photocatalytic membranes: A review. **Journal of Membrane Science**, v. 472, p. 167–184, 15 dez. 2014.

LEVITSKY, I.; TAVOR, D.; GITIS, V. Microbubbles and organic fouling in flat sheet ultrafiltration membranes. **Separation and Purification Technology**, v. 268, p. 118710, 2021.

LI, C. *et al.* Ceramic nanocomposite membranes and membrane fouling: A review. **Water research (Oxford)**, v. 175, 2020.

LI, C. et al. Degradation kinetics and removal efficiencies of pharmaceuticals by photocatalytic ceramic membranes using ultraviolet light-emitting diodes. **Chemical engineering journal (Lausanne, Switzerland : 1996)**, v. 427, p. 130828, 2022.

LI, C. et al. Systematic evaluation of TiO2-GO-modified ceramic membranes for water treatment: Retention properties and fouling mechanisms. **Chemical Engineering Journal**, v. 378, p. 122138, 15 dez. 2019a.

LI, M. et al. Feasibility of concentrating textile wastewater using a hybrid forward osmosis-membrane distillation (FO-MD) process: Performance and economic evaluation. **Water Research**, v. 172, p. 115488, 2020b.

LI, N. *et al.* Catalytic membrane-based oxidation-filtration systems for organic wastewater purification: A review. **Journal of Hazardous Materials**, v. 414, p. 125478, 2021.

LI, T. *et al.* A membrane modified with nitrogen-doped TiO_2/graphene oxide for improved photocatalytic performance. **Applied Sciences (Switzerland),** v. 9, n. 5, 2019.

LIN, Y.-L. Effects of organic, biological and colloidal fouling on the removal of pharmaceuticals and personal care products by nanofiltration and reverse osmosis membranes.(Report). **Journal of Membrane Science**, v. 542, p. 342, 2017.

LIU, H. *et al.* Preparation of Stable Hydrophilic Polyethyleneimine Cross-Linked Graphene Oxide/Titanium Dioxide Membranes for Dye Separation. **Nano**, v. 16, n. 01, p. 2150008, 2021.

LIU, H.; WANG, H.; ZHANG, X. Facile Fabrication of Freestanding Ultrathin Reduced Graphene Oxide Membranes for Water Purification. **Advanced Materials**, v. 27, n. 2, p. 249–254, 2015.

LIU, J. *et al.* Self-Assembling TiO_2 Nanorods on Large Graphene Oxide Sheets at a Two-Phase Interface and Their Anti-Recombination in Photocatalytic Applications. **Advanced Functional Materials**, v. 20, n. 23, p. 4175–4181, 2010.

LIU, S. *et al.* Antibacterial Activity of Graphite, Graphite Oxide, Graphene Oxide, and Reduced Graphene Oxide: Membrane and Oxidative Stress. **ACS Nano**, v. 5, n. 9, p. 6971–6980, 2011.

LIU, Y. *et al.* A novel photocatalytic self-cleaning TiO_2 nanorods inserted graphene oxide-based nanofiltration membrane. **Chemical Physics Letters**, v. 749, jun. 2020.

LUO, Y. *et al.* A review on the occurrence of micropollutants in the aquatic environment and their fate and removal during wastewater treatment. **The Science of the total environment**, v. 473–474, p. 619–641, 2014.

MA, J.; PING, D.; DONG, X. Recent developments of graphene oxide-based membranes: A review. **Membranes**, v. 7, n. 3, 2017.

MANOHARAN, R.; YOUNG-HO, A. Auto-cleaning functionalization of the polyvinylidene fluoride membrane by the biocidal oxine/TiO_2 nanocomposite for anti-biofouling properties**.** **New Journal of Chemistry**, v. 44, n. 3, p. 807–816, 2020.

MANSOURPANAH, Y. et al. Formation of appropriate sites on nanofiltration membrane surface for binding TiO 2 photo-catalyst: Performance, characterization and fouling-resistant capability. **Journal of membrane science**, v. 330, n. 1, p. 297–306, 2009.

MARINHO, B.; DACHAMIR, H. Electrospun TiO2 nanofibers for water and wastewater treatment: a review. **Journal of Materials Science**, v. 56, n. 9, p. 5428–5448, 2021.

MARZOUK, S. S. *et al.* Preparation of TiO_2/SiO_2 ceramic membranes via dip coating for the treatment of produced water. **Chemosphere (Oxford)**, v. 273, 2021.

MENDRET, J. et al. Influence of solution pH on the performance of photocatalytic membranes during dead-end filtration. **Separation and Purification Technology**, v. 118, p. 406–414, 2013.

MENG, N. *et al.* A low-pressure GO nanofiltration membrane crosslinked via ethylenediamine. **Journal of membrane science**, v. 548, p. 363–371, 2018.

MÉRICQ, J.-P. *et al.* High performance PVDF-TiO_2 membranes for water treatment. **Chemical Engineering Science**, v. 123, p. 283–291, 2015.

MIN, K. *et al.* Enhanced chemical interaction between TiO_2 and grapheme oxide for photocatalytic decolorization of methylene blue, **Chem.Eng.J.** 193(2012)203–210.

MITO, M. T. et al. Reverse osmosis (RO) membrane desalination driven by wind and solar photovoltaic (PV) energy: State of the art and challenges for large-scale implementation. **Renewable and Sustainable Energy Reviews**, v. 112, p. 669–685, 2019.

MOLINARI, R.; LAVORATO, C.; ARGURIO, P. Recent progress of photocatalytic membrane reactors in water treatment and in synthesis of organic compounds. A review. **Catalysis Today**, v. 281, p. 144–164, 2017.

MORADI, M. R. et al. End-of-life RO membranes recycling: Reuse as NF membranes by polyelectrolyte layer-by-layer deposition. **Journal of membrane science**, v. 584, p. 300–308, 2019.

MORAL PAJARES, E.; GALLEGO VALERO, L.; ROMÁN SÁNCHEZ, I. M. Cost of urban wastewater treatment and ecotaxes: Evidence from municipalities in southern Europe. **Water**, v. 11, n. 3, p. 423, 2019.

MORALES-TORRES, S. *et al.* Design of graphene-based TiO_2 photocatalysts-a review. **Environmental Science And Pollution Research**, v. 19, n. 9, p. 3676–3687, 2012.

MORALES-TORRES, S. *et al.* Thin-film composite forward osmosis membranes based on polysulfone supports blended with nanostructured carbon materials. **Journal of Membrane Science**, v. 520, n. C, p. 326, 2016.

MOREIRA, V. R. et al. Membrane distillation and dispersive solvent extraction in a closed-loop process for water, sulfuric acid and copper recycling from gold mining wastewater. **Chemical Engineering Journal**, v. 435, p. 133874, 2022.

MOREIRA, V. R. et al. Recycled reverse osmosis membrane combined with pre-oxidation for improved arsenic removal from high turbidity waters and retrofit of conventional drinking water treatment process. **Journal of Cleaner Production**, v. 312, p. 127859, 20 ago. 2021.

MOSER, P. B. *et al.* Effect of MBR-H_2O_2/UV Hybrid pre-treatment on nanofiltration performance for the treatment of petroleum refinery wastewater. **Separation and Purification Technology**, v. 192, p. 176–184, 2018.

MOZIA, S. *et al.* Effect of process parameters on fouling and stability of MF/UF TiO_2 membranes in a photocatalytic membrane reactor. **Separation and Purification Technology,** v. 142, p. 137–148, 2015.

MOZIA, S. Photocatalytic membrane reactors (PMRs) in water and wastewater treatment. A review. **Separation and Purification Technology**, 2010.

MUCHTAR, S. et al. Polydopamine-coated poly (vinylidene fluoride) membranes with high ultraviolet resistance and antifouling properties for a photocatalytic membrane reactor. **Journal of Applied Polymer Science**, v. 136, n. 14, p. 47312, 2019.

MUHULET, A. et al. Synthesis and characterization of polysulfone–TiO2 decorated MWCNT composite membranes by sonochemical method. **Applied Physics A**, v. 126, n. 3, p. 1–9, 2020.

MULDER, M.; ANTAKYALI, D.; ANTE, S. Costs of removal of micropollutants from effluents of municipal wastewater treatment plants-general cost estimates for the Netherlands based on implemented full scale post treatments of effluents of wastewater treatment plants in Germany and Switzerland. **STOWA and Waterboard the Dommel, the Netherlands**, v. 55, 2015.

MÜLLER, J.; DREWES, J. E.; HÜBNER, U. Sequential biofiltration – A novel approach for enhanced biological removal of trace organic chemicals from wastewater treatment plant effluent. **Water Research**, v. 127, p. 127–138, 15 dez. 2017.

MURGOLO, S. *et al.* Degradation of emerging organic pollutants in wastewater effluents by electrochemical photocatalysis on nanostructured TiO_2 meshes. **Water research (Oxford)**, v. 164, 2019.

NAIR, A. K.; JAGADEESH, J. B. TiO2 nanosheet-graphene oxide based photocatalytic hierarchical membrane for water purification. **Surface and Coatings Technology**, v. 320, p. 259–262, 2017.

NASEEM, S. *et al.* Oil-Water Separation of Electrospun Cellulose Triacetate Nanofiber Membranes Modified by Electrophoretically Deposited TiO_2/Graphene Oxide. **Polymers**, v. 10, n. 7, jul. 2018.

NASROLLAHI, N. *et al.* Photocatalytic-membrane technology: a critical review for membrane fouling mitigation. **Journal of industrial and engineering chemistry (Seoul, Korea)**, v. 93, p. 101–116, 2021.

NGO, T. H. A. *et al.* Improvement of Hydrophilicity for Polyamide Composite Membrane by Incorporation of Graphene Oxide-Titanium Dioxide Nanoparticles. **Journal of analytical methods in chemistry,** v. 2020, 2020.

NGUYEN, H. T. V. *et al.* Preparation and Characterization of a Hydrophilic Polysulfone Membrane Using Graphene Oxide. **Journal of Chemistry**, v. 2019, 2019.

NGUYEN-PHAN, T. D. et al. The role of graphene oxide content on the adsorption-enhanced photocatalysis of titanium dioxide/graphene oxide composites. **Chemical Engineering Journal**, v. 170, n. 1, p. 226–232, 15 maio 2011.

NIKBAKHT FINI, M. et al. Performance evaluation of membrane filtration for treatment of H2S scavenging wastewater from offshore oil and gas production. **Separation and Purification Technology**, v. 277, p. 119641, 2021.

NOVOSELOV, K. S. *et al.* Electric Field Effect in Atomically Thin Carbon Films. 2004.

OLIVEIRA, C. P. M. DE; VIANA, M. M.; AMARAL, M. C. S. Coupling photocatalytic degradation using a green TiO2 catalyst to membrane bioreactor for petroleum refinery wastewater reclamation. **Journal of Water Process Engineering**, v. 34, n. November 2019, p. 101093, 2020.

ONG, C. B.; MOHAMMAD, A. W.; NG, L. Y. Integrated adsorption-solar photocatalytic membrane reactor for degradation of hazardous Congo red using Fe-doped ZnO and Fe-doped

ZnO/rGO nanocomposites. **Environmental Science and Pollution Research**, v. 26, n. 33, p. 33856–33869, 2019.

ORVOS, D. R. *et al.* Aquatic toxicity of triclosan. **Environmental Toxicology and Chemistry**, v. 21, n. 7, p. 1338–1349, 2002.

OZGUN, H. et al. Comparative evaluation of cost for preliminary and tertiary municipal wastewater treatment plants in Istanbul. **Science of The Total Environment**, v. 778, p. 146258, 2021.

PAREDES, L. et al. Application of immobilized TiO2 on PVDF dual layer hollow fibre membrane to improve the photocatalytic removal of pharmaceuticals in different water matrices. **Applied Catalysis B: Environmental**, v. 240, p. 9–18, 2019.

PARK, G. et al. One-step sonochemical synthesis of a graphene oxidemanganese oxide nanocomposite for catalytic glycolysis of poly(ethylene terephthalate). **Nanoscale**, v. 4, n. 13, p. 3879–3885, 2012.

PASTRANA-MARTINEZ, L. M. *et al.* Graphene oxide based ultrafiltration membranes for photocatalytic degradation of organic pollutants in salty water. **Water Research**, v. 77, p. 179–190, jun. 2015.

PAULA, E. C.; Avaliação técnica e ambiental da reciclagem via oxidação química de membranas de osmose inversa descartadas; **Tese de doutorado**, UFMG, 2017.

PEDERSEN, M. L. K. *et al.* Investigation of surface energy, wettability and zeta potential of titanium dioxide/graphene oxide membranes. **Journal Of Photochemistry And Photobiology A-Chemistry**, v. 366, n. SI, p. 162–170, nov. 2018.

PENBOON, L.; KHRUEAKHAM, A.; SAIRIAM, S. TiO2 coated on PVDF membrane for dye wastewater treatment by a photocatalytic membrane. **Water Science and Technology**, v. 79, n. 5, p. 958–966, 2019.

PENG, L. *et al.* Microwave-assisted deposition of silver nanoparticles on bamboo pulp fabric through dopamine functionalization. **Applied surface science**, v. 386, p. 151–159, 2016.

PETER-VARBANETS, M. et al. Decentralized systems for potable water and the potential of membrane technology. **Water research**, v. 43, n. 2, p. 245–265, fev. 2009.

PICHARDO-ROMERO, D. *et al.* Current Advances in Biofouling Mitigation in Membranes for Water Treatment: An Overview. **Processes**, v. 8, n. 2, p. 182, 2020.

QING, W. *et al.* Functional catalytic membrane development: A review of catalyst coating techniques. **Advances in Colloid and Interface Science**, v. 282, p. 102207, 2020.

QING, W. et al. Polymeric catalytically active membranes for reaction-separation coupling: A review. **Journal of membrane science**, v. 583, p. 118–138, 2019.

QU, X. *et al.* Nanotechnology for a Safe and Sustainable Water Supply: Enabling Integrated Water Treatment and Reuse. **Accounts of Chemical Research**, v. 46, n. 3, p. 834–843, 2013.

RAMASUNDARAM, S.; YOO, H.N.; SONG, K.G.; LEE, J.; CHOI, K.J.; HONG, S.W. Titanium Dioxide Nanofibers Integrated Stainless Steel Filter for Photocatalytic Degradation of Pharmaceutical Compounds. **J. Hazard. Mater**. 2013, 258–259, 124–132.

RATHI, B. S.; KUMAR, P. S.; SHOW, P.-L. A review on effective removal of emerging contaminants from aquatic systems: Current trends and scope for further research. **Journal of hazardous materials**, v. 409, p. 124413, 2021.

REIS, E. O. et al. Occurrence, removal and seasonal variation of pharmaceuticals in Brasilian drinking water treatment plants. **Environmental Pollution**, v. 250, p. 773–781, 1 jul. 2019.

REMY, C. et al. Comparing environmental impacts of tertiary wastewater treatment technologies for advanced phosphorus removal and disinfection with life cycle assessment. **Water science and technology**, v. 69, n. 8, p. 1742–1750, 2014.

REN, Y. *et al.* A mini review of multifunctional ultrafiltration membranes for wastewater decontamination: Additional functions of adsorption and catalytic oxidation. **The Science of the total environment**, v. 762, 2021.

REZAKAZEMI, M. *et al.* Fouling-resistant membranes for water reuse. **Environmental Chemistry Letters**, v. 16, n. 3, p. 715–763, 2018.

RICCI, B. C. Biorreator anaeróbio osmótico acoplado à destilação assistida por membranas como alternativa para potabilização de esgoto doméstico; **Tese de doutorado**, UFMG, 2019.

ROMAY, M. *et al.* Critical Issues and Guidelines to Improve the Performance of Photocatalytic Polymeric Membranes**. Catalysts**, v. 10, n. 5, 2020.

ROUT, P. R. et al. Treatment technologies for emerging contaminants in wastewater treatment plants: A review. **Science of the Total Environment**, v. 753, p. 141990, 2021.

RÚA-GÓMEZ, P. C.; PÜTTMANN, W. Degradation of lidocaine, tramadol, venlafaxine and the metabolites O-desmethyltramadol and O-desmethylvenlafaxine in surface waters. **Chemosphere**, v. 90, n. 6, p. 1952–1959, 2013.

RUIZ-GARCÍA, A.; MELIÁN-MARTEL, N.; MENA, V. Fouling characterization of RO membranes after 11 years of operation in a brackish water desalination plant. **Desalination**, [s.l.], v. 430, p.180-185, mar. 2018. Elsevier BV.

SAFARPOUR, M. *et al.* Development of a novel high flux and fouling-resistant thin film composite nanofiltration membrane by embedding reduced graphene oxide/TiO_2. **Separation and purification technology**, v. 154, n. C, p. 96–107, 2015.

SAFARPOUR, M.; KHATAEE, A.; VATANPOUR, V. Preparation of a Novel Polyvinylidene Fluoride (PVDF) Ultrafiltration Membrane Modified with Reduced Graphene Oxide/Titanium Dioxide (TiO2) Nanocomposite with Enhanced Hydrophilicity and Antifouling Properties. **Industrial & Engineering Chemistry Research**, v. 53, n. 34, p. 13370–13382, 27 ago. 2014.

SAFARPOUR, M.; VATANPOUR, V.; KHATAEE, A. Preparation and characterization of graphene oxide/TiO2 blended PES nanofiltration membrane with improved antifouling and separation performance. **Desalination**, v. 393, p. 65–78, 2016.

SALEEM, H.; ZAIDI, S. J. Nanoparticles in reverse osmosis membranes for desalination: A state of the art review. **Desalination**, v. 475, 2020.

SALEH, T. A.; GUPTA, V. K. **Nanomaterial and Polymer Membranes**. [s.l: s.n.].

SANTOKE, H. et al. Advanced oxidation treatment and photochemical fate of selected antidepressant pharmaceuticals in solutions of Suwannee River humic acid. **Journal of hazardous materials**, v. 217, p. 382–390, 2012.

SANTOS, A. V. et al. Occurrence and risk assessment of pharmaceutically active compounds in water supply systems in Brazil. **Science of the Total Environment**, v. 746, p. 141011, 2020b.

SANTOS, L.V.S. Utilização de processos biológicos e oxidativos avançados no tratamento dos antibióticos Norfloxacino e Sulfato de Gentamicina presentes em meio aquoso. **Tese de doutorado**. Universidade Federal de Minas Gerais, 2017.

SCHNITTGER, J. *et al.* Hydrophobic ceramic membranes in MD processes – Impact of material selection and layer characteristics. **Journal of membrane science**, v. 618, 2021.

SEHATI, N. *et al.* Application of hollow fiber membrane mediated with titanium dioxide nanowire/reduced graphene oxide nanocomposite in preconcentration of clotrimazole and tylosin. **Journal of Chromatography A**, v. 1420, p. 46–53, 2015.

SEMIAT, R. Energy issues in desalination processes. **Environmental Science & Technology**, v. 42, p. 8193–8201, 2015.

SENÁN-SALINAS, J. et al. Recycling of end-of-life reverse osmosis membranes: Comparative LCA and cost-effectiveness analysis at pilot scale. **Resources, Conservation and Recycling**, v. 150, p. 104423, 2019.

SHAO, F. et al. Layer-by-layer self-assembly TiO2 and graphene oxide on polyamide reverse osmosis membranes with improved membrane durability. **Desalination**, v. 423, p. 21–29, 2017a.

SHENG, C. et al. Removal of Trace Pharmaceuticals from Water using coagulation and powdered activated carbon as pretreatment to ultrafiltration membrane system. **Science of the Total Environment**, v. 550, p. 1075–1083, 2016.

SHENVI, S.S.; ISLOOR, A.M.; ISMAIL, A.F. A review on RO membrane technology: Developments and challenges. **Desalination**, v. 368, p. 10–26, 2015.

SHULTZ, S. et al. Modification of polyamide membranes by hydrophobic molecular plugs for improved boron rejection. **Journal of Membrane Science**, v. 546, p. 165–172, 15 jan. 2018.

SIMONSEN, K. R. *et al.* Principal Component Analysis of the Effect of Batch Variation, TiO2 Content and Reduction Temperature on the Surface Energy of TiO_2/Graphene Oxide Membranes upon UV-C Activation. **Topics in Catalysis**, n. 0123456789, 2020.

SINGH, A. et al. Titanium dioxide doped hydroxyapatite incorporated photocatalytic membranes for the degradation of chloramphenicol antibiotic in water. **Journal of chemical technology and biotechnology (1986)**, v. 96, n. 4, p. 1057–1066, 2021.

SINGH, R.; SINHA, M. K.; PURKAIT, M. K. Stimuli responsive mixed matrix polysulfone ultrafiltration membrane for humic acid and photocatalytic dye removal applications. **Separation and Purification Technology**, v. 250, p. 117247, 2020.

SIRINUPONG, T. *et al.* Synthesis and characterization of thin film composite membranes made of PSF-TiO_2 /GO nanocomposite substrate for forward osmosis applications. **Arabian Journal of Chemistry**, v. 11, n. 7, p. 1144–1153, 2018.

SNYDER, S. A. et al. Role of membranes and activated carbon in the removal of endocrine disruptors and pharmaceuticals. **Desalination**, v. 202, n. 1–3, p. 156–181, 2007.

SONG, N. et al. A review of graphene-based separation membrane: Materials, characteristics, preparation and applications. **Desalination**, v. 437, p. 59–72, 2018.

STADLMAIR, L. F. *et al.* Enzymes in removal of pharmaceuticals from wastewater: A critical review of challenges, applications and screening methods for their selection. **Chemosphere (Oxford),** v. 205, p. 649–661, 2018.

SUBRAMANI, A.; JACANGELO, J. G. Emerging desalination technologies for water treatment: A critical review. **Water research (Oxford),** v. 75, n. C, p. 164–187, 2015.

SUNDARAN, S. P. *et al.* Polyurethane nanofibrous membranes decorated with reduced graphene oxide–TiO_2 for photocatalytic templates in water purification. **Journal of Materials Science**, v. 55, n. 14, 2020.

SURIANI, A. B. *et al.* Incorporation of Electrochemically Exfoliated Graphene Oxide and TiO2 into Polyvinylidene Fluoride-Based Nanofiltration Membrane for Dye Rejection. **Water, Air, and Soil Pollution**, v. 230, n. 8, 2019.

SZYMAŃSKI, K.; MORAWSKI, A. W.; MOZIA, S. Effectiveness of treatment of secondary effluent from a municipal wastewater treatment plant in a photocatalytic membrane reactor and hybrid UV/H2O2 – ultrafiltration system. **Chemical Engineering and Processing - Process Intensification**, v. 125, n. July 2017, p. 318–324, 2018.

SZYMAŃSKI, K.; MORAWSKI, A. W.; MOZIA, S. Humic acids removal in a photocatalytic membrane reactor with a ceramic UF membrane. **Chemical Engineering Journal**, v. 305, p. 19–27, 2016.

TAGHIZADEH, M.; KEBRIA, D. Y.; QADERI, F. Effect of biosurfactant as a novel draw solution on photocatalytic treatment and desalination of produced water by different forward osmosis membranes. **Water Supply**, v. 20, n. 1, p. 240–250, 2019.

TEOW, Y. H. *et al.* Hydroxyl functionalized PVDF–TiO_2 ultrafiltration membrane and its antifouling properties. **Journal of Applied Polymer Science**, v. 132, n. 21, p. n/a--n/a, 2015.

TIWARI, B. *et al.* Review on fate and mechanism of removal of pharmaceutical pollutants from wastewater using biological approach. **Bioresource technology**, v. 224, p. 1–12, 2017.

TRAN, M. L. *et al.* Immobilization of TiO_2 and TiO_2-GO hybrids onto the surface of acrylic acid-grafted polymeric membranes for pollutant removal: Analysis of photocatalytic activity. **Journal of environmental chemical engineering**, v. 8, n. 5, 2020a.

TRAN, M. L. *et al.* Surface coating of titania and graphene oxide onto plasma-activated polymer membranes as efficient photocatalysts for organics removal from water. **Journal of Water Process Engineering**, v. 37, p. 101488, 2020b.

TRAWIŃSKI, J.; SKIBIŃSKI, R. Studies on photodegradation process of psychotropic drugs: a review. **Environmental Science and Pollution Research**, v. 24, n. 2, p. 1152–1199, 2017.

TSAGARAKIS, K. P.; MARA, D. D.; ANGELAKIS, A. N. Application of cost criteria for selection of municipal wastewater treatment systems. **Water, air, and soil pollution**, v. 142, n. 1, p. 187–210, 2003.

UNG-MEDINA, F. et al. Experimental methodology to calculate the local relative light intensity in heterogeneous TiO2/UV-A photocatalytic reactors. **Chemical engineering research & design**, v. 97, p. 28–35, 2015.

UNITED STATES GEOLOGICAL SERVICE. **Contaminants of Emerging Concern in the Environment**. Environmental Health - Toxic Substances Hydrology Program. U.S. Geological Survey. 2017.

URSINO, C. *et al.* Progress of Nanocomposite Membranes for Water Treatment. **Membranes (Basel),** v. 8, n. 2, p. 1–40, 2018.

VARAPRASAD, K.; JAYARAMUDU, T.; SADIKU, E. R. Removal of dye by carboxymethyl cellulose, acrylamide and graphene oxide via a free radical polymerization process. **Carbohydrate Polymers**, v. 164, p. 186–194, 2017.

VASILACHI, I. et al. Occurrence and Fate of Emerging Pollutants in Water Environment and Options for Their Removal. **Water (Basel)**, v. 13, n. 2, p. 181, 2021.

VATANPOUR, V. *et al.* TiO_2 embedded mixed matrix PES nanocomposite membranes: Influence of different sizes and types of nanoparticles on antifouling and performance. **Desalination**, v. 292, p. 19–29, 2012.

VATANPOUR, V. et al. TiO2/CDs modified thin-film nanocomposite polyamide membrane for simultaneous enhancement of antifouling and chlorine-resistance performance. **Desalination**, v. 525, p. 115506, 2022.

VELASCO-SOTO, M. A. *et al.* Selective band gap manipulation of graphene oxide by its reduction with mild reagents. **Carbon (New York),** v. 93, n. C, p. 967–973, 2015.

VERGILI, I. Application of nanofiltration for the removal of carbamazepine, diclofenac and ibuprofen from drinking water sources. **Journal of environmental management**, v. 127, p. 177–187, 2013.

VERGILI, I. et al. Techno-economic analysis of textile dye bath wastewater treatment by integrated membrane processes under the zero liquid discharge approach. **Resources, Conservation and Recycling**, v. 58, p. 25–35, 2012.

WANG, D. et al. Technical, economic and environmental assessment of coagulation/filtration tertiary treatment processes in full-scale wastewater treatment plants. **Journal of cleaner production**, v. 170, p. 1185–1194, 2018.

WANG, H. *et al.* Facile prepared ball-like TiO_2 at GO composites for oxytetracycline removal under solar and visible lights. **Water research (Oxford),** v. 160, p. 197–205, 2019.

WANG, J. et al. Construction of TiO2@graphene oxide incorporated antifouling nanofiltration membrane with elevated filtration performance. **Journal of Membrane Science**, v. 533, p. 279–288, 2017a.

WANG, P.; FANE, A. G.; LIM, T.-T. Evaluation of a submerged membrane vis-LED photoreactor (sMPR) for carbamazepine degradation and TiO2 separation. **Chemical engineering journal**, v. 215, p. 240–251, 2013.

WANG, W. *et al.* Fabrication of an antifouling GO-TiO_2/PES ultrafiltration membrane. **Journal of Applied Polymer Science**, v. n/a, n. n/a, p. 51165, [s.d.].

WANG, X. et al. Photocatalytic and antifouling properties of TiO2-based photocatalytic membranes. **Materials Today Chemistry**, v. 23, p. 100650, 2022.

WAWRYNIUK, M.; PIETRZAK, A.; NAŁĘCZ-JAWECKI, G. Evaluation of direct and indirect photodegradation of mianserin with high-performance liquid chromatography and short-term bioassays. **Ecotoxicology and Environmental Safety**, v. 115, p. 144–151, 2015.

WEI, Y. et al. Declining flux and narrowing nanochannels under wrinkles of compacted graphene oxide nanofiltration membranes. **Carbon (New York)**, v. 108, p. 568–575, 2016.

WILLIAMS, G.; SEGER, B.; KAMT, P. V. TiO 2 -graphene nanocomposites. UV-assisted photocatalytic reduction of graphene oxide. **ACS Nano**, v. 2, n. 7, p. 1487–1491, 2008.

WU, H. et al. Doping polysulfone ultrafiltration membrane with TiO2-PDA nanohybrid for simultaneous self-cleaning and self-protection. **Journal of Membrane Science**, v. 532, p. 20–29, 2017.

WU, L.-G. *et al.* Enhanced performance of polyvinylidene fluoride ultrafiltration membranes by incorporating TiO_2/graphene oxide. **Chemical Engineering Research & Design,** v. 141, p. 492, 2019a.

WU, Y. *et al.* Fabrication and evaluation of GO/TiO_2-based molecularly imprinted nanocomposite membranes by developing a reformative filtering strategy: Application to selective adsorption and separation membrane. **Separation and Purification Technology**, v. 212, p. 245–254, 2019b.

WU, Z. *et al.* Hydrophilic/underwater superoleophobic graphene oxide membrane intercalated by TiO_2 nanotubes for oil/water separation. **Frontiers of Environmental Science & Engineering,** v. 12, n. 3, p. 1–10, 2018.

XIA, C. *et al.* Fabrication of microporous GO-TiO_2 membrane via an improved weak alkaline sol–gel method. **Journal of Membrane Science**, v. 561, p. 10–18, 2018.

XU, C. et al. Graphene oxide–TiO2 composite filtration membranes and their potential application for water purification. **Carbon (New York)**, v. 62, p. 465–471, 2013a.

XU, H. *et al.* Nitrogen-doped GO/TiO_2 nanocomposite ultrafiltration membranes for improved photocatalytic performance. **Separation And Purification Technology**, v. 195, p. 70–82, 2018b.

XU, H. *et al.* Simultaneous removal of dissolved organic matter and nitrate from sewage treatment plant effluents using photocatalytic membranes. **Water research (Oxford),** v. 143, p. 250–259, 2018a.

XU, P.; BELLONA, C.; DREWES, J. E. Fouling of nanofiltration and reverse osmosis membranes during municipal wastewater reclamation: Membrane autopsy results from pilot-scale investigations. **Journal of membrane science**, v. 353, n. 1, p. 111–121, 2010.

XU, T. et al. Atomically Pt implanted nanoporous TiO2 film for photocatalytic degradation of trace organic pollutants in water. **Chemical Engineering Journal**, v. 385, p. 123832, 2020.

XU, Z. *et al.* Photocatalytic antifouling PVDF ultrafiltration membranes based on synergy of graphene oxide and TiO_2 for water treatment. **Journal Of Membrane Science**, v. 520, p. 281–293, 2016b.

YADAV, P. et al. Assessment of the environmental impact of polymeric membrane production. **Journal of Membrane Science**, v. 622, p. 118987, 15 mar. 2021.

YAN, X. *et al.* Layer-by-layer assembly of graphene oxide-TiO_2 membranes for enhanced photocatalytic and self-cleaning performance. **Process safety and environmental protection**, v. 130, p. 257–264, 2019.

YANG, A. *et al.* Membrane concentrate treatment by photosynthetic bacteria: Feasibility and tolerance mechanism analysis. **Bioresource Technology**, v. 253, p. 378–381, 2018.

YANG, X. *et al.* Biochemical characteristics and membrane fouling behaviors of soluble microbial products during the lifecycle of Escherichia coli. **Water research (Oxford),** v. 192, 2021.

YIN, J.; DENG, B. Polymer-matrix nanocomposite membranes for water treatment. **Journal Of Membrane Science**, v. 479, p. 256–275, 2015.

YOO, V.C. *et al.* Enhanced photocatalytic activity of grapheme oxide decorated on TiO_2 films under UV and visible irradiation, **Curr.Appl.Phys.** 11(2011)805–808.

YOUNAS, H. *et al.* Super-hydrophilic and fouling resistant PVDF ultrafiltration membranes based on a facile prefabricated surface. **Journal Of Membrane Science**, v. 541, p. 529–540, nov. 2017.

YUAN, Z. *et al.* Fabrication of antibacterial surface via UV-inducing dopamine polymerization combined with co-deposition Ag nanoparticles. **Materials letters**, v. 183, p. 85–89, 2016.

ZAKERITABAR, S. F. *et al.* Photocatalytic study of nanocomposite membrane modified by CeF_3 catalyst for pharmaceutical wastewater treatment. **Journal of Environmental Health Science and Engineering**, v. 18, n. 2, 2020.

ZHANG, J. et al. Large-scale membrane bioreactors for industrial wastewater treatment in China: Technical and economic features, driving forces, and perspectives. **Engineering**, v. 7, n. 6, p. 868–880, 2021a.

ZHANG, N. et al. Advanced thin-film nanocomposite membranes embedded with organic-based nanomaterials for water and organic solvent purification: A review. **Separation and Purification Technology**, v. 269, p. 118719, 2021b.

ZHANG, Q. et al. Efficient and effective removal of emerging contaminants through the parallel coupling of rapid adsorption and photocatalytic degradation: A case study of fluoroquinolones. **Chemosphere (Oxford)**, v. 280, p. 130770, 2021c.

ZHANG, R. *et al.* Enhanced photocatalytic degradation of organic dyes by ultrasonic-assisted electrospray TiO_2/graphene oxide on polyacrylonitrile/β-cyclodextrin nanofibrous membranes. **Ultrasonics Sonochemistry**, v. 70, p. 105343, 2021.

ZHANG, R.-X. *et al.* Novel binding procedure of TiO_2 nanoparticles to thin film composite membranes via self-polymerized polydopamine. **Journal of membrane science**, v. 437, p. 179–188, 2013.

ZHANG, R.-X. *et al.* Remarkable anti-fouling performance of TiO_2-modified TFC membranes with mussel-inspired polydopamine binding. **Applied Sciences (Switzerland)**, v. 7, n. 1, 2017.

ZHANG, X. *et al.* Developing new adsorptive membrane by modification of support layer with iron oxide microspheres for arsenic removal. **Journal of colloid and interface science**, v. 514, p. 760–768, 2018.

ZHANG, Y. *et al.* Layer-by-layer construction of graphene oxide (GO) framework composite membranes for highly efficient heavy metal removal. **Journal of Membrane Science**, v. 515, p. 230–237, 2016.

ZHANG, Y. *et al.* Catalytic ozonation of emerging pollutant and reduction of toxic by-products in secondary effluent matrix and effluent organic matter reaction activity. **Water research (Oxford),** v. 166, 2019.

ZHANG, Y. et al. Preparation of Ag/β-cyclodextrin co-doped TiO2 floating photocatalytic membrane for dynamic adsorption and photoactivity under visible light. **Applied Catalysis B: Environmental**, v. 267, p. 118715, 2020.

ZHANG, Y. et al. TiO2/BiOI p-n junction-decorated carbon fibers as weavable photocatalyst with UV–vis photoresponsive for efficiently degrading various pollutants. **Chemical Engineering Journal**, v. 415, p. 129019, 2021e.

ZHAO, G. *et al.* Physically Coating Nanofiltration Membranes with Graphene Oxide Quantum Dots for Simultaneously Improved Water Permeability and Salt/Dye Rejection. **Advanced Materials Interfaces**, v. 6, n. 5, p. 1801742, 2019.

ZHAO, Y.; GAO, C.; VAN DER BRUGGEN, B. Technology-driven layer-by-layer assembly of a membrane for selective separation of monovalent anions and antifouling. **Nanoscale**, v. 11, n. 5, p. 2264–2274, 2019.

ZHENG, X. et al. Photocatalytic membrane reactors (PMRs) in water treatment: Configurations and influencing factors. **Catalysts**, v. 7, n. 8, 2017.

ZHOU, C. et al. Degradation of Minocycline by the Adsorption–Catalysis Multifunctional PVDF–PVP–TiO2 Membrane: Degradation Kinetics, Photocatalytic Efficiency, and Toxicity of Products. **International journal of environmental research and public health**, v. 18, n. 23, p. 12339, 2021.

ZHU, C. *et al.* One-step facile synthesis of graphene oxide/TiO_2 composite as efficient photocatalytic membrane for water treatment: Crossflow filtration operation and membrane fouling analysis. **Chemical engineering and processing**, v. 120, p. 20–26, 2017.

ZHU, J. et al. A novel strategy of fabricating high performance UV-resistant aramid fibers with simultaneously improved surface activity, thermal and mechanical properties through building polydopamine and graphene oxide bi-layer coatings. **Chemical Engineering Journal**, v. 310, p. 134–147, 15 fev. 2017b.

ZHU, L. *et al.* Direct production of a free-standing titanate and titania nanofiber membrane with selective permeability and cleaning performance. **Journal Of Materials Chemistry**, v. 21, n. 33, p. 12503–12510, 2011.

ZHU, L. et al. Effect of TiO2 content on the properties of polysulfone nanofiltration membranes modified with a layer of TiO_2–graphene oxide. **Separation and purification technology**, v. 242, 2020a.

ZHU, R. *et al.* Mechanism of humic acid fouling in a photocatalytic membrane system. **Journal of membrane science**, v. 563, p. 531–540, 2018.

ZHUL, C. *et al.* One-step facile synthesis of graphene oxide/TiO_2 composite as efficient photocatalytic membrane for water treatment: Crossflow filtration operation and membrane fouling analysis. **Chemical Engineering And Processing-Process Intensification**, v. 120, p. 20–26, 2017.

ZIMMERMANN, R. et al. Hydroxide and hydronium ion adsorption—A survey. **Current Opinion in Colloid & Interface Science**, v. 15, n. 3, p. 196–202, 2010.

ZONDERVAN, E.; ROFFEL, B. Evaluation of different cleaning agents used for cleaning ultra filtration membranes fouled by surface water. **Journal of Membrane Science**, v. 304, n. 1–2, p. 40–49, 2007.

APPENDIX

APPENDIX

Table A.1 - Different polymeric materials used in TiO_2-GO nanocomposite membranes.

Membrane material	Chemical formula	Chemical structure	Membrane configuration	Benefits of the polymeric material	References
Cellulose acetate (CA)	$(C_{20}H_{28}O_{14})n$	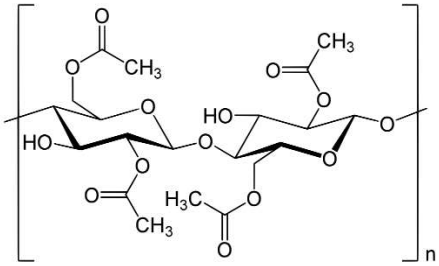	Flat	Good toughness, high biocompatibility, good desalting, high potential flux, and relatively low cost.	(GAO *et al.*, 2013)
Cellulose triacetate (CTA)	$(C_6H_7O_2(OOCH_3)_3)n$	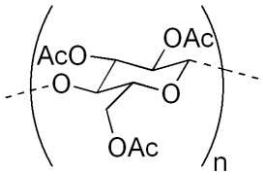	Flat	High transparency, good solvent and heat resistance.	(TAGHIZADEH; KEBRIA; QADERI, 2019)
Polydimethylsiloxane (PDMS)	$(C_2H_6OSi)n$	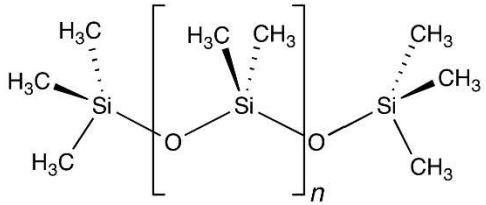	Flat	Biocompatibility, stability, and biomedical antifouling properties.	(CORREA *et al.*, 2017)

Polyethersulfone (PES)	$(C_6H_4–SO_2–C_6H_4–O)n$	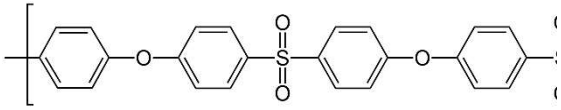	Flat	Commercially available polymer, high mechanical and thermal stability, good heat-aging resistance and environmental endurance as well as easy processing properties.	(DIOGO JANUÁRIO *et al.*, 2020)
Polysulfone (PSF)	$(C_{27}H_{26}O_6S)n$	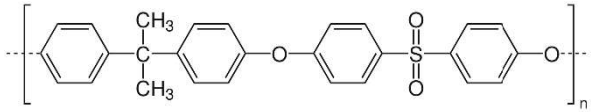	Flat	Semi-hydrophobic polymer, high thermal stability and good mechanical resistance.	(SIRINUPONG *et al.*, 2018)
Polyurethane (PU)	$(C_{17}H_{16}O_4N_2)n$	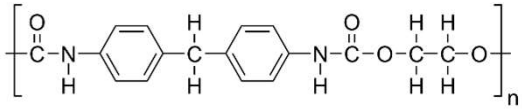	Flat	Possibility of obtaining a nanofibrous polymeric membrane by electrospinning.	(SUNDARAN *et al.*, 2020)
Polyvinylchloride (PVC)	$(C_2H_3Cl)n$	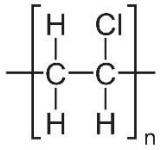	Flat	Low cost, excellent properties such as durability, flexibility, suitable chemical and biological resistance.	(HOSSEINI *et al.*, 2017)
Poly (vinylidene fluoride) (PVDF)	$(CH_2CF_2)n$	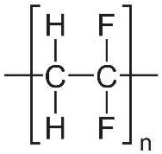	Flat	Strong mechanical property, thermal stability, and chemical resistance.	(TRAN *et al.*, 2020)
Polyamide	[CO-C_6H_4-CO-NH-C_6H_4-NH-]n	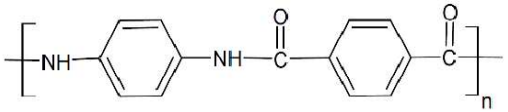	Hollow fiber	High resistance to pressure and temperature, pH compaction, and high stability to biological attack.	(BAIG *et al.*, 2019)

Polypropylene	$(C_3H_6)n$	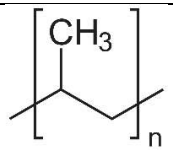	Hollow fiber	Good porosity, high void volume, and high thermal stability.	(SEHATI *et al.*, 2015)

Calibration curve of the eriochrome black T dye

$$y = 32{,}015x + 0{,}1251$$

Where y is the absorbance and x is the concentration of the eriochrome black T dye.

Table A.2. PhACs main physical-chemical properties.

PhACs	Molecular weight (g/mol)	Molar volume (cm^3)	log Kow	pKa	KH ($atm.m^3/mol$)
BET	392	296	3.38	13.4	7.36E-11
KET	254	212	3.12	4.45	1.45E-09
FEN	361	306	5.28	-4.9	4.11E-09
FLU	306	205	0.4	11.01	7.12E-09
LOR	383	304	5.2	4.33	1.6E-08
PRE	358	274	1.46	12.58	1.24E-09

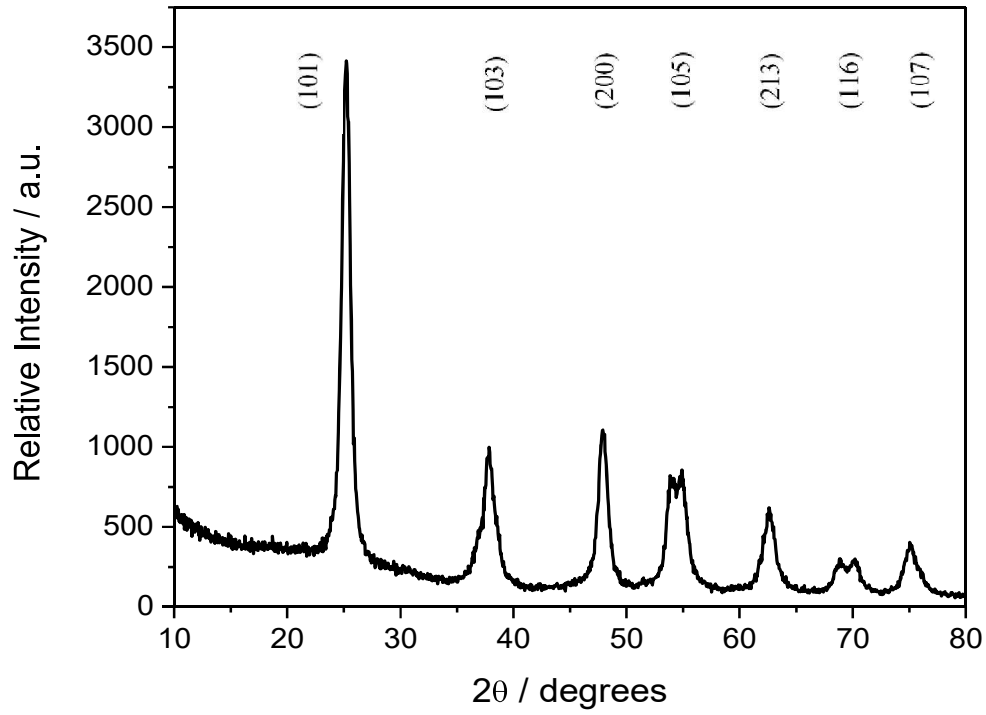

Figure A.1: XRD patterns of TiO_2 nanoparticles.

Scherrer Equation

$D = \frac{k.\lambda}{\beta.cos\theta}$ = 13,54 nm ≈ 14 nm

$\beta^2 = w_{TiO2}{}^2 - w_{NaCl}{}^2$

Where:

D = Average particle diameter

k = Particle shape dependent proportionality constant = 0,94 = assumed value for particles to be spherical

λ = Wavelength of electromagnetic radiation = 0,154184 nm

β = Width at half height of diffraction peak

θ = Diffraction angle = 12,55° = 0,2190 rad

w_{TiO2} = Enlargement due to TiO_2 crystals

w_{NaCl} = Enlargement due to equipment and NaCl standard

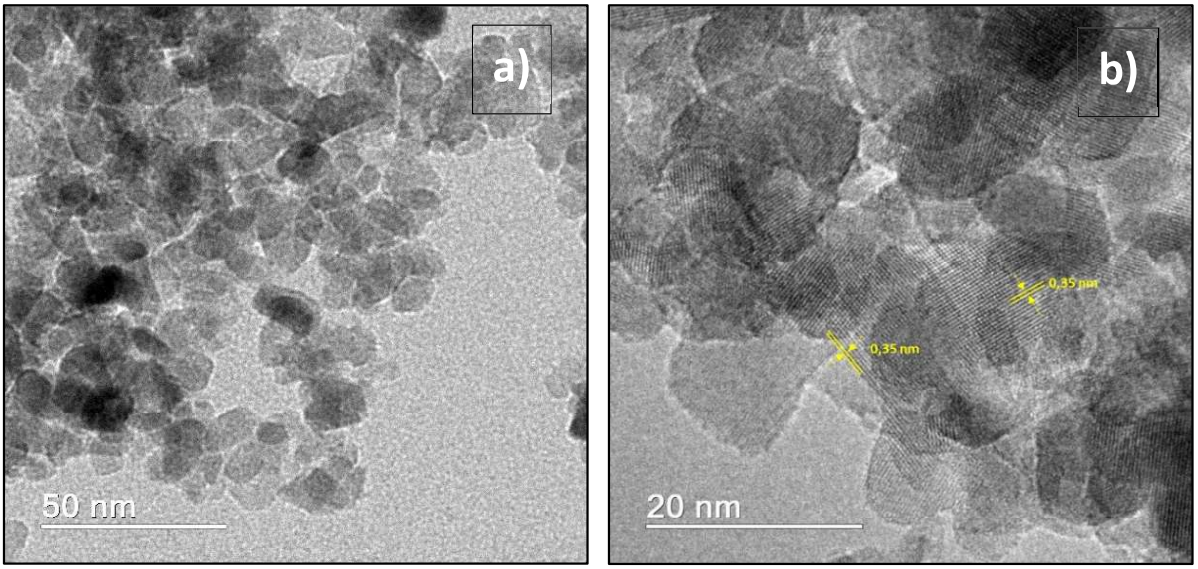

Figure A.2: TEM micrographs of TiO_2.

Figure A.3 - Filtration cell used in the preliminary surface modification of the membranes.

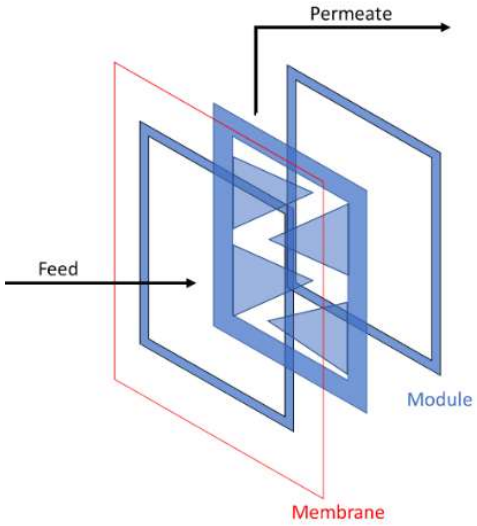

Figure A.4 - PMR module configuration.

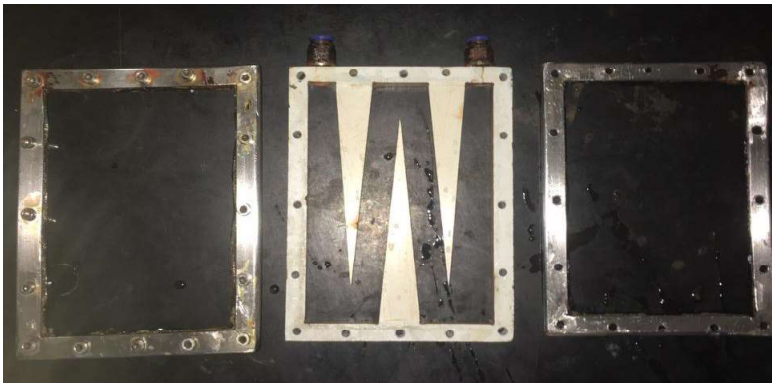

Figure A.5 - PMR module structure.

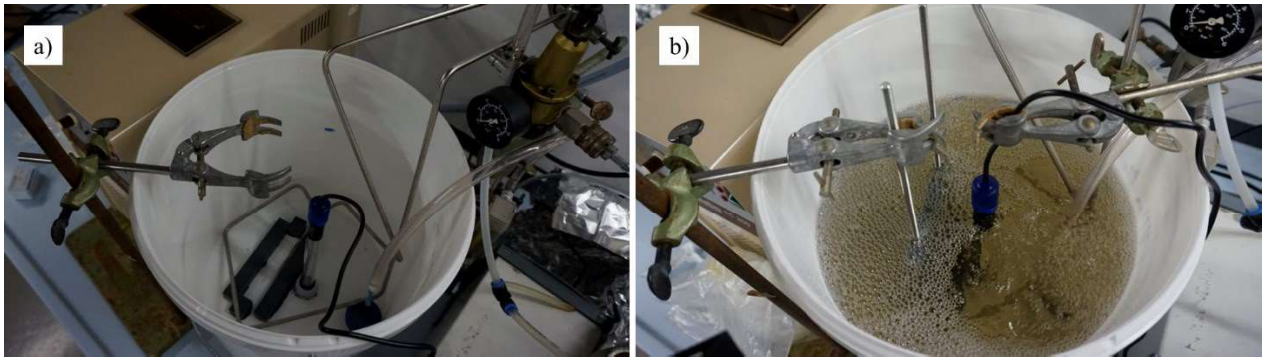

Figure A.6 - PMR module structure.

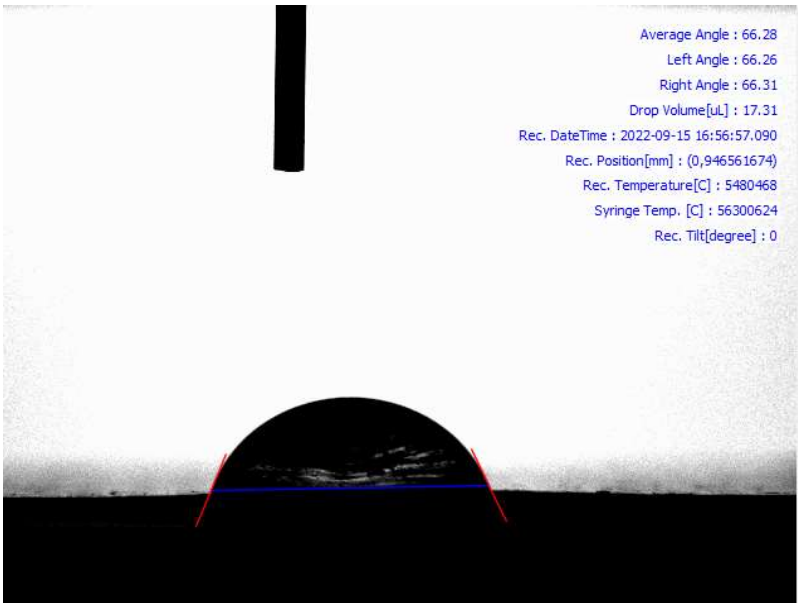

Figure A.7 – Drop on the surface of recycled membrane **–** contact angle measurements.

Figure A.8 – Drop on the surface of the photocatalytic membrane – contact angle measurements.